

DTIC FILE COPY

2

GL-TR-90-0107

AD-A223 490

TGAL-90-03

**MAGNITUDE:YIELD RELATIONSHIP AT VARIOUS NUCLEAR
TEST SITES --- A MAXIMUM-LIKELIHOOD APPROACH
USING HEAVILY CENSORED EXPLOSIVE YIELDS**

Rong-Song Jih
Robert. R. Shumway
D. Wilmer Rivers, Jr.
Robert A. Wagner
Tom W. McElfresh

Teledyne Geotech Alexandria Laboratory
314 Montgomery Street
Alexandria, VA 22314-1581

1 MAY 1990

SCIENTIFIC REPORT NO. 1

APPROVED FOR PUBLIC RELEASE
DISTRIBUTION UNLIMITED

DTIC
S ELECTE D
JUL 03 1990
Ca E

GEOPHYSICS LABORATORY
AIR FORCE SYSTEMS COMMAND
UNITED STATES AIR FORCE
HANSCOM AIR FORCE BASE, MASSACHUSETTS 01731-5000


90 07 . 3 170


SCIENTIFIC REPORT NO.1
16 April 1989 --- 15 April 1990

Project Title:	Numerical and Observational Studies in Seismic Discrimination and Yield Estimation
Name of Contractor:	Task 1: Numerical and Statistical Modeling Studies
Principal Investigator:	Teledyne Geotech Alexandria Laboratories
Institutional Representative:	Rong-Song Jih, (703) 739-7321
Monitoring Agency:	D. Wilmer Rivers, Jr., Director, (703) 836-3882
Contract Manager:	GL/LWH
Contract No.:	James F. Lewkowicz, (617) 377-3028
Sponsoring Agency:	F19628-89-C-0063
ARPA Order No.:	DARPA/NMRO, (703) 697-7523
	5307

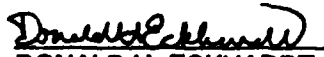
The views and conclusions contained in this document are those of the authors and should not be interpreted as representing the official policies, either expressed or implied, of the Defense Advanced Research Projects Agency or the U.S. Government.

This technical report has been reviewed and is approved for publication.


JAMES F. LEWKOWICZ
Contract Manager
Solid Earth Geophysics Branch
Earth Sciences Division


JAMES F. LEWKOWICZ
Branch Chief
Solid Earth Geophysics Branch
Earth Sciences Division

FOR THE COMMANDER


DONALD H. ECKHARDT
Director
Earth Sciences Division

This report has been reviewed by the ESD Public Affairs Office (PA) and is releasable to the National Technical Information Service (NTIS).

Qualified requestors may obtain additional copies from the Defense Technical Information Center (DTIC). All others should apply to the National Technical Information Service.

If your address has changed, or if you wish to be removed from the mailing list, or if the addressee is no longer employed by your organization, please notify GL/IMA, Hanscom AFB, MA 01731-5000. This will assist us in maintaining current mailing list.

Do not return copies of this report unless contractual obligations or notices on a specific document requires that it be returned.

REPORT DOCUMENTATION PAGE				Form Approved OMB No 0764-0188 Exp Date Jun 30, 1986	
1a REPORT SECURITY CLASSIFICATION Unclassified			1b RESTRICTIVE MARKINGS		
2a SECURITY CLASSIFICATION AUTHORITY			3 DISTRIBUTION/AVAILABILITY OF REPORT Approved for Public Release; Distribution Unlimited		
2b DECLASSIFICATION/DOWNGRADING SCHEDULE					
4 PERFORMING ORGANIZATION REPORT NUMBER(S) TGAL-90-03			5. MONITORING ORGANIZATION REPORT NUMBER(S) GL-TR-90-0107		
6a NAME OF PERFORMING ORGANIZATION Teledyne Geotech and University of California		6b OFFICE SYMBOL (If applicable)	7a. NAME OF MONITORING ORGANIZATION Geophysics Laboratory		
6c. ADDRESS (City, State, and ZIP Code) 314 Montgomery Street Alexandria, VA 22314-1581			7b. ADDRESS (City, State, and ZIP Code) Hanscom AFB, MA 01731-5000		
8a. NAME OF FUNDING/SPONSORING ORGANIZATION DARPA		8b. OFFICE SYMBOL (If applicable) NMRO	9. PROCUREMENT INSTRUMENT IDENTIFICATION NUMBER F19628-89-C-0063		
8c. ADDRESS (City, State, and ZIP Code) 1400 Wilson Boulevard Arlington, VA 22209-2308			10. SOURCE OF FUNDING NUMBERS		
			PROGRAM ELEMENT NO. 62714E	PROJECT NO. 9A10	TASK NO. DA
11. TITLE (Include Security Classification) Magnitude:Yield Relationship at Various Nuclear Test Sites --- A Maximum-Likelihood Approach Using Heavily Censored Explosive Yields					
12. PERSONAL AUTHOR(S) R.-S. Jih, R. H. Shumway, D. W. Rivers, R. A. Wagner, and T. W. McElfresh					
13a. TYPE OF REPORT Scientific #1		13b. TIME COVERED FROM April 1989 to April 1990		14. DATE OF REPORT (Year, Month, Day) 1990 May 1	
15. PAGE COUNT 92					
16. SUPPLEMENTARY NOTATION					
17. COSATI CODES			18. SUBJECT TERMS (Continue on reverse if necessary and identify by block number)		
FIELD	GROUP	SUB-GROUP	Explosive Yield, Seismic Magnitude, Maximum Likelihood, Least Squares, Test Site Bias, EM Algorithm		
19. ABSTRACT (Continue on reverse if necessary and identify by block number) <p>Conventional methods for estimating underground explosion yields from seismic recordings are based on the use of some appropriate "magnitude:yield" relationship. One of the most important parameters used to characterize the seismic signature of an underground explosion is the body-wave magnitude, m_b. Thus obtaining an unbiased measurement of m_b (or auxilarily M_s, P_coda, $m_b(L_p)$, M_o, and RMS L_p values) is obviously a key step in estimating the yield. During the past decade, the m_b which is averaged over a well-distributed global network and which incorporates the maximum-likelihood technique into the inversion scheme has become widely accepted as a means to obtain m_b estimates that avoid bias due to the detection threshold characteristics of individual network stations.</p> <p>Recently Soviet seismologists have published descriptions of 96 nuclear explosions conducted from 1961 through 1972 at the Semipalatinsk Test Site, in Eastern Kazakhstan. With the exception of releasing news about their "peaceful nuclear explosions" [PNE], the Soviets have never before published such a body of information. However, out of the 72 Degelen events with announced yields, only 9 events or 12.5% were of "known" yields. The remaining were either left censored (66.7%) or bounded (20.8%). Similar heavy-censoring pattern can be found for other test sites. Thus the</p>					
20 DISTRIBUTION/AVAILABILITY OF ABSTRACT <input type="checkbox"/> UNCLASSIFIED/UNLIMITED <input type="checkbox"/> SAME AS RPT <input type="checkbox"/> DTIC USERS			21. ABSTRACT SECURITY CLASSIFICATION Unclassified		
22a NAME OF RESPONSIBLE INDIVIDUAL James F. Lewkowicz			22b TELEPHONE (Include Area Code) (617) 377-3028		22c OFFICE SYMBOL GL/LWH

(19. Continued.)

development of a procedure capable of making full use of such censored information would seem very timely and necessary.

In section I of this report, we present a maximum-likelihood regression scheme, "MLE-CY", which takes all the censored yields into account to refine the estimated m_b :yield relationship. This regression routine is very similar to the maximum-likelihood estimator used in computing the optimal network m_b values based on the censored station amplitude measurements due to clipping and to non-detection. In the non-censored case, it gives results identical to those derived by the standard least-squares method. Applications of this scheme to the explosions from several test sites of different geology show that it is a superior procedure, as compared to the conventional least-squares approach. The same algorithm can be applied to other magnitude measurements such as M_S , P_{coda} , $m_b(L_g)$, M_o , $RMS L_g$ and DOB etc.

We have also conducted a systematic analysis of the magnitude:yield relationship at five major test sites using miscellaneous unclassified magnitudes. (A classified annex using the official m_b values will be furnished separately.)

Several noteworthy results are summarized here:

- [1] Including the censored yields in the regression does improve the accuracy of the estimates. In reality, both the magnitude and the yield measurements are subject to error. Pending the determination as to which of the two extreme hypotheses, namely $\sigma(m_b)/\sigma(Y) = 0$ and $\sigma(m_b)/\sigma(Y) = \infty$, is closer to the real situation, we also included the results based on Ericsson's method with various $\sigma(m_b)/\sigma(Y)$. As expected, we can see the smooth transition of estimated parameters (i.e., the slope and the intercept) as $\sigma(m_b)/\sigma(Y)$ varies. Thus the censored cases with non-trivial $\sigma(m_b)/\sigma(Y)$ values could be "interpolated". Our maximum-likelihood regression scheme and Ericsson's method represent two different directions in extending the standard least squares.
- [2] For Shagan events, Ringdal's $RMS L_g$ provides the smallest scatter around the calibration curve, provided that low-yield events with $m_b(RMS L_g) < 5.5$ or yield $< 40KT$ are excluded. Geotech's GLM method gives network m_b values better than almost all other magnitudes based on the teleseismic P waves and $\log(\Psi_{\omega})$, in terms of both the yield estimation and the m_b scaling against Ringdal's $RMS L_g$. For all five test sites we have compared, m_b measurements reported by ISC and NEIS are biased high systematically at low yields.
- [3] A direct estimation of the test site bias suggests that Nuttli's (1987, 1988) Degelen puzzle could be invalid simply because of the relatively poorer quality $m_b(ISC)$ used. Our data indicate that Shagan River Test Site is more efficient in exciting teleseismic P waves than Degelen Mountain, consistent with our previous modeling study. Also, the test site bias is yield dependent, in agreement with other observational study.
- [4] We present an alternative approach to derive the m_b adjustment converting cratering shots to contained explosions of the same yield. The correction derived by this approach seems to match that by the multichannel deconvolution method rather well.
- [5] Degelen Mountain is the only test site that has a decreasing $\log(P_{max}/P_a)$ and $\log(P_b/P_a)$ with increasing yields. It is also the only test site for which the phase "a" (i.e., zero-crossing to first peak) shows the smallest scatter around the calibration curve, as compared to the phases "b" (i.e., first peak to first trough) and "max" (i.e., max peak-to-trough or trough-to-peak in the first 5 seconds). Both the mountainous topography (which causes complex pP interference) as well as the testing practice (e.g., the relatively shallow and abnormal shot depths) could be responsible. At Shagan River, the phase "b" has the smallest scatter around the calibration curve. These observations confirm the conjecture (DARPA, 1981) that in a proper environment the first cycle could give better results than does "max" phase.
- [6] The scale depth for Konystan explosions is 146 ± 1 meters, and the depth of burial [DOB] is roughly proportional to the quartic root of the yield, rather than the cubic root as frequently cited at NTS. This empirical scaling rule is applicable to Shagan River region, but not Degelen Mountain. For Konystan and Shagan regions, the yields estimated using depth scaling have accuracy comparable to those using m_b .

EXECUTIVE SUMMARY

Conventional methods for estimating underground explosion yields from seismic recordings are based on the use of some appropriate "magnitude:yield" relationship. One of the most important parameters used to characterize the seismic signature of an underground explosion is the body-wave magnitude, m_b . Thus obtaining an unbiased measurement of m_b (or auxiliarily M_S , P_{coda} , $m_b(L_g)$, M_o , and RMS L_g values) is obviously a key step in estimating the yield. During the past decade, the m_b which is averaged over a well-distributed global network and which incorporates the maximum-likelihood technique into the inversion scheme has become widely accepted as a means to obtain m_b estimates that avoid bias due to the detection threshold characteristics of individual network stations.

Recently Soviet seismologists have published descriptions of 96 nuclear explosions conducted from 1961 through 1972 at the Semipalatinsk Test Site, in Eastern Kazakhstan. With the exception of releasing news about their "peaceful nuclear explosions" [PNE], the Soviets have never before published such a body of information. However, out of the 72 Degelen events with announced yields, only 9 events or 12.5% were of "known" yields. The remaining were either left censored (66.7%) or bounded (20.8%). Similar heavy-censoring pattern can be found for other test sites. Thus the development of a procedure capable of making full use of such censored information would seem very timely and necessary.

In section I of this report, we present a maximum-likelihood regression scheme, "MLE-CY", which takes all the censored yields into account to refine the estimated m_b :yield relationship. This regression routine is very similar to the maximum-likelihood estimator used in computing the optimal network m_b values based on the censored station amplitude measurements due to clipping and to non-detection. In the non-censored case, it gives results identical to those derived by the standard least-squares method. Applications of this scheme to the explosions from several test sites of different geology show that it is a superior procedure, as compared to the conventional least-squares approach. The same algorithm can be applied to other magnitude measurements such as M_S , P_{coda} , $m_b(L_g)$, M_o , RMS L_g and DOB etc.

We have also conducted a systematic analysis of the magnitude:yield relationship at five major test sites using miscellaneous **unclassified** magnitudes. (A **classified** annex using the official m_b values will be furnished separately.)

Several noteworthy results are summarized here:

- [1] Including the censored yields in the regression does improve the accuracy of the estimates. In reality, both the magnitude and the yield measurements are subject to error. Pending the determination as to which of the two extreme hypotheses, namely $\sigma(m_b)/\sigma(Y) = 0$ and $\sigma(m_b)/\sigma(Y) = \infty$, is closer to the real situation, we also included the results based on Ericsson's method with various $\sigma(m_b)/\sigma(Y)$. As expected, we can see

the smooth transition of estimated parameters (*i.e.*, the slope and the intercept) as $\sigma(m_b)/\sigma(Y)$ varies. Thus the censored cases with nontrivial $\sigma(m_b)/\sigma(Y)$ values could be "interpolated". Our maximum-likelihood regression scheme and Ericsson's method represent two different directions in extending the standard least squares.

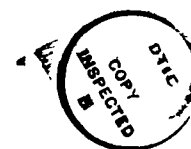
- [2] For Shagan events, Ringdal's $RMS L_g$ provides the smallest scatter around the calibration curve, provided that low-yield events with $m_b(RMS L_g) < 5.5$ or yield $< 40KT$ are excluded. Geotech's GLM method gives network m_b values better than almost all other magnitudes based on the teleseismic P waves and $\log(\Psi_\infty)$, in terms of both the yield estimation and the m_b scaling against Ringdal's $RMS L_g$. For all five test sites we have compared, m_b measurements reported by ISC and NEIS are biased high systematically at low yields.
- [3] A direct estimation of the test site bias suggests that Nuttli's (1987, 1988) Degelen puzzle could be invalid simply because of the relatively poorer quality $m_b(ISC)$ used. Our data indicate that Shagan River Test Site is more efficient in exciting teleseismic P waves than Degelen Mountain, consistent with our previous modeling study. Also, the test site bias is yield dependent, in agreement with other observational study.
- [4] We present an alternative approach to derive the m_b adjustment converting cratering shots to contained explosions of the same yield. The correction derived by this approach seems to match that by the multichannel deconvolution method rather well.
- [5] Degelen Mountain is the only test site that has a decreasing $\log(P_{max}/P_a)$ and $\log(P_b/P_a)$ with increasing yields. It is also the only test site for which the phase "a" (*i.e.*, zero-crossing to first peak) shows the smallest scatter around the calibration curve, as compared to the phases "b" (*i.e.*, first peak to first trough) and "max" (*i.e.*, max peak-to-trough or trough-to-peak in the first 5 seconds). Both the mountainous topography (which causes complex pP interference) as well as the testing practice (*e.g.*, the relatively shallow and abnormal shot depths) could be responsible. At Shagan River, the phase "b" has the smallest scatter around the calibration curve. These observations confirm the conjecture (DARPA, 1981) that in a proper environment the first cycle could give better results than does "max" phase.
- [6] The scale depth for Konystan explosions is 146 ± 1 meters, and the depth of burial [DOB] is roughly proportional to the quartic root of the yield, rather than the cubic root as frequently cited at NTS. This empirical scaling rule is applicable to Shagan River region, but not Degelen Mountain. For Konystan and Shagan regions, the yields estimated using depth scaling have accuracy comparable to those using m_b .

Accession For	
NTIS	GRAND
DTIC	1
Unpublished	1
Justified	1

TABLE OF CONTENTS

	Page
DD Form 1473	i
Executive Summary	iii
Table of Contents	v
List of Tables	vi
Section I. Maximum-Likelihood m_b :Yield Regression with Censored Data	
I.0 Abstract	1
I.1 Introduction	1
I.2 Maximum-Likelihood Yield Estimator	4
I.3 Illustrative Examples	7
I.4 Discussion and conclusions	14
I.5 Acknowledgements	15
I.6 References	16
Section II. Magnitude:Yield Relationship at Various Test Sites	
II.1 Summary	21
II.2 NTS	23
II.3 U.S. and French Sahara Shots in Granite	29
II.4 Eastern Kazakhstan Area	31
II.5 Shagan River Test Site	34
II.6 Degelen Mountain	41
II.7 Konystan (Murzhik) Area	49
II.8 Cratering Versus Non-cratering Explosions	52
II.9 Test Site Bias	54
II.10 Acknowledgements	58
II.11 References	59
Appendix. Geotech's Maximum-Likelihood Network m_b : GLM90A	63
Distribution List	

A-1



LIST OF TABLES

Table No.	Title	Page
I.1	Estimated Yield of French and U.S. Explosions in Granite	9
I.2	Comparison of Yield Estimate of 3 Granite Shots	10
I.3	Explosions at Shagan River Area with Announced Yield	11
I.4	Comparison of NTS Yield Estimates	13
II.2A	m_b :Yield Relation of NTS High-Coupling Shots	23
II.2B	Maximum-Likelihood Yield Estimates of NTS Shots	25
II.2C	Expected Magnitude of NTS High-Coupling Explosions	27
II.2D	Expected Yields of NTS High-Coupling Explosions	28
II.3A	m_b :Yield Relation of Sahara and NTS Events in Granite	29
II.3B	Yield Estimates of French & U.S. Shots in Granite	30
II.3C	Expected m_b of U.S. and French Shots in Granite	30
II.4A	m_b :Yield Calibration Curve at Eastern Kazakhstan	31
II.4B	Least-Squares Yield Estimates of E. Kazakh Shots	32
II.4C	Maximum-Likelihood Yield Estimates of E. Kazakh Shots	33
II.4D	Expected m_b of Eastern Kazakhstan Explosions	34
II.5A	Nuclear Explosions at Shagan River Region	34
II.5B	Reported m_b of Shagan River Explosions	35
II.5C	Magnitude:Yield Calibration Curve at Shagan River Area	36
II.5D	Maximum-Likelihood Yield Estimates of Shagan Explosions	38
II.5E	Expected Magnitudes of Shagan Explosions	39
II.5F	m_b Versus $m_b(RMS L_g)$ for Shagan Explosions	40
II.6A	Nuclear Explosions at Degelen Mountainous Region	41
II.6B	Reported m_b Of Degelen Mountain Explosions	44
II.6C	m_b :Yield Calibration Curve at Degelen Mountain	47
II.6D	Expected m_b of Degelen Mountain Explosions	48
II.7A	Explosions from Konystan (Murzhik) Region	49
II.7B	m_b :Yield Calibration Curve at Konystan Area	50
II.7C	Yield Estimates of Konystan Explosions	51
II.7D	Expected m_b and DOB of Konystan Explosions	51
II.8A	Expected $m_b(P_{max}) - m_b(P_a)$ at Four Test Sites	52
II.8B	Expected $m_b(P_b) - m_b(P_a)$ at Four Test Sites	52
II.9A	Expected $m_b(P) - m_b(L_g)$ at Various Test Sites	54
II.9B	Expected Test Site Bias	55
A1	Geotech's Maximum-Likelihood Network m_b : GLM90A	64
A2	WWSSN Station Corrections	69

SECTION I

MAXIMUM-LIKELIHOOD MAGNITUDE:YIELD REGRESSION WITH CENSORED INFORMATION

Rong-Song Jih, D. Wilmer Rivers, Jr.

Robert H. Shumway

Teledyne Geotech Alexandria Laboratories
314 Montgomery Street
Alexandria, VA 22314-1581

Division of Statistics
University of California
Davis, CA 95616

1.0 ABSTRACT

Officially announced yields of underground nuclear explosions are often truncated or incomplete. So far such censored information has not been fully utilized in the determination of m_b :yield calibration curves. In this study, we present a maximum-likelihood regression scheme which takes all the censored yields into account to refine the empirical m_b :yield relationship. Preliminary applications of this scheme to the explosions from several test sites of different geology show that it is a superior procedure, as compared to the conventional least-squares approach. A joint and direct inversion reveals that the m_b bias between Eastern Kazakhstan, U.S.S.R., and Nevada Test Site, U.S., is about 0.40 and 0.44 at 10KT and 100KT, respectively. The same algorithm can be applied to other magnitude measurements such as M_S , P_{coda} , $m_b(L_g)$, M_o and RMS L_g values *etc.*

1.1 INTRODUCTION

Conventional methods for estimating underground explosion yields from seismic recordings are based on the use of some appropriate "magnitude:yield" relationship. One of the most important parameters used to characterize the seismic signature of an underground explosion is the body-wave magnitude, m_b . Thus obtaining an unbiased measurement of m_b (or similarly M_S , P_{coda} , $m_b(L_g)$, M_o , or RMS L_g values *etc.*) is obviously a key step in estimating the yield. There are already many publications which describe different procedures to infer better estimates of m_b : *e.g.*, Douglas (1966), von Seggern (1973), Ringdal (1976), von Seggern and Rivers (1978), Christoffersson and Ringdal (1981), Blandford and Shumway (1982), Blandford *et al.* (1983), Lilwall (1986), McLaughlin *et al.* (1988b), Lilwall *et al.* (1988), and most recently, Jih and Shumway (1989). During the past decade, the m_b which is

m_b :Yield Regression with Censored Data

averaged over a well-distributed global network and which incorporates the maximum-likelihood technique into the inversion scheme has become widely accepted as a means to obtain m_b estimates that avoid bias due to the detection threshold characteristics of individual network stations.

Officially announced yields of underground nuclear explosions are often truncated or incomplete. In general there are four types of announced yields available:

- [0] W is known as y_0 KT (*e.g.*, the Pahute Mesa event KNICKERBOCKER [5/26/67] had a yield of 71KT).
- [1] W is left censored, *i.e.*, the exact value of W is known only to be less than a certain level t_1 (*e.g.*, the Konystan, U.S.S.R., event on [8/26/72] had a yield less than 20KT).
- [2] W is right censored, *i.e.*, the exact value of W is known only to be larger than a certain level t_2 (*e.g.*, the Pahute Mesa event HANDLEY [3/26/70] had a yield slightly larger than 1000KT), and
- [3] W is known only to lie between two bounds, t_a and t_b (*e.g.*, the Yucca Flat event FLASK [5/26/70] had a yield between 20 and 200KT).

Observations of types 1 through 3 are censored. Regression with right-censored data is an important topic in survival analysis as well as in quality control (Schmee and Hahn, 1979; Aitkin, 1981; and many others), while some biochemical and environmental studies involving the monitoring of toxic material or water quality have inevitably led to the analysis of left-censored data (*e.g.*, Gleit, 1985; Shumway *et al.*, 1989; and many others). Both left-censored and right-censored station recordings due to the ambient noise and signal clipping are crucial in the estimation of network m_b (Ringdal, 1976; von Seggern and Rivers, 1978; Blandford and Shumway, 1982; Jih and Shumway, 1989). For yield determination, likewise, neglecting any of the three aforementioned censoring patterns could cause serious bias, not to mention the waste of useful information. For instance, recently Soviet seismologists (Bocharov *et al.*, 1989) have published descriptions of 96 nuclear explosions conducted from 1961 through 1972 at the Semipalatinsk Test Site, in Eastern Kazakhstan (Vergino, 1989). With the exception of releasing news about their "peaceful nuclear explosions" [PNE] (Nurdyke, 1974), the Soviets have never before published such a body of information. However, out of the 72 Degelen events with announced yields, only 9 events or 12.5% were of type 0. The remaining were either left censored (66.7%) or bounded (20.8%). The U.S. announced yields (Springer and Kinaman, 1971 and 1975) reflect a very similar heavy-censoring pattern. Although many authors have approached the subject of determining yield from m_b or other magnitude measures in a systematic way (*e.g.*, Evernden, 1967; Ericsson, 1971a, 1971b; Springer and Hannon, 1973; von Seggern, 1977; Dahlman and Israelson, 1977; Marshall *et al.*, 1979; Nuttli, 1986a, 1986b, 1988; Heasler *et al.*, 1988; *etc.*), the huge amount of censored information has never been fully utilized in the determination of m_b :yield calibration curves.

m_b :Yield Regression with Censored Data

In this study, we present a maximum-likelihood regression scheme which takes all the censored yields into account to refine the estimated m_b :yield relationship. This regression routine is very similar to the maximum-likelihood estimator used in computing the optimal network m_b values based on the censored station amplitude measurements due to clipping and to non-detection. In the non-censored case, it gives identical results as that derived by the standard least-squares method. The same algorithm can be applied to other magnitude measurements such as M_S , P_{coda} , $m_b(L_g)$, M_o and RMS L_g values *etc.*

1.2 MAXIMUM-LIKELIHOOD YIELD ESTIMATOR

The problem of estimating the yield of an explosion from the seismic magnitude has been handled traditionally using the linear model

$$X = \alpha + \beta \log(W) + v = \alpha + \beta Y + v \quad [1]$$

where X is the measured magnitude, m_b , α and β are intercept and slope estimators, W is the yield in kiloton [KT], and v is an error term. v is assumed to be a Gaussian random variable with mean zero and standard deviation σ . The linear or piecewise-linear relationship between the $\log(\text{yield})$ and the $\log(\text{amplitude})$ is based on both observational study and theoretical prediction (e.g., Mueller and Murphy, 1971; von Seggern and Blandford, 1972; Murphy, 1977).

One may then collect a number of "calibration events", estimating α and β by least squares using a number of known yields and measured magnitudes. This classical calibration approach leads to predicting a future $\log\text{-yield}$ Y at $m_b = \hat{X}$ by inverting equation [1], i.e.,

$$\hat{Y} = \frac{\hat{X} - \hat{\alpha}}{\hat{\beta}} \quad [2]$$

The geometrical interpretation of "regressing X on Y " is that the $(\hat{\alpha}, \hat{\beta})$ thus estimated would be the optimal solution that minimizes the sum of the squared magnitude residuals, $\sum (X - \hat{\alpha} - \hat{\beta}Y)^2$ (and hence the name of " m -regression"). Implicitly, an assumption is been made that the independent variable Y has nearly perfect accuracy and precision as compared to X .

Alternately, one can estimate κ and λ in the inverse regression model

$$Y \equiv \log(W) = \kappa + \lambda X + v' \quad [3]$$

and then predict a future \log yield directly as

$$\hat{Y} = \hat{\kappa} + \hat{\lambda} \hat{X} \quad [4]$$

Likewise, this so-called " Y -regression" approach implicitly assumes that X has perfect accuracy and precision. The optimal estimates $(\hat{\kappa}, \hat{\lambda})$ are the ones that would minimize the sum of the squared \log yield residuals, $\sum (Y - \hat{\kappa} - \hat{\lambda}X)^2$. Thus either the yield or the magnitude must be regarded as error-free independent variable in these two models. In reality, both the m_b and the yield measurements are subject to error. At NTS, where the yields can be measured using the radiochemical method with a precision better than that of the seismic method, $\sigma(m_b) \gg \sigma(\log \text{ yield})$ could be a reasonable assumption. This may not be the case in general, however. Note that [3] can be rewritten in a form similar to [1]:

$$X = \alpha + \beta Y + v'' \quad [3']$$

with the transformations $\alpha = -\kappa/\lambda$, $\beta = 1/\lambda$.

m_b : Yield Regression with Censored Data

Now suppose there are n_0 , n_1 , n_2 , and n_3 events for each type, respectively. We will derive the maximum-likelihood formulation for Y -regression model first (Equations [3] and [3']). The conditional likelihood function of the censored observations (y_0 , t_1 , t_2 , t_a , t_b) given the intercept α , slope β , and the standard deviation σ of error in log yield is

$$L(y_0, t_1, t_2, t_a, t_b | \alpha, \beta, \sigma) = \prod_{j=1}^{n_0} P(Y_j = y_{0j} | \alpha, \beta, \sigma) * \prod_{j=1}^{n_1} P(Y_j < t_{1j} | \alpha, \beta, \sigma) * \prod_{j=1}^{n_2} P(Y_j > t_{2j} | \alpha, \beta, \sigma) * \prod_{j=1}^{n_3} P(t_{aj} < Y_j < t_{bj} | \alpha, \beta, \sigma) \quad [5]$$

and the log-likelihood function is

$$\ln L(y_0, t_1, t_2, t_a, t_b | \alpha, \beta, \sigma) = -\frac{n_0}{2} \ln(2\pi\sigma^2) - \frac{1}{2\sigma^2} \sum_{j=1}^{n_0} (y_{0j} - \frac{x_{0j} - \alpha}{\beta})^2 + \sum_{j=1}^{n_1} \ln \Phi(z_{1j}) + \sum_{j=1}^{n_2} \ln \Phi(-z_{2j}) + \sum_{j=1}^{n_3} \ln [\Phi(z_{bj}) - \Phi(z_{aj})] \quad [6]$$

where x the seismic magnitudes; $z_i \equiv \frac{\alpha + \beta t_i - x_i}{\beta\sigma}$ for $i = 1j, 2j, aj$, and bj ; $\phi(u) \equiv \frac{1}{\sqrt{2\pi}} \exp(-\frac{u^2}{2})$ and $\Phi(u) \equiv \int_{-\infty}^u \phi(x)dx$ are the probability density function [p.d.f.] and the cumulative distribution function [c.d.f.] of the standard normal $N(0,1)$, respectively; and y_0 , t_1 , t_2 , t_a , and t_b are the collection of announced yields. The specific form of the rightmost term in equation [6] reveals the necessity of treating the type 3 censored data as a separate class rather than considering each of type 3 event as two separate events of type 1 and 2.

Solving $\frac{\partial \ln L}{\partial \sigma} \equiv 0$ implies immediately that the maximum-likelihood solution of σ must satisfy the following necessary condition:

$$\sigma(\log \text{yield})^2 = \frac{\sum_{j=1}^{n_0} (y_{0j} - \frac{x_{0j} - \alpha}{\beta})^2}{n_0 + \sum_{j=1}^{n_1} \frac{\phi(z_{1j})}{\Phi(z_{1j})} z_{1j} - \sum_{j=1}^{n_2} \frac{\phi(z_{2j})}{\Phi(-z_{2j})} z_{2j} + \sum_{j=1}^{n_3} \frac{\phi(z_{bj})z_{bj} - \phi(z_{aj})z_{aj}}{\Phi(z_{bj}) - \Phi(z_{aj})}} \quad [7]$$

(α, β, σ) can be solved iteratively with the Expectation Maximization (EM) algorithm (Dempster *et al.*, 1977) as follows:

- Initialization Step:

Infer the initial guess of the unknown parameters, (α, β, σ) , from the standard regression with the type 0 data alone.

m_b : Yield Regression with Censored Data

- E Step:

Replace the censored yields by their conditional expectations based on the current estimate of the parameters.

- M Step:

Recompute σ with [7] and update α and β by regressing with the refined pseudo observations computed in the E step. Then repeat steps E and M until α , β , and σ converge.

Dempster *et al.* (1977) proved that such iterative procedure guarantees the monotonic increase of the likelihood function of the new estimate, which in turn guarantees the convergence of the whole procedure since the log-likelihood function defined in [6] is bounded above, say, by 0.

The following prerequisite mathematics are used in the E step. Let X be an arbitrary Gaussian random variable with mean μ and variance σ^2 , p.d.f. g , c.d.f. G , then

- $E(X | X < a) = \mu - \sigma^2 g(a)/G(a)$,
- $E(X | X > a) = \mu + \sigma^2 g(a)/G(-a)$,
- $E(X | a < X < b) = \mu - \sigma^2 [g(b) - g(a)]/[G(b) - G(a)]$.

The calculation of $g(x)$ and $G(x)$ can be accomplished easily by the following transformations: $g(x) = \phi(\frac{x-\mu}{\sigma})/\sigma$, $G(x) = \Phi(\frac{x-\mu}{\sigma})$, as was done in Equations [6]-[7].

If we regress the magnitudes on the log yields, Equation [7] becomes

$$\sigma(m_b)^2 = \frac{\sum_{j=1}^{n_0} (\alpha + \beta y_{0j} - x_{0j})^2}{n_0 + \sum_{j=1}^{n_1} \frac{\phi(z_{1j})}{\Phi(z_{1j})} z_{1j} - \sum_{j=1}^{n_2} \frac{\phi(z_{2j})}{\Phi(-z_{2j})} z_{2j} + \sum_{j=1}^{n_3} \frac{\phi(z_{bj})z_{bj} - \phi(z_{aj})z_{aj}}{\Phi(z_{bj}) - \Phi(z_{aj})}} \quad [8]$$

where $z_i \equiv \frac{\alpha + \beta t_i - x_i}{\sigma}$ for $i = 1j, 2j, aj$, and bj .

Essentially the same procedure can be used for both the m - and Y -regression models. The major difference in the M step is whether we regress Y on X (and then transform κ and λ to α and β) or regress X on Y to estimate α and β directly. The other minor difference is in the calculation of σ and z . The σ in [7] represents the standard deviation of the residual log yield, while the σ in [8] is actually that for the residual magnitude. For the m -regression model, $\sigma(m_b)$ in [8] is frequently used as a measure of goodness of fit. If the Y -regression model is used, $\sigma(m_b)$ can be computed as $\sigma(\log \text{ yield}) \cdot \beta$. The 2σ uncertainty factor in yield is defined as $10^{(2\sigma/\beta)}$ and $10^{(2\sigma)}$ for the m - and Y -regression models, respectively. Recently the m -regression model has been given greater attention in the nuclear monitoring study, and hence examples and discussions in the subsequent sections will be limited to the m -regression model for brevity. If $n_1 = n_2 = n_3 = 0$, then both algorithms presented here

reduce to the standard least-squares method, and σ in [7] and [8] becomes the simple RMS residuals in the usual sense.

1.3 ILLUSTRATIVE EXAMPLES

During the past several years, WWSSN (World-Wide Standard Seismograph Network) m_b database measured at Teledyne Geotech (TG) has been gradually expanded to 124 events, totaling 366 usable "a", "b", and "max" event phases (Blandford and Shumway, 1982; Blandford *et al.*, 1983; McLaughlin *et al.*, 1988b; Jih and Shumway, 1989; Jih *et al.*, 1990a; 1990b). We have applied the maximum-likelihood network m_b estimator, GLM [General Linear Model] (Blandford and Shumway, 1982), to the complete data set consisting of 15,288 teleseismic magnitude measurements in the distance range from 20 degrees to 95 degrees at 127 stations to determine our best m_b values to date, which we denote as $m_b(TG)$. The $m_b(P_{max},TG)$ and $m_b(P_b,TG)$ of the events from the same test site are then fed to the maximum-likelihood m_b :yield regression scheme we just proposed to derive the optimal calibration curve. The resulting calibration curves are summarized as follow:

- (#1) $m_b(P_{max},TG) = 3.747[\pm 0.075] + 0.857[\pm 0.034] \log(W)$ for NTS shots in high-coupling media; $\sigma = 0.091$; 95% confidence factor = 1.630; *i.e.*, we are 95% confident that the actual yield lies in the range from $Y_{est}/1.630$ to $Y_{est} \cdot 1.630$. In this regression $(n_0, n_1, n_2, n_3) = (9, 2, 1, 2)$.¹
- (#2) $m_b(P_b,TG) = 3.484[\pm 0.089] + 0.866[\pm 0.040] \log(W)$ for NTS shots in high-coupling media; $\sigma = 0.108$; 95% confidence factor = 1.775. $(n_0, n_1, n_2, n_3) = (9, 2, 1, 2)$.
- (#3) $m_b(P_{max},TG) = 3.659[\pm 0.022] + 1.008[\pm 0.018] \log(W)$ for Sahara and NTS shots in granite; $\sigma = 0.032$; 95% confidence factor = 1.157; $(n_0, n_1, n_2, n_3) = (4, 6, 1, 0)$ (*cf.* Table 1).
- (#4) $m_b(P_b,TG) = 3.348[\pm 0.028] + 1.040[\pm 0.022] \log(W)$ for Sahara and NTS shots in granite; $\sigma = 0.037$; 95% confidence factor = 1.178; $(n_0, n_1, n_2, n_3) = (4, 6, 1, 0)$ (*cf.* Table 1).
- (#5) $m_b(P_{max},TG) = 4.110[\pm 0.062] + 0.892[\pm 0.039] \log(W)$ at Eastern Kazakhstan; $\sigma = 0.093$; 95% confidence factor = 1.617. $(n_0, n_1, n_2, n_3) = (13, 3, 0, 5)$.
- (#6) $m_b(P_b,TG) = 3.837[\pm 0.059] + 0.924[\pm 0.037] \log(W)$ at Eastern Kazakhstan; $\sigma = 0.091$; 95% confidence factor = 1.571. $(n_0, n_1, n_2, n_3) = (13, 3, 0, 5)$.

Although the formulae (#1) through (#6) are preliminary, there are a few observations worth noting. First, the slope in (#1) matches Murphy's (1977) theoretical prediction, 0.85,

¹9 events of type 0: BILBY, SHOAL, HANDCAR, REX, CHARTREUSE, PILEDRIIVER, SCOTCH, BOXCAR, and BENHAM; 2 events of type 1: ALMENDRO and MAST; 1 event of type 2: HANDLEY; 2 events of type 3: CORDUROV and NASH. See Appendix (page 64) for the m_b values.

m_b :Yield Regression with Censored Data

rather well. Secondly, putting the representative explosions from various test sites recorded at a global network (such as WWSSN) into a single GLM inversion not only yields a consistent set of station corrections for global use, but it also provides a **direct** estimate of the m_b bias between any two test sites of interest. For instance, the m_b bias between Eastern Kazakhstan and NTS can be estimated easily from (#1) and (#5) as 0.40 and 0.436 magnitude unit at 10KT and 100KT, respectively. This value is very close to that based on some indirect methods using P_n velocity or surface waves (Evernden and Marsh, 1987), and slightly larger than that in Der *et al.* (1985) and Stewart (1988). It includes the combined effects of the net bias due to the clustering of stations on the focal sphere (McLaughlin, 1988) as well as the difference of Q, coupling, and pP interferences between two test sites.

In deriving (#3) and (#4), we have supplemented the French explosions in Hoggar Massif, south Algeria, with U.S. shots PILEDRIIVER and SHOAL detonated at Climax Stock, Nevada. The French Test Site is in the volcanic terrain, apparently in an incipient rift zone (Duclaux and Michaud, 1970; Schock *et al.*, 1972; Faure, 1972). The \bar{t} of Hoggar Massif as estimated by Der *et al.* (1985) is 0.35 sec, which shows no significant difference in the attenuation from that of NTS (McLaughlin *et al.*, 1988a). There exists fair agreement between U.S. and French granite shots in the yield-scaled peak values of acceleration, velocity, and displacement (Heuze, 1983). On the other hand, although the Semipalatinsk Test Site of U.S.S.R. has hard-rock geology as well, it is inappropriate to include the Soviet events in the same regression with French explosions unless care is taken in advance to correct for the test site bias. Table 1 lists the regression results using the least-squares (LS) and the maximum-likelihood estimator (MLE) along with the announced yields of U.S. and French tests in granite taken from Bolt (1976) and Stimpson (1988). The yield estimates in column "MLE" of Table 1 are predicted by formulae (#3) and (#4), respectively. Although the network m_b values we use are not corrected for the pP interference as suggested in Marshall *et al.* (1979), they fit the theoretical scaling rather well. The slope of the m_b :yield curve for this region is nearly 1 for these low-yield tests, consistent with an earlier study by Blandford and Shumway (1982) using fewer events. Because of the nearly ideal fit, the MLE changes the yields only slightly as estimated by the standard least squares method in this particular case.

m_b :Yield Regression with Censored Data

Table 1. Estimated Yield of French and U.S. Explosions in Granite

Event	Announced	$m_b(P_{\max}, TG)$	LS	MLE	$m_b(P_b, TG)$	LS	MLE
	[KT]		[KT]	[KT]		[KT]	[KT]
BERYL	>20.0	4.986	20.6	20.8	4.779	23.8	23.8
CORUNDON	<20.0	4.214	3.5	3.6	3.900	3.4	3.4
EMERAUDE	<20.0	4.569	7.9	8.0	4.263	7.6	7.6
GRENAT	<20.0	4.766	12.4	12.6	4.497	12.7	12.7
OPALE	<20.0	3.894	1.7	1.7	3.853	3.1	3.1
RUBIS	52.0	5.432	57.2	57.5	5.170	56.4	56.5
SAPHIR	120.0	5.720	110.7	111.1	5.468	109.2	109.2
TOURMALINE	<20.0	4.646	9.4	9.5	4.429	10.9	11.0
TURQUOISE	<20.0	4.223	3.6	3.6	3.942	3.7	3.7
SHOAL	12.2	4.739	11.7	11.8	4.455	11.6	11.6
PILEDRIIVER	56.0	5.436	57.7	58.0	5.195	59.7	59.7

We have also derived the maximum-likelihood calibration curves using Nuttli's (1986a) $m_b(L_g)$ as well as Marshall's (1988) m_b values for NTS:

(#7) Marshall's $m_b = 3.892[\pm 0.105] + 0.833[\pm 0.049] \log(W)$ for high-coupling material at NTS; $\sigma = 0.186$; 95% confidence factor = 2.799. Note that the mean slope, 0.833, is very close to that in (#1). $(n_0, n_1, n_2, n_3) = (19, 13, 1, 27)$.

(#8) Nuttli's $m_b(L_g) = 4.402[\pm 0.038] + 0.730[\pm 0.018] \log(W)$ for high-coupling material at NTS; $\sigma = 0.086$; 95% confidence factor = 1.717. $(n_0, n_1, n_2, n_3) = (22, 14, 1, 30)$.

(#9) Nuttli's $m_b(L_g) = 4.020[\pm 0.038] + 0.841[\pm 0.032] \log(W)$ for low-coupling material at NTS; $\sigma = 0.170$; 95% confidence factor = 2.536. $(n_0, n_1, n_2, n_3) = (14, 41, 0, 24)$.

To illustrate the robustness of the present approach, we have tabulated below (Table 2) the best yield estimate of several often analyzed nuclear tests in hard rock computed using our formulae based on Marshall's, Nuttli's, and our magnitudes.

m_b :Yield Regression with Censored Data

Table 2. Comparison of Yield Estimate of 3 Granite Shots			
Events	RUBIS	SAPHIR	Kazakhstan 01/15/65
Announced Yield	52KT	120KT	100-150KT
Nordyke ^{*1}	—	—	125KT
Dahlman and Israelson ^{*2}	—	—	110KT
Marshall <i>et al.</i> ^{*3}	45.4KT [$m_Q=5.97$]	91.6KT [$m_Q=6.29$]	68.9KT [$m_Q=6.16$]
Nuttli ^{*4} $m_b(L_g)$, Quadratic Fit Nuttli ^{*5} $m_b(L_g)$, Linear Fit	68KT 70KT [$m_b(L_g)=5.72$]	110KT 117KT [$m_b(L_g)=5.89$]	103KT 109KT [$m_b(L_g)=5.87$]
Stimpson ^{*6}	68KT [$m_b=5.49$]	127KT [$m_b=5.70$]	—
This Study, $m_b(P_{max},TG)$	57.5KT [$m_b(P_{max})=5.432$]	111.1KT [$m_b(P_{max})=5.720$]	96.7KT [$m_b(P_{max})=5.882$]
This Study, $m_b(P_b,TG)$	56.5KT [$m_b(P_b)=5.170$]	109.2KT [$m_b(P_b)=5.468$]	112.9KT [$m_b(P_b)=5.735$]

*1) Nordyke (1974): based on the crater size.

*2) Dahlman and Israelson (1977): slope = 0.74.

*3) Marshall *et al.* (1979): $m_Q = 4.23[\pm 0.15] + 1.05[\pm 0.06] \log(W)$ for salt and granite

*4) Nuttli (1986a, b): $m_b(L_g) = 3.943 + 1.124 \log(W) - 0.0829 (\log(W))^2$ for $5.2 < m_b(L_g) < 6.7$

*5) Nuttli (1986a, b): $m_b(L_g) = 4.307 + 0.765 \log(W)$ for $5.2 < m_b(L_g) < 6.7$

*6) Stimpson (1988): $m_b = 4.08 + 0.77 \log(W)$ for hard rock

Patton (1988), Ringdal and Marshall (1989), Hansen *et al.* (1989), and Ringdal and Hansen (1989) confirmed that the L_g phase is very promising for use in yield estimation, as originally proposed by Nuttli (1986a, 1986b). Table 2 indicates that the yields estimated by our MLE regression scheme using our m_b measurements have equally good or better accuracy as does $m_b(L_g)$. The improvements over other conventional regression schemes can be attributed to two factors:

- [1] the maximum-likelihood magnitude:yield regression method presented in this study is superior to the conventional least-squares magnitude:yield regression, regardless of what magnitude is used; and
- [2] Geotech's GLM method results in a smaller bias in the network m_b estimates.

To explore the validity of the first claim, we analyzed 7 events with announced yields from the Shagan River Test Site (*i.e.*, Balapan region) as listed in Table 3 using Marshall's

m_b :Yield Regression with Censored Data

(1987) m_b measurements and those of Sykes and Ruggi (1989).

When the standard least-squares (LS) is applied to Marshall's m_b values of the four events with known yields, the predicted yield of event [01/15/65] is 87.9KT. Once the remaining events of censored yields are added into our maximum-likelihood regression, the estimate becomes 92.0KT. If Sykes' m_b values were used instead, the yield estimate would change from 91.2KT (LS) to 94.9KT (MLE). Both cases show an obvious improvement relative to the announced yields by incorporating the censored yields into the regression. Furthermore, such improvement is not an isolated case. Out of 4 events with known yield, 3 events had significantly improved estimates.

Table 3. Explosions at Shagan River Area with Announced Yield							
Date	Lat	Long	Depth	Yield	NEIS	Sykes	Marshall
	[N]	[E]	[m]	[KT]	m_b	m_b	m_b
650115	49.9350	79.0094	178	100-150	6.3	5.905	5.931
680619	49.9803	78.9855	316	<20	5.5	5.350	5.354
691130	49.9243	78.9558	472	125	6.0	5.954	6.048
710630	49.9460	78.9805	217	<20	5.4	5.290	5.027
720210	50.0243	78.8781	295	16	5.5	5.370	5.370
721102	49.9270	78.8173	521	165	6.2	6.181	6.224
721210	50.0270	78.9956	478	140	6.0	5.989	5.996

[from Bocharov *et al.* (1989) and Vergino (1989)]

The maximum-likelihood calibration curves at Shagan River region using m_b values in Table 3 ($(n_0, n_1, n_2, n_3) = (4, 2, 0, 1)$) are listed as follow:

(#10)

Marshall's $m_b = 4.476[\pm 0.090] + 0.741[\pm 0.052] \log(W)$ with 95% confidence factor 1.605 and σ 0.076.

(#11)

Sykes' $m_b = 4.525[\pm 0.096] + 0.698[\pm 0.054] \log(W)$ with 95% confidence factor 1.577 and σ 0.069.

(#12)

NEIS' $m_b = 4.807[\pm 0.164] + 0.614[\pm 0.093] \log(W)$ with 95% confidence factor 2.671 and σ 0.131.

Bocharov *et al.* (1989) and Vergino (1989) also listed the yields of Soviet nuclear explosions in Konystan (Murzhik) and Degelen regions. Using Marshall's m_b measurements, the

m_b :Yield Regression with Censored Data

maximum-likelihood calibration curves are:

(#13)

Marshall's $m_b = 4.535[\pm 0.045] + 0.768[\pm 0.039] \log(W)$ at Konystan; $\sigma = 0.069$; 95% confidence factor = 1.516. $(n_0, n_1, n_2, n_3) = (6, 7, 0, 1)$.

(#14)

Marshall's $m_b = 4.370[\pm 0.020] + 0.869[\pm 0.017] \log(W)$ at Degelen with $\sigma = 0.076$ and 95% confidence factor 1.494. $(n_0, n_1, n_2, n_3) = (9, 46, 0, 15)$.

It remains to examine the second claim we made earlier, namely that the m_b values computed with Geotech's GLM method are better than those computed with other methods. We have separately regressed Marshall's (1988) and our m_b on the announced yields of the high-coupling shots detonated at NTS, using the same maximum-likelihood regression scheme. The results in Table 4 clearly indicate that for each event in common, our predicted yield is systematically closer to the announced yield than that based on Marshall's m_b values. About half of Geotech's NTS events in common with Nuttli's have the announced yields closer to the predictions based on our formula derived with Nuttli's $m_b(L_g)$, in accordance with Nuttli's claim that $m_b(L_g)$ could provide yield estimates as good as those based on the "good" m_b .

m_b :Yield Regression with Censored Data

Table 4. Comparison of NTS Yield Estimates					
Date	Event Code	Announced W	Estimated W		
		[KT]	$m_b(L_g)$	$m_b(\text{Marshall})$	$m_b(P_{\max}, \text{TG})$
621005	MISSISSIPPI	110	87.8	—	—
630913	BILBY	235	205.8	—	171.5
631026	SHOAL	12.2	12.0	—	14.4
641105	HANDCAR	12	7.3	7.5	10.7
660224	REX	16	16.0	8.3	13.7
660414	DURYEA	65	53.0	28.0	—
660506	CHARTREUSE	70	72.6	44.6	56.5
660527	DISCUSTHROWER	21	14.5	11.9	—
660602	PILEDRIIVER	56	93.5	113.9	93.7
660630	HALFBEAK	300	351.9	412.1	—
661220	GREELEY	825	727.2	644.9	—
670520	COMMODORE	250	175.7	229.3	—
670523	SCOTCH	150	199.4	131.5	146
670526	KNICKERBOCKER	71	70.4	51.5	—
680426	BOXCAR	1200	1096	825	1293
681219	BENHAM	1100	1205	899	1122
691029	CALABASH	110	106.1	113.0	—
700526b	FLASK	105	99.6	98.9	—
701217	CARPETBAG	220	240.9	183.3	—
701218	BANE BERRY	10	12.8	21.9	—
710708	MINIATA	80	124.2	82.4	—
730426	STARWORT	85	96.5	100.0	—
# of Events			22+14+1+30	19+13+1+27	9+2+1+2
$\hat{\sigma}_{MLE}(m_b)$			0.086	0.186	0.091
2σ Factor			1.717	2.799	1.630

$\hat{W}(m_b(L_g))$ estimated with the formula #8.

$\hat{W}(m_b, \text{Marshall})$ estimated with the formula #7.

$\hat{W}(m_b, \text{TG})$ estimated with the formula #1.

m_b :Yield Regression with Censored Data

Patton (1988) repeated Nuttli's (1986a) procedure to estimate the yields of 69 NTS high-coupling shots recorded at LLNL's high-quality digital network. Based on his regression result, the predicted $m_b(L_g)$ at explosive yields of 10, 50, 100, 150KT are 5.159, 5.687, 5.914, and 6.047, respectively. Nuttli's (1986a) original regression with 22 NTS shots recorded at WWSSN stations gave 5.072, 5.607, 5.837, and 5.972, respectively (*cf.* formula *5 in Table 2). Our formula (#8), which is based on Nuttli's (1986a) $m_b(L_g)$ measurements exclusively, gives 5.132, 5.642, 5.861, and 5.990 at 10, 50, 100, and 150KT, respectively. It is obvious that our maximum-likelihood scheme gives $m_b(L_g)$ estimates closer to Patton's results at all levels of explosive yield. In other words, including the censored information in the regression as proposed in this study does improve the determination of the calibration curve, regardless of what type of magnitude is used.

1.4 DISCUSSION AND CONCLUSIONS

Officially announced yields of underground nuclear explosions are often truncated or incomplete. In this study, we have presented a maximum-likelihood regression scheme which takes all the censored yields into account to refine the estimated m_b :yield relationship with an attempt to make the maximum use of the available data. Preliminary applications of this scheme to events from several test sites of different geology show that it is indeed a superior procedure, as compared to the conventional least-squares approach. The same algorithm can be applied to other magnitude measurements such as M_S , $m_b(L_g)$ or RMS L_g values *etc.*

Nuttli's L_g work (1986a, 1986b) proposed that careful analysis of L_g peak amplitude data from explosions could produce yield estimates nearly as accurate as the best teleseismic estimates. Based on the assumption that his $m_b(L_g)$:yield formulae are site independent, he obtained a m_b bias estimate (relative to NTS) of 0.35 and 0.54 at Shagan River and Degelen Mountain, respectively. The combination of these two values would seem to be consistent with our preliminary m_b bias estimates of 0.40 (10KT) and 0.435 (100KT) based on events from Eastern Kazakhstan including Shagan River and Degelen Mountain.

Our regression with Marshall's (1987) m_b values suggests that there is a m_b bias of 0.112 and 0.150 at Konystan and Degelen, respectively, relative to Shagan River for 100KT shots. At 150KT, the bias becomes 0.117 and 0.173, respectively. Marshall's m_b values generally have better quality than the ISC (International Seismological Centre, Newbury, U.K.) bulletin data which Nuttli (1987) used. Thus combining this m_b (Marshall) bias estimate with Nuttli's $m_b - m_b(L_g)$ offset, 0.23, would imply that there is a $m_b(L_g)$ bias of approximately $0.23 - 0.15 = 0.08$ and $0.23 - 0.173 = 0.057$ at 100KT and 150KT, respectively, between Shagan River and Degelen Mountain. Linear finite-difference calculations by Jih and McLaughlin (1988) and Jih *et al.* (1989) also suggest that there should be observable coupling variations

affecting L_g amplitude. We are currently expanding Geotech's m_b database to investigate such spatial variation among three subregions of Eastern Kazakhstan (Jih *et al.*, 1990a; 1990b). At any rate, our preliminary analysis using Nuttli's $m_b(L_g)$ values tends to suggest that the regionalized calibration curves should provide a better result. For instance, formulae (#8) and (#9) would give a better fit than the formula (*5) in Table 2 for NTS events. In principle, this should be true not just for $m_b(L_g)$ alone. Porting any empirical magnitude:yield calibration curve from one site to another could be unreliable in some cases. The difference between formula (#10) for Shagan River and formula (#14) for Degelen Mountain is an example.

Recent theoretical studies on L_g (Lilwall, 1988; Jih *et al.*, 1989; Frankel, 1989) seem to agree that in a medium where the velocity increases with depth a smaller and smaller focal sphere of pS will be trapped as depth increases, thus decreasing the L_g amplitude. Since the larger shots are buried more deeply, this would imply that in general the slope in $m_b(L_g)$:yield relationship would be less than that in the m_b :yield relationship, as indicated in formulae (#1) through (#9).

Special purpose magnitudes, like m_Q in Marshall *et al.* (1979) which include corrections for source depth and source region attenuation should be, in principle, superior to m_b for estimating the explosive yield. However, the present study has shown that this may not be the case (*cf.* Table 2). The success of the pP and t^* corrections depends on the accuracy of the corrections. In our examples, the network m_b (or, m_2 in Marshall *et al.*, 1979), which were only corrected for the instrument gain, geometrical spreading (Veith and Clawson, 1972) as well as the station terms, would give fairly good yield estimates. Finally, the results in Table 2 seem to indicate that the phase "b" (*i.e.*, the first peak to the first trough) of the teleseismic P wave could give the yield estimate equally well as does the phase "max". However, further investigation is necessary.

1.5 ACKNOWLEDGEMENTS

R.S.J. is indebted to Robert R. Blandford for his insightful discussions throughout the whole course of study. Peter D. Marshall and Paul G. Richards kindly provided Marshall's m_b measurements of U.S. and Soviet explosions, respectively. M. A. Brennan (at CSS) and C. S. Lynnes gave useful suggestions on software development. Geotech's WWSSN SPZ amplitudes were measured by R. A. Wagner, M. Marshall, R. Ahner, and J. A. Burnett under various projects. This research was supported under DARPA contract F19628-89-C-0063 (Task1), monitored by Geophysics Laboratory. The views and conclusions contained in this paper are those of the authors and should not be interpreted as representing the official policies, either expressed or implied, of the Defense Advanced Research Projects Agency or the U.S. Government.

1.6 REFERENCES

- Aitkin, M. (1981). A note on the regression analysis of censored data, *Technometrics*, **23**, 161-163.
- Blandford, R. R., and R. H. Shumway (1982). Magnitude:Yield for nuclear explosions in granite at the Nevada Test Site and Algeria: joint determination with station effects and with data containing clipped and low-amplitude signals, *Report VSC-TR-82-12*, Teledyne Geotech, Alexandria, Virginia.
- Blandford, R. R., R. H. Shumway, R. Wagner, and K. L. McLaughlin (1983). Magnitude:yield for nuclear explosions at several test sites with allowance for effects of truncated data, amplitude correlation between events within test sites, absorption, and pP, *Report TGAL-TR-83-06*, Teledyne Geotech, Alexandria, Virginia.
- Bocharov, V. S., S. A. Zelentsov, and V. Mikhailov (1989). Characteristics of 96 underground nuclear explosions at the Semipalatinsk test site, *Atomic Energy*, **67**, 210-214 (*in Russian*).
- Bolt, B. A. (1976). *Nuclear Explosions And Earthquakes: The Parted Veil*. W. H. Freeman & Company, San Francisco, CA.
- Christofferson, A. and F. Ringdal (1981). Optimum approaches to magnitude measurements, in *Identification of Seismic Sources - Earthquakes or Underground Explosions*, E. S. Husebye and S. Mykkeltveit, Editors, D. Reidel Publishing Co., Dordrecht, Holland.
- Dahlman, O. and H. Israelson (1977). *Monitoring Underground Nuclear Explosions*, Elsevier Scientific Publishing Co., New York.
- Dempster, A. P., N. M. Laird, and D. B. Rubin (1977). Maximum:likelihood estimation from incomplete data via the EM algorithm, *J. Roy. Statist. Soc. B.*, **39**, 1-38.
- Der, Z. A., T. W. McElfresh, R. A. Wagner, and J. Burnett (1985). Errata to "Spectral characteristics of P waves from nuclear explosions and yield estimation", *Bull. Seism. Soc. Am.*, **75**, 1222.
- Douglas, A. (1966). A special purpose least squares programme, *AWRE Report No. O-54/66*, HMSO, London, UK.
- Duclaux, F. and M. L. Michaud (1970), Conditions experimentales des tirs nucleaires souterrains Francais au Sahara, *R. Acad. Sc. Paris*, **270**, Serie B, 189-192.
- Ericsson, U. (1971a). Maximum-likelihood linear fitting when both variables have normal and correlated error, *Report C4474-A1*, Research Institute of National Defense, Stockholm, Sweden.

- Ericsson, U. (1971b). A linear model for the yield dependence of magnitudes measured by a seismographic network, *Geophys. J. R. Astr. Soc.*, **25**, 49-69.
- Evernden, J. F. (1967). Magnitude determination at regional and near-regional distance in the U.S., *Bull. Seism. Soc. Am.*, **57**, 591-639.
- Evernden, J. F. and G. E. Marsh (1987). Yields of U.S. and Soviet nuclear tests, *Physics Today*, **8-1**, 37-44.
- Faure, J. (1972) Recherches sur les effets geologiques d'explosions nucleaires souterraines dans un massif de granite saharien, Centre d'Etudes de Bruyeres-le-Chatel, Commissariat a l'Energie Atomique, *Report CEA-R-4257*, Service de Documentation CEN-SACLAY, B.P. no. 2, 91-GIF-sur-Yvette, France.
- Frankel, A. (1989). Effects of source depth and crustal structure on the spectra of regional phases determined from synthetic seismograms, *Proceedings of AFTAC/DARPA 1989 Seismic Research Review* (28-29 Nov 1989, Patrick AFB, Florida), 97-118.
- Gleit, A. (1985). Estimation for small normal data sets with detection limits, *Env. Sci. Tech.*, **19**, 1206-1213.
- Hansen, R. A., Ringdal, F. and P. G. Richards (1989). Analysis of IRIS data for Soviet nuclear explosions, in *Semiannual Technical Summary*, 1 Oct 1988 - 31 Mar 1989 (L. B. Loughran ed.), *NORSAR Sci. Rep. 2-88/89*, NTN/NORSAR, Kjeller, Norway.
- Heasler, P. G., R. C. Hanlen, D. A. Thurman, and W. L. Nicholson (1988). Application of general linear models to event yield estimation, *Report PNL-CC-1801 171*, Pacific Northwest laboratories of Battelle Memorial Institute, Richland, WA.
- Heuze, F. E. (1983). A review of geomechanics data from French nuclear explosions in the Hoggar granite, with some comparisons to tests in U.S. granite, *LLNL Report UCID-19812*, Lawrence Livermore Laboratory, Livermore, CA.
- Jih, R.-S., C. S. Lynnes, D. W. Rivers, and I. N. Gupta (1989). Simultaneous modeling of teleseismic and near regional phases with linear finite-difference method (*abstract*), *EOS, Trans. A.G.U.*, **70-43**, 1189.
- Jih, R.-S. and K. L. McLaughlin (1988). Investigation of explosion generated SV Lg waves in 2-D heterogeneous crustal models by finite-difference method. *Report AFGL-TR-88-0025 (=TGAL-88-01)*, Teledyne Geotech, Alexandria, VA.
- Jih, R.-S., and R. H. Shumway (1989). Iterative network magnitude estimation and uncertainty assessment with noisy and clipped data, *Bull. Seism. Soc. Am.*, **79**, 1122-1141.
- Jih, R.-S., R. H. Shumway, R. A. Wagners, D. W. Rivers, C. S. Lynnes, and T. W. McElfresh (1990a). Maximum-likelihood magnitude:yield regression with heavily censored data

m_b :Yield Regression with Censored Data

- (preliminary results), (*abstract*), *EOS, Trans. A.G.U.*, **71**.
- Jih, R.-S., R. A. Wagner, and T. W. McElfresh (1990b). Maximum-likelihood m_b :yield calibration curve at various test sites, *Section 2 of Report TGAL-90-03*, Teledyne Geotech, Alexandria, VA.
- Lilwall, R. C. (1986). Some simulation studies on seismic magnitude estimations, *AWRE Report No. O-22/86*, HMSO, London, UK.
- Lilwall, R. C. (1988). Regional $m_b:M_S$, L_g/P_g amplitude ratios and L_g spectral ratios as criteria for distinguishing between earthquakes and explosions: a theoretical study, *Geophys. J.*, **93**, 137-147.
- Lilwall, R. C., P. D. Marshall, and D. W. Rivers (1988). Body wave magnitudes of some underground nuclear explosions at the Nevada (USA) and Shagan River (USSR) Test Sites, *AWE Report O-15/88*, HMSO, London, UK.
- Marshall, P.D. (1987). (Written communication to Paul G. Richards on Nov 11, 1987)
- Marshall, P.D. (1988). (Electronic communication to Teledyne Geotech on Apr 6, 1988)
- Marshall, P. D., O. L. Springer, and H. C. Rodean (1979). Magnitude corrections for attenuation in the upper mantle, *Geophys. J. R. astr. Soc.*, **57**, 609-638.
- McLaughlin, K. L., A. C. Lees, Z. A. Der, and M. E. Marshall (1988a). Teleseismic spectral and temporal M_0 and Ψ_∞ estimates for four French explosions in Southern Sahara, *Bull. Seism. Soc. Am.*, **78**, 1580-1596.
- McLaughlin, K. L., R. H. Shumway, and T. W. McElfresh (1988b). Determination of event magnitudes with correlated data and censoring: a maximum likelihood approach, *Geophys. J.*, **95**, 31-44.
- Mueller, R. A. and J. Murphy (1971). Seismic characteristics of underground nuclear detonations, *Bull. Seism. Soc. Am.*, **61**, 1675-1692.
- Murphy, J. (1977). Seismic source functions and magnitude determinations for underground nuclear detonations, *Bull. Seism. Soc. Am.*, **67**, 135-158.
- Nordyke, M. D. (1973), A review of Soviet data on the peaceful uses of nuclear explosions, *Report UCRL-51414-REV1*, Lawrence Livermore Laboratory, University of California, CA.
- Nuttli, O. W. (1986a). Yield estimates of Nevada Test Site explosions obtained from seismic L_g waves, *J. Geophys. Res.*, **91**, 2137-2151.
- Nuttli, O. W. (1986b). L_g magnitudes of selected East Kazakhstan underground explosions, *Bull. Seism. Soc. Am.*, **76**, 1241-1251.

- Nuttli, O. W. (1987). Lg magnitudes of Degelen, East Kazakhstan, underground explosions, *Bull. Seism. Soc. Am.*, **77**, 679-681.
- Nuttli, O. W. (1988). Lg magnitudes and yield estimates for underground Novaya Zemlya nuclear explosions, *Bull. Seism. Soc. Am.*, **78**, 873-884.
- Patton, H. J. (1988). Application of Nuttli's method to estimate yield of Nevada Test Site explosions recorded on Lawrence Livermore National Laboratory's digital seismic system, *Bull. Seism. Soc. Am.*, **78**, 1759-1772.
- Ringdal, F. (1976). Maximum likelihood estimation of seismic magnitude, *Bull. Seism. Soc. Am.*, **66**, 789-802.
- Ringdal, F. and P. D. Marshall (1989). Yield determination of Soviet underground nuclear explosions at the Shagan River Test Site, Semiannual Technical Summary, 1 Oct 1988 - 31 Mar 1989 (L. B. Loughran ed.), *NORSAR Sci. Rep. 2-88/89*, NTN/NORSAR, Kjeller, Norway.
- Ringdal, F. and R. A. Hansen (1989). NORSAR yield estimation studies, *Proceedings of AFTAC/DARPA 1989 Seismic Research Review* (28-29 Nov 1989, Patrick AFB, Florida), 145-156.
- Schmee, J. and G. J. Hahn (1979). A simple method for regression analysis with censored data, *Technometrics*, **21**, 417-432.
- Schock, R. N., A. E. Abey, H. C. Heard, H. Louis, (1972). Mechanical properties of granite from the Taourirt Tan Afella Massif, Algeria, *LLNL Report UCID-51296*, Lawrence Livermore Laboratory, Livermore, CA.
- Shumway, R. H., A. S. Azari, and P. Johnson (1989). Estimating mean concentrations under transformation for environmental data with detection limits, *Technometrics*, **31**, 347-356.
- Springer, D. L. and W. J. Hannon (1973). Amplitude:yield scaling for underground nuclear explosions, *Bull. Seism. Soc. Am.*, **63**, 477-500.
- Springer, D. L. and R. L. Kinaman (1971). Seismic source summary for U.S. underground nuclear explosions, 1961-1970, *Bull. Seism. Soc. Am.*, **61**, 1073-1098.
- Springer, D. L. and R. L. Kinaman (1975). Seismic source summary for U.S. underground nuclear explosions, 1971-1973, *Bull. Seism. Soc. Am.*, **65**, 343-349.
- Stewart, R. C. (1988). P-wave seismograms from underground explosions at the Shagan River Test Site recorded at 4 arrays, *AWE Report O-4/88*, HMSO, London, UK.
- Stimpson, I. G. (1988). Source parameters of explosions in granite at the French Test Site in Algeria, *AWE Report O-11/88*, HMSO, London, UK.

m_b :Yield Regression with Censored Data

- Sykes, L. R. and S. Ruggi (1989). Soviet nuclear testing, in *Nuclear Weapon Databook (Volume IV, Chapter 10)*, Natural Resources Defense Council, Washington D. C.
- Veith, K. F. and G. E. Clawson (1972). Magnitude from short-period P-wave data, *Bull. Seism. Soc. Am.*, **62**, 435-452.
- Vergino, E. S. (1989). Soviet test yields, *EOS, Trans. A.G.U.*, Nov 28, 1989.
- von Seggern, D. H. (1973). Joint magnitude determination and analysis of variance for explosion magnitude estimates, *Bull. Seism. Soc. Am.*, **63**, 827-845.
- von Seggern, D. H. (1977). Intersite magnitude yield bias exemplified by the underground explosions MILROW, BOXCAR, and HANDLEY, *Report SDAC-TR-77-4*, Teledyne Geotech, Alexandria, VA.
- von Seggern, D. and R. R. Blandford (1972). Source time functions and spectra for underground nuclear explosions, *Geophys. J. R. astr. Soc.*, **31**, 83-97.
- von Seggern, D. and D. W. Rivers (1978). Comments on the use of truncated distribution theory for improved magnitude estimation, *Bull. Seism. Soc. Am.*, **68**, 1543-1546.

SECTION II

MAGNITUDE:YIELD RELATIONSHIP AT VARIOUS TEST SITES

Rong-Song Jih, Robert A. Wagner, and T. W. McElfresh

Teledyne Geotech Alexandria Laboratories
314 Montgomery Street
Alexandria, VA 22314-1581

II.1 SUMMARY

We have conducted a systematic analysis of the magnitude:yield relationship at several test sites using miscellaneous magnitudes. The main tool of this study is a linear-regression scheme "MLE-CY" (Jih *et al.*, 1990a; 1990b) which takes all censored yields (*e.g.*, yield < 20 KT or 100 KT < yield < 150 KT) into account to refine the determination of the calibration curve. The majority of the recently published 96 Soviet explosive yields (Bocharov *et al.*, 1989; Vergino, 1989) and the U.S. announced yields (Springer and Kinaman, 1971, 1975) were heavily truncated or rounded, and hence the maximum-likelihood approach would seem ideal to make full use of the yield information. The regression routine we use is very similar to the maximum-likelihood estimator used in computing the optimal network m_b values based on the censored station amplitude measurements due to clipping and to noise (Blandford and Shumway, 1982; Jih and Shumway, 1989). In the non-censored case, it gives results identical to those derived by the standard least squares, corresponding to the two extreme cases of Ericsson's (1971) curve-fitting method which puts different variances in both the independent and the dependent variables.

In the following sections, we will tabulate the maximum-likelihood m_b :yield calibration curves which symbolically correspond to $\sigma(m_b)/\sigma(Y) = 0$ and ∞ , respectively. Several noteworthy results are summarized here:

- [1] Including the censored yields in the regression does improve the accuracy of the estimates (*cf.* Tables 2C and 2D). In reality, both the magnitude and the yield measurements are subject to error. Pending the determination as to which of the two extreme hypotheses, namely $\sigma(m_b)/\sigma(Y) = 0$ and $\sigma(m_b)/\sigma(Y) = \infty$, is closer to the real situation, we also included the results based on Ericsson's method with various $\sigma(m_b)/\sigma(Y)$. As expected, we can see the smooth transition of estimated parameters (*i.e.*, the slope and the intercept) as $\sigma(m_b)/\sigma(Y)$ varies (*cf.* Tables 2A, 4A, 5C, 6C, and 7B). Thus the censored cases with nontrivial $\sigma(m_b)/\sigma(Y)$ values could be "interpolated". Our maximum-likelihood regression scheme and Ericsson's method represent two different directions in

m_b -Yield Calibration Curves

extending the standard least squares. In the future, Efron's bootstrap (Efron, 1979; Efron and Tibshirani, 1985) or other resampling techniques could be incorporated into Ericsson's curve-fitting routine to estimate the confidence interval.

- [2] For Shagan events, Ringdal's $RMS L_g$ provides the smallest scatter around the calibration curve, provided that low-yield events with $m_b(RMS L_g) < 5.5$ or yield $< 40KT$ (e.g. the explosion on 10 Feb 72) are excluded. Geotech's GLM method (Blandford and Shumway, 1982) gives network m_b values better than almost all other magnitudes based on teleseismic P waves and $\log(\Psi_\infty)$, in terms of both the yield estimation (cf. Tables 2B and 5C) and the m_b scaling against Ringdal's $RMS L_g$ (cf. Tables 5F and 9A). For all five test sites we have compared, m_b measurements reported by ISC and NEIS are biased high systematically at low yields (cf. Tables 2C, 4D, 5E, and 5D).
- [3] A direct estimation of the test site bias (cf. Tables 9A and 9B) suggests that Nuttli's (1987, 1988) Degelen puzzle could be invalid simply because of the relatively poorer quality m_b (ISC) used. Our data indicate that the Shagan River Test Site is more efficient in exciting teleseismic P waves than Degelen Mountain, consistent with our previous modeling study (Jih and McLaughlin, 1988). Also, the test site bias is yield dependent, in agreement with other observational study.
- [4] We present an alternative approach to derive the m_b adjustment converting cratering shots to contained explosions of the same yield (cf. Tables 8A and 8B). The correction derived by this approach seems to match that by the multichannel deconvolution method (Der *et al.*, 1985) rather well.
- [5] Degelen Mountain is the only test site that has a decreasing $\log(P_{max}/P_a)$ and $\log(P_b/P_a)$ with increasing yields (cf. Tables 6D, 8A, and 8B). It is also the only test site for which the phase "a" (i.e., zero-crossing to first peak) shows the smallest scatter around the calibration curve, as compared to the phases "b" (i.e., first peak to first trough) and "max" (i.e., max peak-to-trough or trough-to-peak in the first 5 seconds). Both the mountainous topography (which causes complex pP interference) as well as the testing practice (e.g., the relatively shallow and abnormal shot depths) could be responsible. At Shagan River, the phase "b" has the smallest scatter around the calibration curve (cf. Tables 5C and 5D). These observations confirm the conjecture (DARPA, 1981) that in a proper environment the first cycle could give better results than does "max" phase.
- [6] The scale depth for Konystan explosions is 146 ± 1 meters, and the depth of burial [DOB] is roughly proportional to the quartic root of the yield, rather than the cubic root as frequently cited at NTS (cf. Table 7B). This empirical scaling rule is applicable to Shagan River test site, but not Degelen Mountain. For Konystan and Shagan regions, the yields estimated using depth scaling have accuracy comparable to those using m_b .

m_b -Yield Calibration Curves

II.2 NTS

Table 2A. m_b :Yield Relation of NTS High-Coupling Shots

(Earlier Studies)							
# of Events ¹	Magnitude	$\frac{\sigma(m_b)}{\sigma(Y)}$	Slope	Intercept	$\sigma(m_b)$	2 σ Factor ²	Method
22+0+0+0	Nuttli (1986a)	?	0.765±0.027	4.307±0.067	—	—	LS
69+0+0+0	Patton (1988)	∞	0.755±0.022	4.404±0.048	0.098	1.818	LS
(This Study)							
# of Events	Magnitude	$\frac{\sigma(m_b)}{\sigma(Y)}$	Slope	Intercept	$\sigma(m_b)$	2 σ Factor	Method
22+14+1+30	Nuttli, $m_b(L_g)$	0	0.761±0.033	4.336±0.193	0.116	2.019	MLE-CY
22+14+1+30	Nuttli, $m_b(L_g)$	∞	0.730±0.018	4.402±0.038	0.086	1.717	MLE-CY
19+13+1+29	ISC	0	0.787±0.067	4.006±0.379	0.190	3.036	MLE-CY
19+13+1+29	ISC	∞	0.693±0.035	4.199±0.074	0.136	2.475	MLE-CY
19+13+1+27	Marshall	0	0.982±0.062	3.581±0.351	0.210	2.672	MLE-CY
19+13+1+27	Marshall	∞	0.833±0.049	3.892±0.105	0.186	2.799	MLE-CY
9+2+1+2	TG, P_a	0	0.893±0.088	3.165±0.450	0.204	2.863	MLE-CY
9+2+1+2	TG, P_a	∞	0.835±0.065	3.283±0.147	0.175	2.632	MLE-CY
9+2+1+2	TG, P_b	0	0.887±0.052	3.441±0.279	0.124	1.901	MLE-CY
9+2+1+2	TG, P_b	∞	0.866±0.040	3.484±0.089	0.108	1.775	MLE-CY
9+2+1+2	TG, P_{max}	0	0.872±0.045	3.716±0.253	0.105	1.744	MLE-CY
9+2+1+2	TG, P_{max}	∞	0.857±0.034	3.747±0.075	0.091	1.630	MLE-CY
22+0+0+0	Nuttli, $m_b(L_g)$	0	0.760±0.040	4.340±0.232	0.082	1.646	LS
22+0+0+0	Nuttli, $m_b(L_g)$	0.1	0.759±—	4.342±—	—	—	Ericsson
22+0+0+0	Nuttli, $m_b(L_g)$	1	0.745±—	4.370±—	—	—	Ericsson
22+0+0+0	Nuttli, $m_b(L_g)$	5	0.737±—	4.385±—	—	—	Ericsson
22+0+0+0	Nuttli, $m_b(L_g)$	100	0.737±—	4.386±—	—	—	Ericsson
22+0+0+0	Nuttli, $m_b(L_g)$	∞	0.737±0.029	4.386±0.060	0.081	1.659	LS

1) # of "exact" yields, # of left-censored yields, # of right-censored yields, and # of bounded yields.

2) the multiplicative uncertainty factor in the yield [KT] at 95% confidence level.

m_b -Yield Calibration Curves

Table 2A. m_b :Yield Relation of NTS High-Coupling Shots (Continued)

(This Studies)							
# of Events	Magnitude	$\frac{\sigma(m_b)}{\sigma(Y)}$	Slope	Intercept	$\sigma(m_b)$	2σ Factor	Method
9+0+0+0	TG, P_{\max}	0	0.870±0.052	3.719±0.284	0.098	1.684	LS
9+0+0+0	TG, P_{\max}	0.1	0.869±___	3.720±___	___	___	Ericsson
9+0+0+0	TG, P_{\max}	1	0.860±___	3.738±___	___	___	Ericsson
9+0+0+0	TG, P_{\max}	5	0.854±___	3.750±___	___	___	Ericsson
9+0+0+0	TG, P_{\max}	100	0.854±___	3.751±___	___	___	Ericsson
9+0+0+0	TG, P_{\max}	∞	0.854±0.044	3.751±0.093	0.097	1.692	LS

For purposes of estimating explosion yields, the media are divided into three types: unsaturated material, *e.g.*, alluvium and dry tuff; water-saturated rock; and granite. The U.S. granite shots PILEDRIVER and SHOAL will be discussed in the next section again.

If we ignore the different corner frequencies between events of large and small yields, and put all high-coupling shots in one single regression, then both Geotech's $m_b(P_{\max})$'s and Marshall's m_b give a slope matching Murphy's (1977) theoretical prediction, 0.85, rather well (*cf.* Table 2A).

At NTS, yields estimated from m_b alone have a random uncertainty factor of 1.45 at the 95% confidence (*i.e.*, 2σ) level, provided the best “official” m_b values are used (U.S. Congress/OTA, 1988). None of the magnitudes listed in Table 2A reaches such a precision. However, it is also clear that the m_b based on our P_{\max} is relatively more precise than other unclassified m_b measurements. The phase “a” has much larger variance than the phase “max” at NTS, possibly because of the small amplitudes measured were near the noise.

m_b -Yield Calibration Curves

Table 2B. Maximum-Likelihood Yield Estimates of NTS Shots					
Date	Event Code	Announced W	Estimated W		
		[KT]	$m_b(L_g)$	$m_b(\text{Marshall})$	$m_b(P_{\max}, \text{TG})$
621005	MISSISSIPPI	110	87.8	—	—
630913	BILBY	235	205.8	—	171.5
631026	SHOAL	12.2	12.0	—	14.4
641105	HANDCAR	12	7.3	7.5	10.7
660224	REX	16	16.0	8.3	13.7
660414	DURYEA	65	53.0	28.0	—
660506	CHARTREUSE	70	72.6	44.6	56.5
660527	DISCUSTHROWER	21	14.5	11.9	—
660602	PILEDRIIVER	56	93.5	113.9	93.7
660630	HALFBEAK	300	351.9	412.1	—
661220	GREELEY	825	727.2	644.9	—
670520	COMMODORE	250	175.7	229.3	—
670523	SCOTCH	150	199.4	131.5	146
670526	KNICKERBOCKER	71	70.4	51.5	—
680426	BOXCAR	1200	1096	825	1293
681219	BENHAM	1100	1205	899	1122
691029	CALABASH	110	106.1	113.0	—
700526b	FLASK	105	99.6	98.9	—
701217	CARPETBAG	220	240.9	183.3	—
701218	BANEBERRY	10	12.8	21.9	—
710708	MINIATA	80	124.2	82.4	—
730426	STARWORT	85	96.5	100.0	—
# of Events			22+14+1+30	19+13+1+27	9+2+1+2
$\hat{\sigma}_{\text{MLE}}(m_b)$			0.086	0.186	0.091
2σ Factor			1.717	2.799	1.630
ρ			0.990	0.942	0.994

* ρ : the correlation coefficient between the magnitudes and the log yields.

m_b -Yield Calibration Curves

For each event in common with Marshall's in Table 2B, the yield predicted with Geotech's $m_b(P_{\max})$ is always closer to the announced value than that based on Marshall's m_b values. As noted in Jih *et al.* (1990a), this would strongly suggest that Geotech's m_b values have smaller systematic error, since the same regression methodology was used.

Patton (1988) utilized Nuttli's procedure to estimate the yields for 69 high-coupling shots at NTS. The NTS explosions Patton used were clustered around $m_b(L_g) \approx 5.8$. Beyond that level, the difference in yield estimates between Nuttli's and Patton's predictions are by no means negligible. For $m_b(L_g) \approx 6.0$, they predict the yield to be 163KT (N) and 130KT (P), respectively. At $m_b(L_g) \approx 6.5$, the predictions are 736KT (N) and 597KT (P), respectively.

Since Patton (1988) did not release the individual yields or $m_b(L_g)$ in his paper, we need an alternative approach to make the comparison. The data recorded at LLNL's regional digital network have quality better than those WWSSN film chips which Nuttli (1986a) read. It would seem reasonable to assume that the m_b predicted by Patton's regression is more accurate than Nuttli's. Table 2c below indicates that regressing Nuttli's $m_b(L_g)$ measurements against the censored yields with our maximum-likelihood scheme gives m_b estimates very close to Patton's results at all levels of explosive yield. In other words, including the censored information in the regression as proposed in Jih *et al.* (1990a, 1990b) does improve the determination of the calibration curves, regardless of what magnitude is used.

m_b -Yield Calibration Curves

Table 2C. Expected magnitudes of NTS High-Coupling Explosions					
(Regressing the magnitudes on the yields)					
(Earlier Studies)					
m_b :Y Curve	# of Events	10KT	50KT	100KT	150KT
Nuttli ¹	22+0+0+0	5.072	5.607	5.837	5.972
Patton ²	69+0+0+0	5.159	5.687	5.914	6.047
(This Study)					
m_b :Y Curve	# of Events	10KT	50KT	100KT	150KT
Nuttli ³	22+0+0+0	5.123	5.638	5.860	5.989
Nuttli ⁴	22+14+1+30	5.132	5.642	5.861	5.990
ISC	19+13+1+26	4.892	5.376	5.585	5.707
Marshall	19+13+1+27	4.725	5.307	5.558	5.704
TG, P_a	9+2+1+2	4.118	4.701	4.953	5.100
TG, P_b	9+2+1+2	4.350	4.955	5.216	5.368
TG, P_{max}	9+2+1+2	4.604	5.202	5.460	5.610

- 1) Nuttli (1986a): $m_b(L_g) = 4.307[\pm 0.067] + 0.765[\pm 0.027]\log(W)$ for $5.2 < m_b(L_g) < 6.7$.
- 2) Patton (1988): $m_b(L_g) = 4.404[\pm 0.048] + 0.755[\pm 0.022]\log(W)$ for $4.22 < m_b(L_g) < 6.7$.
- 3) Nuttli's $m_b(L_g)$ values regressed with the least square, $\sigma(m_b)/\sigma(Y) = \infty$ (cf. Table 2A).
- 4) Nuttli's $m_b(L_g)$ values regressed with MLE-CY, $\sigma(m_b)/\sigma(Y) = \infty$ (cf. Table 2A).

Table 2C raises a question as how to evaluate different calibration curves. Apparently the trade off between α and β should be taken into account. Judging on the slope, β , alone could be very misleading. For instance, in comparison with the 2 slopes which we obtained with Nuttli's $m_b(L_g)$ measurements, his original slope is closer to that of Patton's (cf. Table 2A), and yet our formulae actually predict the yields as well as the magnitudes closer to those of Patton's (Tables 2C and 2D).

m_b -Yield Calibration Curves

Table 2D. Expected Yields [KT] of NTS High-Coupling Explosions				
(Earlier Studies)				
m_b :Y Curve	$m_b(L_g)=4.5$	$m_b(L_g)=5.0$	$m_b(L_g)=5.5$	$m_b(L_g)=6.0$
Nuttli ¹	1.8	8.1	36.3	163.3
Patton ²	1.3	6.2	28.3	130.0
(This Study)				
m_b :Y Curve	$m_b(L_g)=4.5$	$m_b(L_g)=5.0$	$m_b(L_g)=5.5$	$m_b(L_g)=6.0$
Nuttli ³	1.4	6.8	32.5	155.1
Nuttli ⁴	1.4	6.6	32.0	154.9
m_b :Y Curve	$m_b=4.5$	$m_b=5.0$	$m_b=5.5$	$m_b=6.0$
Marshall	5.4	21.4	85.2	339.5
TG, P_{max}	7.6	29.0	111.3	426.4

- 1) Nuttli (1986a): $m_b(L_g) = 4.307[\pm 0.067] + 0.765[\pm 0.027]\log(W)$ for $5.2 < m_b(L_g) < 6.7$.
- 2) Patton (1988): $m_b(L_g) = 4.404[\pm 0.048] + 0.755[\pm 0.022]\log(W)$ for $4.22 < m_b(L_g) < 6.7$.
- 3) Nuttli's $m_b(L_g)$ values regressed with the least square (cf. Table 2A).
- 4) Nuttli's $m_b(L_g)$ values regressed with MLE-CY (cf. Table 2A).

Due to the different yield relationships for teleseismic P and L_g at NTS, the yield estimates at the same "magnitude" level are very different. We will compare the $m_b(P) - m_b(L_g)$ offset of various test sites in a later section (cf. Table 9A).

In comparing with Nuttli's regression results, we noticed that his original formula (Equation 1 in Table 2C) seems not reproducible. His data set (cf. Nuttli, 1986a, page 2144) included the Pahute Mesa event HANDLEY which had a bounded yield of >1000 KT. However, Nuttli seemed to have treated the yield as exactly 1000KT in his calculations (cf. Figures 7 and 9 of Nuttli, 1986a). Different symbols for the 2 granite events PILEDRIIVER and SHOAL were used in his figures (cf. Nuttli, 1986a, pages 2145 and 2147). Also, Nuttli imposed a $m_b(L_g)$ range of applicability (from 5.2 to 6.7) on his calibration curve.

We have tested eight possible combinations with Nuttli's $m_b(L_g)$ measurements:

- including NTS granite events or not,
- limiting $m_b(L_g)$ to [5.2,6.7] or not,
- assuming HANDLEY was 1000KT or deleting HANDLEY from the regression.

m_b -Yield Calibration Curves

None of the eight extra experiments could give an "exactly identical" formula to that given by Nuttli (1986a), even if the computer's "machine ϵ " is accounted for. It seems very likely that Nuttli was using the "Y-regression" models, *i.e.*, $\sigma(m_b)/\sigma(Y) = 0$, with some unspecified constraint on the data set. However, for all cases we have tested, the comparisons of MLE results (using Nuttli's data) against Patton's result confirmed consistently that including the censored data would improve the regression.

II.3 U.S. AND FRENCH SAHARA SHOTS IN GRANITE

Table 3A. m_b :Yield Relation of French Sahara and NTS Events in Granite*							
# of Events	m_b	$\frac{\sigma(m_b)}{\sigma(Y)}$	Slope	Intercept	$\sigma(m_b)$	2σ Factor	Method
4+0+0+0	TG, P_a	0	0.875 \pm 0.056	3.365 \pm 0.270	0.035	1.203	LS
4+0+0+0	TG, P_a	∞	0.869 \pm 0.049	3.374 \pm 0.083	0.035	1.203	LS
4+0+0+0	TG, P_b	0	1.048 \pm 0.064	3.334 \pm 0.325	0.048	1.234	LS
4+0+0+0	TG, P_b	∞	1.040 \pm 0.066	3.348 \pm 0.113	0.048	1.235	LS
4+0+0+0	TG, P_{\max}	0	1.011 \pm 0.058	3.657 \pm 0.310	0.042	1.211	LS
4+0+0+0	TG, P_{\max}	∞	1.004 \pm 0.058	3.668 \pm 0.099	0.042	1.212	LS
4+4+1+0	TG, P_a	0	0.928 \pm 0.044	3.258 \pm 0.195	0.061	1.353	MLE-CY
4+4+1+0	TG, P_a	∞	0.905 \pm 0.036	3.296 \pm 0.048	0.056	1.328	MLE-CY
4+6+1+0	TG, P_b	0	1.049 \pm 0.020	3.334 \pm 0.092	0.035	1.169	MLE-CY
4+6+1+0	TG, P_b	∞	1.040 \pm 0.022	3.348 \pm 0.028	0.037	1.178	MLE-CY
4+6+1+0	TG, P_{\max}	0	1.014 \pm 0.018	3.658 \pm 0.084	0.032	1.154	MLE-CY
4+6+1+0	TG, P_{\max}	∞	1.008 \pm 0.018	3.659 \pm 0.022	0.032	1.157	MLE-CY

*) 2 NTS events in granite and 9 French Sahara explosions; no P_a for EMERAUDE and TURQUOISE.

m_b -Yield Calibration Curves

Table 3B. Yield Estimates of French & U.S. Shots in Granite							
Event	Official W	$m_b(P_{\max})$	LS	MLE	$m_b(P_b)$	LS	MLE
	[KT]		[KT]	[KT]		[KT]	[KT]
BERYL	>20.0	4.986	20.6	20.8	4.779	23.8	23.8
CORUNDON	<20.0	4.214	3.5	3.6	3.900	3.4	3.4
EMERAUDE	<20.0	4.569	7.9	8.0	4.263	7.6	7.6
GRENAT	<20.0	4.766	12.4	12.6	4.497	12.7	12.7
OPALE	<20.0	3.894	1.7	1.7	3.853	3.1	3.1
RUBIS	52.0	5.432	57.2	57.5	5.170	56.4	56.5
SAPHIR	120.0	5.720	110.7	111.1	5.468	109.2	109.2
TOURMALINE	<20.0	4.646	9.4	9.5	4.429	10.9	11.0
TURQUOISE	<20.0	4.223	3.6	3.6	3.942	3.7	3.7
SHOAL	12.2	4.739	11.7	11.8	4.455	11.6	11.6
PILEDRIIVER	56.0	5.436	57.7	58.0	5.195	59.7	59.7
# of Events			4+0+0+0	4+6+1+0		4+0+0+0	4+6+1+0
$\delta_{MLE}(m_b)$			0.042	0.032		0.048	0.037
2σ Factor			1.212	1.157		1.235	1.178
ρ			0.997	0.999		0.996	0.999

Table 3C. Expected m_b of U.S. and French Shots in Granite					
m_b :Y Curve	# of Events	10KT	50KT	100KT	150KT
TG, P_a	4+4+1+0	4.201	4.833	5.106	5.265
TG, P_b	4+6+1+0	4.388	5.115	5.428	5.611
TG, P_{\max}	4+6+1+0	4.668	5.372	5.675	5.853

m_b -Yield Calibration Curves

II.4 EASTERN KAZAKHSTAN AREA

# of Events	m_b	$\frac{\sigma(m_b)}{\sigma(Y)}$	Slope	Intercept	$\sigma(m_b)$	2 σ Factor	Method
19+55+0+17	ISC	0	0.715±0.029	4.532±0.156	0.105	1.972	MLE-CY
19+55+0+17	ISC	∞	0.687±0.014	4.570±0.018	0.076	1.660	MLE-CY
19+55+0+17	NEIS	0	0.745±0.039	4.607±0.213	0.157	2.639	MLE-CY
19+55+0+17	NEIS	∞	0.655±0.019	4.725±0.023	0.113	2.222	MLE-CY
19+55+0+17	Sykes	0	0.717±0.024	4.535±0.129	0.088	1.755	MLE-CY
19+55+0+17	Sykes	∞	0.696±0.012	4.563±0.015	0.063	1.520	MLE-CY
19+0+0+0	Marshall	0	0.823±0.050	4.419±0.279	0.098	1.728	LS
19+0+0+0	Marshall	0.1	0.822±___	4.420±___	___	___	Ericsson
19+0+0+0	Marshall	1	0.802±___	4.448±___	___	___	Ericsson
19+0+0+0	Marshall	5	0.791±___	4.466±___	___	___	Ericsson
19+0+0+0	Marshall	∞	0.789±0.039	4.466±0.060	0.096	1.748	LS
19+55+0+17	Marshall	0	0.798±0.025	4.462±0.133	0.109	1.872	MLE-CY
19+55+0+17	Marshall	∞	0.759±0.015	4.516±0.018	0.087	1.696	MLE-CY
12+3+0+5	TG, P_a	0	0.951±0.042	3.497±0.208	0.094	1.577	MLE-CY
12+3+0+5	TG, P_a	∞	0.926±0.037	3.537±0.059	0.088	1.552	MLE-CY
13+3+0+5	TG, P_b	0	0.951±0.042	3.795±0.220	0.096	1.594	MLE-CY
13+3+0+5	TG, P_b	∞	0.924±0.037	3.837±0.059	0.091	1.571	MLE-CY
13+3+0+5	TG, P_{max}	0	0.921±0.047	4.064±0.257	0.102	1.666	MLE-CY
13+3+0+5	TG, P_{max}	∞	0.892±0.039	4.110±0.062	0.093	1.617	MLE-CY

*) including Shagan River (Balapan), Konystan (Murzhik), and Degelen Mountain.

In Table 4A, we regressed all Eastern Kazakh explosions with announced yields (Bocharov *et al.*, 1989) against various m_b values of Marshall (1987), ISC, NEIS, and ours. Detailed descriptions of the explosions are listed in later sections according to the subregion they belong to.

m_b -Yield Calibration Curves

Table 4B. Least-Squares Yield Estimates of E. Kazakh Shots						
Event, Region	Official W	ISC	NEIS	Sykes	Marshall	TG, P_{\max}
	[KT]	[KT]	[KT]	[KT]	[KT]	[KT]
651121, D	29.0	32.0	48.0	31.0	27.7	25.6
660213, D	125.0	159.6	188.5	155.8	185.1	159.0
660320, D	100.0	115.7	188.5	112.8	98.6	88.2
660507, D	4.0	2.4	1.6	2.3	2.2	2.8
670922, M	10.0	8.8	8.7	8.5	7.6	—
680929, D	60.0	60.8	48.0	59.1	58.5	50.1
690723, D	16.0	16.8	17.2	16.2	20.6	15.6
691130, S	125.0	115.7	95.2	97.2	100.9	121.2
691228, M	40.0	44.1	34.1	42.8	47.7	—
710425, D	90.0	83.9	67.6	92.9	109.5	69.5
710606, M	16.0	23.2	17.2	21.0	22.0	—
711009, M	12.0	12.2	12.2	12.5	14.0	—
711021, M	23.0	23.2	24.3	23.1	25.8	—
720210, S	16.0	16.8	17.2	14.7	14.0	22.1
720328, D	6.0	6.4	6.2	7.0	8.0	9.2
720816, D	8.0	4.6	6.2	6.8	6.4	7.6
720902, M	2.0	3.4	4.4	3.0	2.6	—
721102, S	165.0	159.6	188.5	202.4	168.6	207.6
721210, S	140.0	115.7	95.2	108.8	86.7	133.4
# of Events		19+0+0+0	19+0+0+0	19+0+0+0	19+0+0+0	13+0+0+0
$\sigma_{MLE}(m_b)$		0.080	0.120	0.070	0.096	0.097
2σ Factor		1.669	2.278	1.570	1.748	1.638
ρ		0.983	0.957	0.987	0.980	0.984

D = Degelen, S = Shagan (Balapan), M = Murzhik (Konystan).

m_b -Yield Calibration Curves

Table 4C. Maximum-Likelihood Yield Estimates of E. Kazakh Shots

Event, Region	Official W	ISC	NEIS	Sykes	Marshall	TG, P_{max}
	[KT]	[KT]	[KT]	[KT]	[KT]	[KT]
651121, D	29.0	31.7	43.9	30.8	27.3	25.4
660213, D	125.0	169.5	179.1	160.8	196.8	162.9
660320, D	100.0	121.2	179.1	115.5	102.1	89.5
660507, D	4.0	2.2	1.3	2.2	1.9	2.7
670922, M	10.0	8.3	7.6	8.2	7.1	—
680929, D	60.0	62.0	43.9	59.6	59.3	50.4
690723, D	16.0	16.2	15.3	15.9	20.1	15.4
691130, S	125.0	121.2	88.6	99.2	104.7	123.6
691228, M	40.0	44.3	30.9	42.9	48.0	—
710425, D	90.0	86.7	62.4	94.8	113.9	70.2
710606, M	16.0	22.7	15.3	20.7	21.5	—
711009, M	12.0	11.6	10.7	12.2	13.4	—
711021, M	23.0	22.7	21.7	22.9	25.3	—
720210, S	16.0	16.2	15.3	14.4	13.4	21.9
720328, D	6.0	5.9	5.3	6.7	7.4	9.0
720816, D	8.0	4.2	5.3	6.5	6.0	7.4
720902, M	2.0	3.0	3.7	2.8	2.3	—
721102, S	165.0	169.5	179.1	210.2	178.5	213.6
721210, S	140.0	121.2	88.6	111.4	89.4	136.4
# of Events		19+55+0+17	19+55+0+17	19+55+0+17	19+55+0+17	13+3+0+5
$\delta_{MLE}(m_b)$		0.076	0.113	0.063	0.087	0.093
2σ Factor		1.660	2.222	1.520	1.696	1.617
ρ		0.993	0.985	0.996	0.994	0.988

D = Degelen, S = Shagan (Balapan), M = Murzhik (Konystan).

m_b -Yield Calibration Curves

Table 4D. Expected m_b of Eastern Kazakhstan Explosions					
m_b :Y Curve	# of Events	10KT	50KT	100KT	150KT
ISC	19+55+0+17	5.256	5.736	5.943	6.064
NEIS	19+55+0+17	5.380	5.837	6.034	6.150
Sykes	19+55+0+17	5.260	5.747	5.956	6.079
Marshall	19+55+0+17	5.274	5.805	6.033	6.167
TG, P_a	12+3+0+5	4.462	5.109	5.388	5.551
TG, P_b	13+3+0+5	4.761	5.407	5.685	5.848
TG, P_{max}	13+3+5+4	5.003	5.626	5.895	6.052

II.5 SHAGAN RIVER TEST SITE

Table 5A. Nuclear Explosions at Shagan River (Balapan) Region					
Date	Lat	Long	Depth	Yield	Rock
	[N]	[E]	[m]	[KT]	
650115	49.9350	79.0094	178	100-150	Sa
680619	49.9803	78.9855	316	<20	Sa
691130	49.9243	78.9558	472	125	Co
710630	49.9460	78.9805	217	<20	Co
720210	50.0243	78.8781	295	16	Al
721102	49.9270	78.8173	521	165	Al
721210	50.0270	78.9956	478	140	TS

Sa = Sandstone, Al = Aleurolite (Siltstone),
 Co = Conglomerate, TS = Tuffaceous Sandstone
 [from Bocharov *et al.* (1989) and Vergino (1989)]

m_b -Yield Calibration Curves

Table 5B. Reported m_b of Shagan River Explosions							
Date	ISC	NEIS	Sykes	Marshall	Stewart	Stewart	Stewart
	m_b	m_b	m_b	m_b	m_b	$\log(\Psi_\infty)$	M_o
650115	5.8	6.3	5.905	5.931	5.96	3.87	15.80
680619	5.4	5.5	5.350	5.354	5.60	3.31	15.24
691130	6.0	6.0	5.954	6.048	6.14	4.00	15.93
710630	5.2	5.4	5.290	5.027	5.29	2.98	14.91
720210	5.4	5.5	5.370	5.370	5.58	3.22	15.15
721102	6.1	6.2	6.181	6.224	6.39	4.38	16.31
721210	6.0	6.0	5.989	5.996	6.06	4.38	16.31

*) Averaged over EKA, YKA, GBA, and WRA.

Table 5B. Reported m_b of Shagan River Explosions (Continued)						
Date	EKA	Nuttli	Ringdal	TG	TG	TG
	m_b	$m_b(L_g)$	$RMS L_g$	$m_b(P_a)$	$m_b(P_b)$	$m_b(P_{max})$
650115	5.98	5.87	5.950 [*]	5.495	5.734	5.882
680619	5.70	—	—	4.620	5.002	5.263
691130	6.30	—	6.043	5.380	5.770	5.977
710630	5.34	—	—	4.472	4.768	5.041
720210	5.58	5.55	5.4 ^{**}	4.805	5.074	5.306
721102	6.41	6.04	6.118	5.592	5.940	6.189
721210	6.08	6.09	6.095	—	5.786	6.015
710425 ^{***}	N/A	N/A	5.862	N/A	N/A	N/A

*) Inferred indirectly from Nuttli's $m_b(L_g) = 5.87$ (Ringdal and Marshall, 1989).

**) Low SNR for L_g phase (see text).

**) A Degelen event used in Ringdal (1989).

m_b -Yield Calibration Curves

Table 5C. Magnitude:Yield Calibration Curve at Shagan River Area							
# of Events	Magnitude	$\frac{\sigma(m_b)}{\sigma(Y)}$	Slope	Intercept	$\sigma(m_b)$	2 σ Factor	Method
4+2+0+1	ISC	0	0.655±0.132	4.584±0.753	0.116	2.267	MLE-CY
4+2+0+1	ISC	∞	0.628±0.055	4.645±0.097	0.077	1.753	MLE-CY
4+2+0+1	NEIS	0	0.722±0.709	4.621±1.225	0.189	3.346	MLE-CY
4+2+0+1	NEIS	∞	0.614±0.093	4.807±0.131	0.131	2.671	MLE-CY
4+2+0+1	Sykes	0	0.720±0.105	4.481±0.600	0.095	1.833	MLE-CY
4+2+0+1	Sykes	∞	0.698±0.054	4.525±0.096	0.069	1.577	MLE-CY
4+0+0+0	Marshall	0	0.795±0.137	4.385±0.811	0.088	1.669	LS
4+0+0+0	Marshall	0.1	0.795±___	4.387±___	___	___	Ericsson
4+0+0+0	Marshall	1	0.777±___	4.420±___	___	___	Ericsson
4+0+0+0	Marshall	5	0.767±___	4.439±___	___	___	Ericsson
4+0+0+0	Marshall	∞	0.767±0.105	4.441±0.206	0.087	1.685	LS
4+2+0+1	Marshall	0	0.768±0.089	4.421±0.510	0.098	1.803	MLE-CY
4+2+0+1	Marshall	∞	0.741±0.052	4.476±0.090	0.076	1.606	MLE-CY
4+2+0+1	EKA, m_b	0	0.705±0.246	4.724±1.457	0.236	4.654	MLE-CY
4+2+0+1	EKA, m_b	∞	0.568±0.104	4.983±0.181	0.165	3.809	MLE-CY
4+2+0+1	Stewart, m_b	0	0.667±0.220	4.738±1.293	0.207	4.170	MLE-CY
4+2+0+1	Stewart, m_b	∞	0.570±0.087	4.926±0.152	0.138	3.044	MLE-CY
4+2+0+1	Stewart, $\log(\Psi_\infty)$	0	1.098±0.124	1.865±0.467	0.172	2.061	MLE-CY
4+2+0+1	Stewart, $\log(\Psi_\infty)$	∞	0.953±0.135	2.134±0.237	0.189	2.498	MLE-CY
4+2+0+1	Stewart, M_o	0	1.099±0.124	13.795±1.942	0.172	2.061	MLE-CY
4+2+0+1	Stewart, M_o	∞	0.953±0.135	14.064±0.237	0.189	2.497	MLE-CY
3+0+0+1	Nuttli, $m_b(L_g)$	0	0.587±0.346	4.742±2.035	0.160	3.516	MLE-CY
3+0+0+1	Nuttli, $m_b(L_g)$	∞	0.546±0.106	4.835±0.207	0.087	2.085	MLE-CY
4+0+0+1	Ringdal, $RMS L_g$	0	1.075±0.123	3.768±0.741	0.026	1.119	MLE-CY
4+0+0+1	Ringdal, $RMS L_g$	∞	1.025±0.134	3.873±0.281	0.027	1.130	MLE-CY

*) Degelen event 710425 was used instead of Shagan event 720210.

m_b -Yield Calibration Curves

Table 5C. Magnitude:Yield Calibration Curve at Shagan River Area (Continued)

# of Events	Magnitude	$\frac{\sigma(m_b)}{\sigma(Y)}$	Slope	Intercept	$\sigma(m_b)$	2 σ Factor	Method
3+2+0+1	TG, P_a	0	0.759 \pm 0.075	3.873 \pm 0.382	0.082	1.640	MLE-CY
3+2+0+1	TG, P_a	∞	0.738 \pm 0.041	3.910 \pm 0.069	0.060	1.456	MLE-CY
4+2+0+1	TG, P_b	0	0.812 \pm 0.044	4.083 \pm 0.238	0.051	1.332	MLE-CY
4+2+0+1	TG, P_b	∞	0.803 \pm 0.028	4.101 \pm 0.050	0.041	1.264	MLE-CY
4+2+0+1	TG, P_{\max}	0	0.811 \pm 0.074	4.298 \pm 0.422	0.082	1.593	MLE-CY
4+2+0+1	TG, P_{\max}	∞	0.788 \pm 0.039	4.336 \pm 0.068	0.067	1.475	MLE-CY

m_b (NEIS) are biased high at low yields for Shagan explosions simply because NEIS averages the signals reported. Consequently their m_b vs. $\log(W)$ slope is underestimated, which in turn causes the yields of the high-yield explosions to be overestimated. The yields estimated by Geotech's P_b seem to have accuracy at least as good as that based on P_{\max} .

In Tables 5B and 5C, Stewart's m_b , $\log(\Psi_\infty)$, and M_0 are those which are averaged over four arrays: Eskdalemuir (EKA) Scotland, Yellowknife (YKA) Canada, Gauribidanur (GBA) India, and Warramunga (WRA) Australia. The scatter is slightly reduced as compared to that based on a single array EKA. Marshall's m_b values are based on the ISC bulletin recordings (Marshall, personal communication).

Apparently the $RMS L_g$ averaged over the bandpassed multi-channel signals recorded at NORSAR fit the announced yields very well. However, more data may be needed to further quantify its performance (Ringdal and Hansen, 1989) (cf. Table 5D). If Shagan event 720210 (which had poor L_g SNR at NORSAR) is included, the results would show a slightly greater scatter ($\sigma = 0.056$ and 0.040 for cases 0 and ∞ , respectively). In Tables 5C through 5E, we have excluded this event at Ringdal's suggestion (Ringdal, personal communication).

Zavadil and Eisenhower conjectured that the first or "b" phase could replace the phase "max." However, these AFTAC researchers and many others did not find convincing evidence to support their argument (DARPA, 1981). It seems this conjecture could well be valid at least for Shagan River. Among the three phases we measured, the phase "b" has the smallest scatter (cf. Table 5C), and it gives the best yield estimates (cf. Table 5D). At NTS and Sahara, the phase "b" has precision much better than the phase "a". At Degelen Mountain, phase "a" shows the smallest scatter, possibly because phases "b" and "max" are severely contaminated by the scattering at the free-surface topography (cf. Table 6C).

m_b -Yield Calibration Curves

Table 5D. Maximum-Likelihood Yield Estimates of Shagan Explosions							
Date & Official W	ISC	NEIS	Sykes	Marshall	Stewart m_b	$\log(\Psi_\infty)$	M_o
[KT]	[KT]	[KT]	[KT]	[KT]	[KT]	[KT]	[KT]
650115, 100-150	69.2	269.6	94.9	92.0	65.0	66.3	66.4
680619, <20	16.0	13.4	15.2	15.3	15.2	17.1	17.1
691130, 125	144.2	87.6	111.6	132.4	134.5	90.8	90.8
710630, <20	7.7	9.2	12.5	5.5	4.3	7.7	7.7
720210, 16	16.0	13.4	16.5	16.1	14.0	13.8	13.8
721102, 165	208.1	185.3	235.9	226.0	369.2	227.6	227.6
721210, 140	144.2	87.6	125.2	112.7	97.4	227.6	227.6
$\sigma_{MLE}(m_b)$	0.077	0.131	0.069	0.076	0.138	0.189	0.189
2 σ Factor	1.753	2.671	1.577	1.606	3.044	2.498	2.497
ρ	0.986	0.958	0.989	0.991	0.957	0.962	0.963

Table 5D. Maximum-Likelihood Yield Estimates of Shagan Explosions (Continued)							
Date & Official W	EKA	Nuttli*	Nuttli**	Ringdal***	P_a	P_b	P_{max}
[KT]	[KT]	[KT]	[KT]	[KT]	[KT]	[KT]	[KT]
650115, 100-150	56.9	109	78.8	106.3	140.6	108.2	89.3
680619, <20	18.3	—	—	—	9.2	13.3	14.6
691130, 125	208.5	—	—	131.0	98.2	119.9	117.8
710630, <20	4.2	—	—	—	5.8	6.8	7.6
720210, 16	11.2	42	16.5	—	16.3	16.3	16.6
721102, 165	325.8	183	161.5	155.0	190.3	195.3	218.9
721210, 140	85.4	212	199.4	147.2	—	125.6	131.7
$\sigma_{MLE}(m_b)$	0.165	—	0.087	0.027	0.060	0.041	0.067
2 σ Factor	3.809	—	2.085	1.130	1.456	1.264	1.475
ρ	0.939	—	0.965	0.979	0.996	0.998	0.994

*) Nuttli (1986b): $m_b(L_g) = 4.307[\pm 0.067] + 0.765[\pm 0.027]\log(W)$ for $5.2 < m_b(L_g) < 6.7$.

**) Nuttli's $m_b(L_g)$ regressed by our maximum-likelihood code.

***) Degelen event 710425 was used instead of Shagan event 720210.

m_b -Yield Calibration Curves

In 1988 the United States and the Soviet Union signed a bilateral agreement whereby each country was permitted to monitor at close distance an underground nuclear explosion at the other's main test site. The Soviet JVE (Joint Verification Experiment) shot was detonated on September 14, 1988, near the southern edge of the Shagan River Test Site. The New York Times states that the American and Soviet on-site measurements are said to give yields of 115KT and 122KT, respectively, for the Soviet JVE explosions (Sykes and Ekstrom, 1989). NORSAR's $RMS L_g$ measurement for this event was 5.969 (Ringdal and Marshall, 1989). Assuming that the actual yield was between 100 and 150KT, as suggested by P. G. Richards, the regression using NORSAR's $RMS L_g$ data including this event would give an estimate of 111.2KT, which is very close to Sykes' 113KT based on the average of m_b and M_S (Sykes and Ekstrom, 1989). The $\sigma(m_b)$ and the 95% factor in yield associated with NORSAR's data reduce from 0.027 and 1.130 (*cf.* Table 5D) to 0.026 and 1.122, respectively.

Table 5E. Expected Magnitudes of Shagan Explosions					
m_b :Y Curve	# of Events	10KT	50KT	100KT	150KT
ISC	4+2+0+1	5.273	5.711	5.900	6.011
NEIS	4+2+0+1	5.421	5.850	6.035	6.144
Sykes	4+2+0+1	5.223	5.711	5.921	6.044
Marshall	4+2+0+1	5.217	5.735	5.958	6.088
EKA, m_b	4+2+0+1	5.551	5.948	6.119	6.219
Stewart, m_b	4+2+0+1	5.496	5.895	6.067	6.167
Stewart, $\log(\Psi_\infty)$	4+2+0+1	3.087	3.753	4.040	4.208
Stewart, M_o	4+2+0+1	15.017	15.683	15.970	16.138
Nuttli, $m_b(L_g)$	3+0+0+1	5.381	5.762	5.926	6.023
Ringdal, $RMS L_g$	4+0+0+1	—	5.614	5.923	6.103
TG, P_a	3+2+0+1	4.648	5.164	5.386	5.516
TG, P_b	4+2+0+1	4.904	5.465	5.707	5.848
TG, P_{max}	4+2+0+1	5.133	5.684	5.922	6.062

In Table 5D, we have listed two sets of yield estimates based on Nuttli's (1986b) $m_b(L_g)$ measurements. Although Nuttli's $m_b(L_g)$ database for Shagan had only four events in common with that of Bocharov, it is clear that regressing the $m_b(L_g)$ (or m_b) on each test site

m_b -Yield Calibration Curves

separately, whenever the data are available, would give better results than the global calibration curve as recommended by Nuttli.

Table 5E indicates that our $m_b(P_{max})$ matches Ringdal's $RMS L_g$ very well (except at low yields). Note that $m_b(L_g)$ is defined to be equal to m_b in eastern North America, which has geology similar to Eastern Kazakhstan. Thus relative to $m_b(L_g)$ scaling, our $m_b(P_{max})$ seem to have the smallest bias, as compared to other m_b . We have also regressed various magnitudes on Ringdal's $RMS L_g$ with slope fixed at 1 (Table 5F). As expected, our $m_b(P_b)$ and $m_b(P_{max})$ possess the strongest correlation, the smallest scatter around the fitted straight line, as well as the smallest standard error in the estimated intercept.

Table 5F. Various Magnitudes Versus Ringdal's $RMS L_g$ for Shagan Events*			
Magnitude	$\sigma(m_b)$	Intercept	ρ
ISC	0.068	-0.034±0.028	0.968
NEIS	0.143	0.066±0.058	0.840
Sykes	0.094	0.002±0.039	0.960
Marshall	0.112	0.030±0.050	0.926
EKA, m_b	0.136	0.149±0.068	0.907
Stewart, m_b	0.125	0.105±0.062	0.912
Stewart, $\log(\Psi_\infty)$	0.211	-1.951±0.106	0.955
Stewart, M_o	0.211	9.979±0.106	0.955
Nuttli, $m_b(L_g)$	0.085	-0.016±0.049	0.986
TG, P_a	0.077	-0.560±0.039	0.968
TG, P_b	0.058	-0.266±0.026	0.988
TG, P_{max}	0.064	-0.057±0.029	0.982

*) Regressed on $RMS L_g$ with slope 1 and free intercept.

It should not be surprising that M_o and $\log(\Psi_\infty)$ reported by the four British arrays give identical slope, σ , ρ , and yield estimates *etc.* (Tables 5C, 5D, and 5F) since Stewart (1988) computed the seismic moment, M_o , as

$$M_o \equiv 4 \pi d V_p^2 \Psi_\infty$$

m_b -Yield Calibration Curves

where $d = 2.4$ g/cc and $V_p = 5.0$ km/sec are the presumed density and the P -wave velocity of the source material.

II.6 DEGELEN MOUNTAIN

Table 6A. Nuclear Explosions at Degelen Mountainous Region					
Date	Lat	Long	Depth	Yield	Rock
	[N]	[E]	[m]	[KT]	
611011	49.77272	77.99500	116	<20	Gr
620202	49.77747	78.00164	238	<20	Gr
640315	49.81597	78.07517	220	20-150	Gr
640516	49.80772	78.10197	253	20-150	Gr
640719	49.80908	78.09292	168	<20	Gr
641116	49.80872	78.13344	194	20-150	QP
650303	49.82472	78.05267	196	<20	Gr
650511	49.77022	77.99428	103	<20	Gr
650617	49.82836	78.06686	152	<20	Gr
650729	49.77972	77.99808	126	<20	Gr
650917	49.81158	78.14669	156	<20	QP
651008	49.82592	78.11144	204	<20	QP
651121	49.81919	78.06358	278	29	Gr
651224	49.80450	78.10667	213	<20	QP
660213	49.80894	78.12100	297	125	QP
660320	49.76164	78.02389	294	100	QP
660421	49.80967	78.10003	178	<20	Gr
660507	49.74286	78.10497	274	4	QP
660629	49.83442	78.07336	187	20-150	Gr
660721	49.73667	78.09703	170	<20	QP

Gr = Granite, QP = Quartz Porphyrite, Po = Porphyrite, QS = Quartz Syenite
[from Bocharov *et al.* (1989) and Vergino (1989)]

m_b -Yield Calibration Curves

Table 6A. Nuclear Explosions at Degelen Mountainous Region (Continued)					
Date	Lat	Long	Depth	Yield	Rock
	[N]	[E]	[m]	[KT]	
660805	49.76431	78.04242	171	<20	Gr
660819	49.82708	78.10875	134	<20	QP
660907	49.82883	78.06375	117	<20	Gr
661019	49.74711	78.02053	185	20-150	Gr
661203	49.74689	78.03336	153	<20	Gr
670130	49.76744	77.99139	131	<20	QS
670226	49.74569	78.08231	241	20-150	QP
670325	49.75361	78.06300	152	<20	Gr
670420	49.74161	78.10542	225	20-150	QP
670528	49.75642	78.01689	262	<20	QP
670629	49.81669	78.04903	195	<20	Gr
670715	49.83592	78.11817	161	<20	QP
670804	49.76028	78.05550	160	<20	Gr
671017	49.78089	78.00383	181	20-150	Gr
671030	49.79436	78.00786	173	<20	Gr
671208	49.81714	78.16378	150	<20	QP
680107	49.75442	78.03094	237	<20	Gr
680424	49.84519	78.10322	127	<20	QP
680611	49.79300	78.14508	149	<20	QP
680712	49.75469	78.08994	172	<20	Gr
680820	49.82264	78.07447	208	<20	Gr
680905	49.74161	78.07558	162	<20	Gr
680929	49.81197	78.12194	290	60	QP
681109	49.80053	78.13911	125	<20	QP
681218	49.74594	78.09203	194	<20	Gr
690307	49.82147	78.06267	214	20-150	Gr

Gr = Granite, QP = Quartz Porphyrite, Po = Porphyrite, QS = Quartz Syenite
[from Bocharov *et al.* (1989) and Vergino (1989)]

m_b -Yield Calibration Curves

Table 6A. Nuclear Explosions at Degelen Mountainous Region (Continued)					
Date	Lat	Long	Depth	Yield	Rock
	[N]	[E]	[m]	[KT]	
690516	49.75942	78.07578	184	<20	Gr
690704	49.74603	78.11133	219	<20	QP
690723	49.81564	78.12961	175	16	QP
690911	49.77631	77.99669	190	<20	Gr
691001	49.78250	78.09831	144	<20	Gr
691229	49.73367	78.10225	86	<20	QP
700129	49.79558	78.12389	214	20-150	Po
700327	49.74781	77.99897	138	<20	Gr
700527	49.73131	78.09861	66	<20	QP
700628	49.80150	78.10681	332	20-150	Gr
700724	49.80972	78.12839	154	<20	QP
700906	49.75975	78.00539	212	<20	Gr
701217	49.74564	78.09917	193	<20	Gr
710322	49.79847	78.10897	283	20-150	Gr
710425	49.76853	78.03392	296	90	Gr
710525	49.80164	78.13883	132	<20	Gr
711129	49.74342	78.07850	203	<20	Gr
711215	49.82639	77.99731	115	<20	Gr
711230	49.76003	78.03714	249	20-150	Gr
720310	49.74531	78.11969	171	<20	QP
720328	49.73306	78.07569	124	6	QP
720607	49.82675	78.11547	208	20-150	QP
720706	49.73750	78.11006	81	<20	QP
720816	49.76547	78.05883	139	8	Gr
721210	49.81939	78.05822	264	20-150	Gr
721228	49.73919	78.10625	132	<20	QP

Gr = Granite, QP = Quartz Porphyrite, Po = Porphyrite, QS = Quartz Syenite
[from Bocharov *et al.* (1989) and Vergino (1989)]

m_b -Yield Calibration Curves

Table 6B. Reported m_b of Degelen Mountain Explosions							
Date	ISC	NEIS	Sykes	Marshall	TG, P_a	TG, P_b	TG, P_{max}
	m_b	m_b	m_b	m_b	m_b	m_b	m_b
611011	—	—	—	—	—	—	—
620202	—	—	—	—	—	—	—
640315	5.6	5.6	5.600	5.563	—	—	—
640516	5.6	5.6	5.600	5.549	—	—	—
640719	5.4	5.5	5.400	5.433	—	—	—
641116	5.6	6.0	—	5.642	—	—	—
650303	5.5	5.6	5.500	5.443	—	—	—
650511	4.9	5.2	4.900	4.742	—	—	—
650617	5.2	5.4	5.200	5.244	—	—	—
650729	4.5	4.5	4.500	—	—	—	—
650917	5.2	5.6	5.200	5.219	—	—	—
651008	5.4	5.7	5.400	5.471	—	—	—
651121	5.6	5.8	5.600	5.605	4.877	5.154	5.364
651224	5.0	5.0	5.000	4.944	—	—	—
660213	6.1	6.2	6.100	6.256	5.642	5.892	6.084
660320	6.0	6.2	6.000	6.040	5.337	5.626	5.852
660421	5.3	5.4	5.300	5.370	—	—	—
660507	4.8	4.8	4.800	4.734	3.994	4.235	4.488
660629	5.6	5.6	5.600	5.508	—	—	—
660721	5.3	5.4	5.300	5.360	—	—	—
660805	5.4	5.5	5.400	5.390	—	—	—
660819	5.1	4.8	5.100	4.633	—	—	—
660907	4.8	4.7	4.800	4.661	—	—	—
661019	5.6	5.7	5.600	5.669	—	—	—
661203	4.8	4.8	4.800	4.600	—	—	—
670130	4.8	4.8	4.800	4.627	—	—	—
670226	6.0	6.0	6.000	6.034	5.355	5.599	5.823
670325	5.3	5.3	5.300	5.320	—	—	—

m_b -Yield Calibration Curves

Table 6B. Reported m_b of Degelen Mountain Explosions (Continued)							
Date	ISC	NEIS	Sykes	Marshall	TG, P_a	TG, P_b	TG, P_{max}
	m_b	m_b	m_b	m_b	m_b	m_b	m_b
670420	5.5	5.7	5.500	5.556	—	—	—
670528	5.4	5.4	5.400	5.464	—	—	—
670629	5.3	5.3	5.300	5.336	—	—	—
670715	5.4	5.4	5.400	5.387	—	—	—
670804	5.3	5.3	5.300	5.316	—	—	—
671017	5.6	5.7	5.600	5.629	—	—	—
671030	5.3	5.5	5.300	5.413	—	—	—
671208	5.4	5.4	5.400	5.314	—	—	—
680107	5.1	5.3	5.100	4.977	—	—	—
680424	5.0	5.0	5.000	4.911	—	—	—
680611	5.2	5.3	5.200	5.240	—	—	—
680712	5.3	5.4	5.300	5.169	—	—	—
680820	4.8	4.8	4.800	4.761	—	—	—
680905	5.4	5.5	5.400	5.439	—	—	—
680929	5.8	5.8	5.800	5.861	5.127	5.434	5.629
681109	4.9	4.9	4.900	4.751	—	—	—
681218	5.0	5.2	5.000	5.044	—	—	—
690307	5.6	5.5	5.600	5.664	—	—	—
690516	5.2	5.3	5.200	5.264	—	—	—
690704	5.2	5.3	5.200	5.241	—	—	—
690723	5.4	5.5	5.400	5.504	4.596	4.922	5.169
690911	5.0	5.0	5.000	4.910	3.977	4.236	4.578
691001	5.2	5.3	5.200	5.256	—	—	—
691229	5.1	4.6	5.100	4.217	—	—	—
700129	5.5	5.6	5.500	5.599	—	—	—
700327	5.0	5.2	5.000	4.929	—	—	—
700527	3.8	—	3.800	—	—	—	—
700628	5.7	5.9	5.700	5.870	—	—	—

m_b -Yield Calibration Curves

Table 6B. Reported m_b of Degelen Mountain Explosions (Continued)							
Date	ISC	NEIS	Sykes	Marshall	TG, P_a	TG, P_b	TG, P_{max}
	m_b	m_b	m_b	m_b	m_b	m_b	m_b
700724	5.3	5.3	5.300	5.337	—	—	—
700906	5.4	5.6	5.400	5.533	—	—	—
701217	5.4	5.5	5.400	5.433	—	—	—
710322	5.7	5.8	5.700	5.767	—	—	—
710425	5.9	5.9	5.940	6.076	5.301	5.568	5.758
710525	5.1	5.2	5.020	5.048	—	—	—
711129	5.4	5.5	5.440	5.462	—	—	—
711215	4.9	4.9	4.900	4.677	—	—	—
711230	5.7	5.8	5.780	5.838	4.984	5.349	5.526
720310	5.4	5.5	5.410	5.453	—	—	—
720328	5.1	5.2	5.140	5.177	4.353	4.728	4.961
720607	5.4	5.5	5.400	5.422	—	—	—
720706	4.4	4.4	4.420	4.275	—	—	—
720816	5.0	5.2	5.130	5.105	4.339	4.622	4.887
721210	5.6	5.7	5.600	5.715	4.977	5.355	5.534
721228	—	—	4.900	—	—	—	—

Table 6B indicates that for Degelen events, all other m_b 's are systematically larger than ours by a Δm_b of approximately 0.2 to 0.3. The m_b offset is less significant for Shagan events (*cf.* Tables 6B and 5E), however. This is possibly due to the different focusing and defocusing patterns between Shagan-Europe and Degelen-Europe paths. In our WWSSN database, there were 8 and 10 European stations which detected the Shagan event 650115 (100-150KT) and Degelen event 710425 (90KT), respectively. The averaged m_b residuals of the European WWSSN stations for these two events are 0.07 ± 0.133 and 0.122 ± 0.057 , respectively. Marshall's database has a heavy clustering of ISC stations in Europe, and hence the resulting m_b offset may just be reflecting the even more severe path focusing effects enhanced by the ISC clustering in the western Europe.

m_b -Yield Calibration Curves

Table 6C. m_b -Yield Calibration Curve at Degelen Mountain

# of Events	m_b	$\frac{\sigma(m_b)}{\sigma(Y)}$	Slope	Intercept	$\sigma(m_b)$	2σ Factor	Method
9+46+0+15	ISC	0	0.833±0.022	4.362±0.114	0.069	1.466	MLE-CY
9+46+0+15	ISC	∞	0.809±0.015	4.392±0.018	0.058	1.392	MLE-CY
9+46+0+15	NEIS	0	0.861±0.036	4.445±0.195	0.129	1.997	MLE-CY
9+46+0+15	NEIS	∞	0.773±0.024	4.556±0.028	0.110	1.920	MLE-CY
9+46+0+15	Sykes	0	0.803±0.019	4.414±0.102	0.062	1.426	MLE-CY
9+46+0+15	Sykes	∞	0.786±0.012	4.438±0.015	0.051	1.345	MLE-CY
9+0+0+0	Marshall	0	0.912±0.067	4.300±0.377	0.097	1.635	LS
9+0+0+0	Marshall	0.1	0.912±___	4.300±___	___	___	Ericsson
9+0+0+0	Marshall	1	0.897±___	4.322±___	___	___	Ericsson
9+0+0+0	Marshall	5	0.885±___	4.338±___	___	___	Ericsson
9+0+0+0	Marshall	100	0.884±___	4.340±___	___	___	Ericsson
9+0+0+0	Marshall	∞	0.884±0.059	4.340±0.090	0.096	1.647	LS
9+46+0+15	Marshall	0	0.908±0.022	4.318±0.115	0.083	1.525	MLE-CY
9+46+0+15	Marshall	∞	0.869±0.017	4.370±0.020	0.076	1.494	MLE-CY
9+1+0+3	TG, P_a	0	0.981±0.048	3.449±0.226	0.087	1.505	MLE-CY
9+1+0+3	TG, P_a	∞	0.959±0.044	3.479±0.066	0.084	1.499	MLE-CY
9+1+0+3	TG, P_b	0	0.972±0.058	3.752±0.297	0.108	1.665	MLE-CY
9+1+0+3	TG, P_b	∞	0.939±0.052	3.798±0.079	0.103	1.654	MLE-CY
9+1+0+3	TG, P_{max}	0	0.931±0.062	4.033±0.333	0.108	1.709	MLE-CY
9+1+0+3	TG, P_{max}	∞	0.899±0.051	4.079±0.078	0.099	1.660	MLE-CY

m_b -Yield Calibration Curves

Table 6D. Expected m_b of Degelen Explosions					
m_b :Y Curve	# of Events	10KT	50KT	100KT	150KT
ISC	9+46+0+15	5.201	5.767	6.010	6.153
NEIS	9+46+0+15	5.329	5.870	6.103	6.239
Sykes	9+46+0+15	5.223	5.772	6.009	6.147
Marshall	9+46+0+15	5.239	5.846	6.108	6.261
TG, P_a	9+1+0+2	4.438	5.108	5.397	5.566
TG, P_b	9+1+0+2	4.737	5.393	5.676	5.841
TG, P_{max}	9+1+0+2	4.978	5.606	5.876	6.034

m_b -Yield Calibration Curves

II.7 KONYSTAN (MURZHIK) AREA

Table 7A. Explosions at Konystan (Murzhik) Region									
Date	Lat	Long	Depth	Yield	Rock	ISC	NEIS	Sykes	Marshall
	[N]	[E]	[m]	[KT]		m_b	m_b	m_b	m_b
651014	49.9906	77.6357	048	1.1	Al	—	—	—	—
661218	49.9246	77.7472	427	20-150	Po	5.8	5.9	5.800	5.922
670916	49.9372	77.7281	230	<20	Sa	5.3	5.3	5.300	5.245
670922	49.9596	77.6911	229	10	Al	5.2	5.3	5.200	5.160
671122	49.9419	77.6868	227	<20	Al	4.8	—	4.800	4.410
681021	49.7279	78.4863	31	0.2	Ar	—	—	—	—
681112	49.7124	78.4613	31	0.2x3	Gs	—	—	—	—
690531	49.9503	77.6942	258	<20	Al	5.3	5.4	5.300	5.290
691228	49.9373	77.7142	388	46	Al	5.7	5.7	5.700	5.791
700721	49.9524	77.6729	225	<20	Sa	5.4	5.4	5.400	5.376
701104	49.9892	77.7624	249	<20	Po	5.4	5.4	5.400	5.439
710606	49.9754	77.6603	299	16	Al	5.5	5.5	5.480	5.526
710619	49.9690	77.6408	290	<20	Po	5.4	5.5	5.410	5.538
711009	49.9779	77.6414	237	12	Al	5.3	5.4	5.320	5.371
711021	49.9738	77.5973	324	23	Sa	5.5	5.6	5.510	5.580
720826	49.9820	77.7166	285	<20	Al	5.3	5.5	5.370	5.363
720902	49.9594	77.6409	185	2	Sa	4.9	5.1	4.880	4.788

Sa = Sandstone, Al = Aleurolite (Siltstone), Po = Porphyrite, Gs = Gritstone
 [from Bocharov *et al.* (1989) and Vergino (1989)]

m_b -Yield Calibration Curves

Table 7B. m_b :Yield Calibration Curve at Konystan Area							
# of Events	m_b	$\frac{\sigma(m_b)}{\sigma(Y)}$	Slope	Intercept	$\sigma(m_b)$	2 σ Factor	Method
6+7+0+1	ISC	0	0.632 \pm 0.097	4.659 \pm 0.518	0.093	1.962	MLE-CY
6+7+0+1	ISC	∞	0.602 \pm 0.036	4.691 \pm 0.042	0.057	1.542	MLE-CY
6+7+0+1	NEIS	0	0.500 \pm 0.106	4.894 \pm 0.573	0.099	2.490	MLE-CY
6+7+0+1	NEIS	∞	0.472 \pm 0.023	4.920 \pm 0.027	0.046	1.562	MLE-CY
6+7+0+1	Sykes	0	0.638 \pm 0.080	4.650 \pm 0.426	0.077	1.740	MLE-CY
6+7+0+1	Sykes	∞	0.617 \pm 0.031	4.671 \pm 0.036	0.048	1.429	MLE-CY
6+0+0+0	Marshall	0	0.791 \pm 0.102	4.498 \pm 0.547	0.081	1.598	LS
6+0+0+0	Marshall	0.1	0.790 \pm ___	4.498 \pm ___	___	___	Ericsson
6+0+0+0	Marshall	1	0.772 \pm ___	4.519 \pm ___	___	___	Ericsson
6+0+0+0	Marshall	5	0.761 \pm ___	4.531 \pm ___	___	___	Ericsson
6+0+0+0	Marshall	100	0.760 \pm ___	4.532 \pm ___	___	___	Ericsson
6+0+0+0	Marshall	∞	0.760 \pm 0.077	4.532 \pm 0.091	0.079	1.613	LS
6+7+0+1	Marshall	0	0.806 \pm 0.065	4.495 \pm 0.347	0.089	1.666	MLE-CY
6+7+0+1	Marshall	∞	0.768 \pm 0.039	4.535 \pm 0.045	0.069	1.516	MLE-CY
6+7+0+1	DOB*	0	0.278 \pm 0.400	2.136 \pm 0.972	0.143	10.713	MLE-CY
6+7+0+1	DOB	∞	0.245 \pm 0.024	2.164 \pm 0.028	0.035	1.915	MLE-CY

*) Depth of Burial.

Our maximum-likelihood regression routine can be applied to estimate the depth scaling rule as well (Jih, 1990). The result in Table 7B indicates that the scale depth for Konystan explosions is 146 \pm 1 meters. Furthermore, The depth of burial [DOB] is proportional to the quartic root of the yield, rather than the cubic root as frequently cited at NTS (e.g., Evernden and Marsh, 1987). For Konystan test site, the yields estimated using DOB seem to have accuracy comparable to m_b (Table 7C). This is not the case for Degelen region, however (Jih, 1990).

m_b -Yield Calibration Curves

Table 7C. Maximum-Likelihood Yield Estimates of Konystan Explosions						
Date	Official W	ISC	NEIS	Sykes	Marshall	DOB
	[KT]	[KT]	[KT]	[KT]	[KT]	[KT]
661218	20-150	69.5	118.8	67.4	64.2	80.1
670916	<20	10.3	6.4	10.4	8.4	6.4
670922	10	7.0	6.4	7.2	6.5	6.3
671122	<20	1.5	0.6	1.6	0.7	6.1
690531	<20	10.3	10.4	10.4	9.6	10.2
691228	46	47.4	44.8	46.4	43.3	54.2
700721	<20	15.0	10.4	15.2	12.5	5.8
701104	<20	15.0	10.4	15.2	15.1	8.8
710606	16	22.1	16.9	20.4	19.6	18.7
710619	<20	15.0	16.9	15.7	20.3	16.5
711009	12	10.3	10.4	11.2	12.3	7.2
711021	23	22.1	27.5	22.8	23.0	25.9
720826	<20	10.3	16.9	13.6	12.0	15.4
720902	2.0	2.2	2.4	2.2	2.1	2.6
$\sigma_{MLE}(m_b)$ or $\sigma_{MLE}(\text{DOB})$		0.057	0.046	0.048	0.069	0.035
2 σ Factor		1.542	1.562	1.429	1.516	1.915
ρ		0.990	0.993	0.993	0.992	0.971

Table 7D. Expected m_b & DOB of Konystan Explosions					
m_b :Y Curve	# of Events	10KT	50KT	100KT	150KT
ISC	6+7+0+1	5.293	5.714	5.895	6.001
NEIS	6+7+0+1	5.392	5.723	5.865	5.948
Sykes	6+7+0+1	5.289	5.720	5.906	6.014
Marshall	6+7+0+1	5.302	5.839	6.070	6.205
DOB (meter)	6+7+0+1	257	380	451	498

m_b -Yield Calibration Curves

II.8 CRATERING VERSUS NON_CRATERING EXPLOSIONS

Tables 8A and 8B list the $\Delta_1 m_b \equiv \hat{m}_b(P_{\max}) - \hat{m}_b(P_a)$ and $\Delta_2 m_b \equiv \hat{m}_b(P_b) - \hat{m}_b(P_a)$ at four different test sites. As the yield increases from 10KT to 150KT, the Δm_b decreases steadily, except at Degelen Mountain. This could be yet another indication that the D.O.B. at Degelen does not quite follow the depth scaling. Note that Sahara Test Site has the same trend as Shagan.

Table 8A. Expected $\hat{m}_b(P_{\max}) - \hat{m}_b(P_a)$ At 4 Test Sites				
Test Site	10KT	50KT	100KT	150KT
NTS	0.486	0.501	0.507	0.510
Sahara	0.467	0.539	0.569	0.588
KTS	0.541	0.517	0.507	0.501
Shagan River	0.485	0.520	0.536	0.546
Degelen	0.540	0.498	0.479	0.468

Table 8B. Expected $\hat{m}_b(P_b) - \hat{m}_b(P_a)$ At 4 Test Sites				
Test Site	10KT	50KT	100KT	150KT
NTS	0.232	0.254	0.263	0.268
Sahara	0.187	0.282	0.322	0.346
KTS	0.299	0.298	0.297	0.297
Shagan River	0.256	0.301	0.321	0.332
Degelen	0.299	0.285	0.279	0.275

McLaughlin *et al.* (1985) studied the ratio of the P_a phase and P_{\max} phase of presumed Shagan River contained and cratering explosions by comparing the WWSSN station m_b 's. The motivation was that the logarithm of amplitude ratio of P_{\max}/P_a of event 650115 was significantly smaller than other presumed contained explosions in the vicinity. Assuming the phase P_a is unaffected by the influence of the non-linear free-surface interference, then an adjustment to the $m_b(P_{\max})$ should be able to convert that to a contained explosion of the

m_b -Yield Calibration Curves

same yield. McLaughlin *et al.* (1985) concluded that a correction between 0.17 and 0.27 is needed for this conversion, assuming a yield of 125KT.

Based on 46 Shagan River explosions recorded at EKA, Ringdal and Marshall (1989) derived a value of 0.75 as their mean $\log(P_{\max}/P_a)$ across the EKA array using the same techniques as used in McLaughlin *et al.* (1985). The cratering event 650115 had $m_b(P_{\max}) - m_b(P_a) = 0.62$ at EKA, and hence they apply a correction of $5.87 + 0.75 - 0.62 = 6.00$ for a hypothetical contained explosion with equivalent yield. Both Ringdal and Marshall (1989) and McLaughlin *et al.* (1985) have the same methodological drawback in that they did not take the yields of those reference contained explosions into account, due to the lack of data at the time.

We utilize the statistics in Tables 8A and 8B to illustrate that the correction by Ringdal and Marshall (1989) might be slightly more accurate than that in McLaughlin *et al.* (1985). In Table 8A, we have $\hat{m}_b(P_{\max}) - \hat{m}_b(P_a) = 0.536$ at 100KT, and 0.546 at 150KT. Since for event 650115 our $m_b(P_{\max}, TG) - m_b(P_a, TG) = 0.387$ (Table 5B), this would imply an adjustment of 0.149 (100KT) and 0.159 (150KT), and a corrected m_b of about 6.031 (100KT) and 6.041 (150KT), respectively. Note that the adjusted m_b at 150KT, 6.041, is almost identical to the "expected $m_b(P_{\max})$ " of 6.062 (*cf.* Table 5E). The corrected m_b at 100KT would match that of Ringdal's rather well if the standard error in the uncorrected $m_b(P_{\max})$, 5.882 ± 0.046 , is taken into account.

Der *et al.* (1985) deconvolved four contained and the cratering Shagan events [650115] recorded at EKA, and then they convolved the Green's functions with an appropriate attenuation operator as well as the source-time function of various yields of interest. By comparing the phases P_a and P_{\max} of the synthetics, they obtained a cratering-to-contained correction of 0.15, 0.15, and 0.18 at 60, 125, and 300KT, respectively. The match with our result is remarkably good. This approach would seem very attractive if the database can be expanded to events covering a wide range of yields (and hence depths) and then the method can be applied to events in the same yield range.

m_b -Yield Calibration Curves

II.9 TEST SITE BIAS

Table 9A. Expected $\hat{m}_b(P) - \hat{m}_b(L_g)$ at Various Test Sites					
(Earlier Studies*)					
Test Site	Description	10KT	50KT	100KT	150KT
NTS	$m_b(\text{ISC}) - \text{Nuttli's } m_b(L_g)$	-0.31	-0.31	-0.31	-0.31
Shagan River	$m_b(\text{ISC}) - \text{Nuttli's } m_b(L_g)$	0.04	0.04	0.04	0.04
Degelen	$m_b(\text{ISC}) - \text{Nuttli's } m_b(L_g)$	0.27	0.27	0.27	0.27
Degelen	$m_b(\text{Sykes}) - \text{Nuttli's } m_b(L_g)$	0.23	0.23	0.23	0.23
Novaya Zemlya	$m_b(\text{ISC}) - \text{Nuttli's } m_b(L_g)$	-0.11	-0.11	-0.11	-0.11
(This Study)					
Test Site	Description	10KT	50KT	100KT	150KT
NTS	$m_b(\text{Marshall}) - \text{Patton's } m_b(L_g)$	-0.434	-0.380	-0.356	-0.343
NTS	$m_b(P_{\max}, \text{TG}) - \text{Patton's } m_b(L_g)$	-0.555	-0.485	-0.454	-0.437
Shagan River	$m_b(\text{Marshall}) - \text{Ringdal's RMS } L_g$	—	0.121	0.035	-0.015
Shagan River	$m_b(P_{\max}, \text{TG}) - \text{Ringdal's RMS } L_g$	—	0.070	-0.001	-0.041
Degelen	$m_b(\text{Marshall}) - \text{Ringdal's RMS } L_g$	—	0.232	0.185	0.158
Degelen	$m_b(P_{\max}, \text{TG}) - \text{Ringdal's RMS } L_g$	—	-0.008	-0.047	-0.069

*) Nuttli (1987, 1988).

At Degelen and Shagan, our results show that the $m_b(P) - m_b(L_g)$ has a decreasing tendency with increasing yield, contrary to the increasing trend at NTS. Results based on Marshall's m_b are consistent with ours.

m_b -Yield Calibration Curves

Table 9B. Expected Test Site Bias

(Earlier Studies)					
Test Sites	Description	10KT	50KT	100KT	150KT
Shagan - NTS	Nuttli (1987)	0.35	0.35	0.35	0.35
Degelen - NTS	Nuttli (1987)	0.54	0.54	0.54	0.54
Shagan - Degelen	Nuttli (1987)	-0.19	-0.19	-0.19	-0.19
Novaya Zemlya - NTS	Nuttli (1987)	0.20	0.20	0.20	0.20
(This Study)					
Test Sites	Description	10KT	50KT	100KT	150KT
Ringdal's $RMS L_g$ (Shagan) - $m_b(P_{max}, TG, Sahara)$		—	0.243	0.253	0.251
Ringdal's $RMS L_g$ (Shagan) - $m_b(L_g)$ (Patton, NTS)		—	-0.073	0.009	0.056
KTS - NTS	m_b (Marshall)	0.549	0.498	0.475	0.463
KTS - NTS	$m_b(P_a, TG)$	0.344	0.408	0.435	0.451
KTS - NTS	$m_b(P_b, TG)$	0.411	0.452	0.469	0.480
KTS - NTS	$m_b(P_{max}, TG)$	0.399	0.424	0.435	0.442
Shagan - NTS	m_b (Marshall)	0.492	0.428	0.400	0.384
Shagan - NTS	$m_b(P_a, TG)$	0.530	0.463	0.433	0.416
Shagan - NTS	$m_b(P_b, TG)$	0.554	0.510	0.491	0.480
Shagan - NTS	$m_b(P_{max}, TG)$	0.529	0.482	0.462	0.452
Degelen - NTS	m_b (Marshall)	0.514	0.539	0.550	0.557
Degelen - NTS	$m_b(P_a, TG)$	0.320	0.407	0.444	0.466
Degelen - NTS	$m_b(P_b, TG)$	0.387	0.438	0.460	0.473
Degelen - NTS	$m_b(P_{max}, TG)$	0.374	0.404	0.416	0.424
Sahara - NTS	$m_b(P_a, TG)$	0.083	0.132	0.153	0.165
Sahara - NTS	$m_b(P_b, TG)$	0.038	0.160	0.212	0.243
Sahara - NTS	$m_b(P_{max}, TG)$	0.063	0.168	0.214	0.240
KTS - Sahara	$m_b(P_a, TG)$	0.261	0.276	0.282	0.286
KTS - Sahara	$m_b(P_b, TG)$	0.373	0.292	0.257	0.237
KTS - Sahara	$m_b(P_{max}, TG)$	0.335	0.254	0.220	0.199

m_b -Yield Calibration Curves

Table 9B. Expected Test Site Bias (Continued)

(This Study)					
Test Sites	Description	10KT	50KT	100KT	150KT
Shagan - Sahara	$m_b(P_a, TG)$	0.447	0.331	0.280	0.251
Shagan - Sahara	$m_b(P_b, TG)$	0.516	0.350	0.279	0.237
Shagan - Sahara	$m_b(P_{max}, TG)$	0.465	0.312	0.247	0.209
Degelen - Sahara	$m_b(P_a, TG)$	0.237	0.275	0.291	0.301
Degelen - Sahara	$m_b(P_b, TG)$	0.349	0.278	0.248	0.230
Degelen - Sahara	$m_b(P_{max}, TG)$	0.310	0.234	0.201	0.181
Shagan - Degelen	$m_b(ISC)$	0.072	-0.056	-0.110	-0.142
Shagan - Degelen	$m_b(NEIS)$	0.092	-0.020	-0.068	-0.095
Shagan - Degelen	$m_b(Sykes)$	0.000	-0.061	-0.088	-0.103
Shagan - Degelen	$m_b(Marshall)$	-0.022	-0.111	-0.150	-0.173
Shagan - Degelen	$m_b(P_a, TG)$	0.210	0.056	-0.011	-0.050
Shagan - Degelen	$m_b(P_b, TG)$	0.167	0.072	0.031	0.007
Shagan - Degelen	$m_b(P_{max}, TG)$	0.155	0.078	0.046	0.028
Konystan - Degelen	$m_b(ISC)$	0.092	-0.053	-0.115	-0.152
Konystan - Degelen	$m_b(NEIS)$	0.063	-0.147	-0.238	-0.291
Konystan - Degelen	$m_b(Sykes)$	0.066	-0.052	-0.103	-0.133
Konystan - Degelen	$m_b(Marshall)$	0.063	-0.007	-0.038	-0.056
Konystan - Shagan	$m_b(ISC)$	0.020	0.003	-0.005	-0.010
Konystan - Shagan	$m_b(NEIS)$	-0.029	-0.127	-0.170	-0.196
Konystan - Shagan	$m_b(Sykes)$	0.066	0.009	-0.015	-0.030
Konystan - Shagan	$m_b(Marshall)$	0.085	0.104	0.112	0.117

The m_b bias between Sahara and Degelen is interesting in that different phases exhibit opposite tendency of bias change with yields. The bias determined with phase "a" increases with yields, while that of phases "b" and "max" decrease.

Based on Geotech's m_b -yield calibration curves, Shagan River would have more efficient P -wave coupling than does Degelen River by an offset of about 0.155 m.u. (magnitude unit)

m_b -Yield Calibration Curves

and 0.046 m.u. at 10KT and 100KT, respectively. This m_b bias can be explained by the profound topography at Degelen Mountain which could cause strong P -to- S conversion, as illustrated by the linear finite-difference calculations (Jih and McLaughlin, 1988). The bias value currently used by the U.S. government is intended to be the most appropriate value for yields near the 150KT threshold of the 1974 Threshold Test Ban Treaty (TTBT). Our results in Table 9B provide a direct clues of how different the bias could be at lower yields.

A brief review of earlier work on test site bias may be interesting. Based on the P -wave seismograms of three granite explosions (PILEDRIIVER, Shagan 680619, and Shagan 710630) recorded at EKA, Douglas (1987) concluded that the Shagan-NTS bias is about 0.5, which is very close to what we got with phases P_b and P_{max} (Table 9B). Stewart (1988) predicted a bias of 0.37 at $m_b=5.0$ and of 0.32 at $m_b=6.5$, based on the m_b averaged across four arrays: Eskdalemuir (EKA) Scotland, Yellowknife (YKA) Canada, Gauribidanur (GBA) India, and Warramunga (WRA) Australia. His predicted bias is yield-dependent, and it has a decreasing trend with increasing yield, which is consistent with our maximum-likelihood results in Table 9B. This tendency should not be surprising. Large-yield explosions generate predominantly low-frequency signals and low-yield explosions are relatively richer in higher frequencies, so a relatively large amount of energy is removed by the attenuation from low yield tests, hence the bias is greater for such low yield explosions. Furthermore, the bias between two sites is made up of more than just the attenuation in the mantle beneath the test site. A difference in depth containment laws and up-hole velocities between the test sites can have an effect on the observed amplitudes and hence on the final value of bias (Marshall, personal communication). The bias between any two test sites should be a sum of these effects. Murphy and Tzeng (1982) estimated the bias by comparing signals recorded near NTS and Semipalatinsk from Aleutian Islands earthquakes. They estimated the bias as 0.24 magnitude unit. Priestley *et al.* (1987) used a similar approach, and they estimated the bias as 0.34. It should be noted, however, that all these earlier bias estimates were made before the publication of Bocharov *et al.* (1989) and Vergino (1989).

II.10 ACKNOWLEDGEMENTS

R.S.J. is indebted to Robert R. Blandford for his many insightful discussions throughout the whole course of study. R.S.J. also likes to thank Paul G. Richards, P. D. Marshall, Frode Ringdal, and Robert Herrmann for their discussions and comments. Robert R. Blandford, Paul G. Richards, and D. Wilmer Rivers, Jr. reviewed the manuscript. This study would not be possible without the efforts from Vergino and Bocharov that made Soviet yields more accessible. Richard R. Baumstark (Boomer) gave useful suggestions in writing elegant UNIX scripts. Research reported herein was supported under DARPA contract F19628-89-C-0063 (Task 1), monitored by Geophysics Laboratory. The views and conclusions contained in this report are those of the authors and should not be interpreted as representing the official policies, either expressed or implied, of the Defense Advanced Research Projects Agency or the U.S. Government.

II.11 REFERENCES

- Blandford, R. R., and R. H. Shumway (1982). Magnitude:Yield for nuclear explosions in granite at the Nevada Test Site and Algeria: joint determination with station effects and with data containing clipped and low-amplitude signals, *Report VSC-TR-82-12*, Teledyne Geotech, Alexandria, Virginia.
- Bocharov, V. S., S. A. Zelentsov, and V. Mikhailov (1989). Characteristics of 96 underground nuclear explosions at the Semipalatinsk test site, **67** (3), 210-214 (*in Russian*).
- DARPA (1981). A technical assessment of seismic yield estimation, *Report DARPA-NMR-81-02*, DARPA/NMRO, Arlington, VA.
- Der, Z. A., R. H. Shumway, A. C. Lees, and E. Smart (1985). Multichannel deconvolution of *P* waves at seismic arrays, *Report TGAL-85-04*, Teledyne Geotech, Alexandria, VA.
- Douglas, A. (1987). Differences in upper mantle attenuation between the Nevada and Shagan River Test Sites: Can the effects be seen in *P*-wave seismograms? *Bull. Seism. Soc. Am.*, **77**, 270-276.
- Efron, B. (1979). Bootstrap methods: Another look at the jackknife, *Ann. Statist.*, **7**, 1-26.
- Efron, B. and R. Tibshirani (1985). The bootstrap method for assessing statistical accuracy, *Behaviormetrika*, **17**, 1-35.
- Ericsson, U. (1971). Maximum-likelihood linear fitting when both variables have normal and correlated error, *Report C4474-A1*, Research Institute of National Defense, Stockholm, Sweden.
- Evernden, J. F. and G. E. Marsh (1987). Yields of U.S. and Soviet nuclear tests, *Physics Today*, **8-1**, 37-44.
- Jih, R.-S. (1990). Depth scaling at Eastern Kazakhstan: a maximum-likelihood approach, *Report TGAL-90-05*, Teledyne Geotech, Alexandria, VA (*manuscript in preparation*).
- Jih, R.-S. and K. L. McLaughlin (1988). Investigation of explosion generated SV Lg waves in 2-D heterogeneous crustal models by finite-difference method, *Report AFGL-TR-88-0025 (=TGAL-88-01)*, Teledyne Geotech, Alexandria, VA. **ADA213586**
- Jih, R.-S., and R. H. Shumway (1989). Iterative network magnitude estimation and uncertainty assessment with noisy and clipped data, *Bull. Seism. Soc. Am.*, **79**, 1122-1141.
- Jih, R.-S., D. W. Rivers, and R. H. Shumway (1990a). Maximum-likelihood magnitude:yield regression with heavily censored information, *Section 1 of Report TGAL-90-03*, Teledyne Geotech, Alexandria, VA (submitted to *Bull. Seism. Soc. Am.*).

m_b -Yield Calibration Curves

- Jih, R.-S., R. H. Shumway, R. A. Wagners, D. W. Rivers, C. S. Lynnes, and T. W. McElfresh (1990b). Maximum-likelihood magnitude:yield regression with heavily censored data (preliminary results), (*abstract*), *EOS, Trans. A.G.U.*, **71**.
- Marshall, P. D., O. L. Springer, and H. C. Rodean (1979). Magnitude corrections for attenuation in the upper mantle, *Geophys. J. R. astr. Soc.*, **57**, 609-638.
- McLaughlin, K. L., I. N. Gupta, and R. A. Wagner (1985). Magnitude determination of cratering and non-cratering nuclear explosions, *Report TGAL-85-03*, Teledyne Geotech, Alexandria Laboratory, Alexandria, VA.
- Murphy, J. (1977). Seismic source functions and magnitude determinations for underground nuclear detonations, *Bull. Seism. Soc. Am.*, **67**, 135-158.
- Murphy, J. and T. K. Tzeng (1982). Estimation of magnitude/yield bias between NTS and Semipalatinsk Nuclear Testing areas, *Report SSS-R-82-5603*, Systems, Sciences, and Software, Reston, VA.
- Nordyke, M. D. (1973). A review of Soviet data on the peaceful uses of nuclear explosions, *Report UCRL-51414-REV1*, Lawrence Livermore Laboratory, University of California, CA.
- Nuttli, O. W. (1986a). Yield estimates of Nevada Test Site explosions obtained from seismic L_g waves, *J. Geophys. Res.*, **91**, 2137-2151.
- Nuttli, O. W. (1986b). L_g magnitudes of selected East Kazakhstan underground explosions, *Bull. Seism. Soc. Am.*, **76**, 1241-1251.
- Nuttli, O. W. (1987). L_g magnitudes of Degelen, East Kazakhstan, underground explosions, *Bull. Seism. Soc. Am.*, **77**, 679-681.
- Nuttli, O. W. (1988). L_g magnitudes and yield estimates for underground Novaya Zemlya nuclear explosions, *Bull. Seism. Soc. Am.*, **78**, 873-884.
- Patton, H. J. (1988). Application of Nuttli's method to estimate yield of Nevada Test Site explosions recorded on Lawrence Livermore National Laboratory's digital seismic system, *Bull. Seism. Soc. Am.*, **78**, 1759-1772.
- Priestley, K. F., D. E. Charez, and J. N. Brune (1987). A direct estimate of m_b bias between Eastern Kazakh and Nevada, *EOS, Trans. A.G.U.*, **68**, 362.
- Ringdal, F. and P. D. Marshall (1989). Yield determination of Soviet underground nuclear explosions at the Shagan River Test Site, Semiannual Technical Summary, 1 Oct 1988 - 31 Mar 1989, *NORSAR Sci. Rep. 2-88/89*, Kjeller, Norway.
- Ringdal, F. and R. A. Hansen (1989). NORSAR yield estimation studies, *Proceedings of AFTAC/DARPA 1989 Seismic Research Review* (28-29 Nov 1989, Patrick AFB, Florida),

m_b -Yield Calibration Curves

145-156.

- Springer, D. L. and R. L. Kinaman (1971). Seismic source summary for U.S. underground nuclear explosions, 1961-1970, *Bull. Seism. Soc. Am.*, **61**, 1073-1098.
- Springer, D. L. and R. L. Kinaman (1975). Seismic source summary for U.S. underground nuclear explosions, 1971-1973, *Bull. Seism. Soc. Am.*, **65**, 343-349.
- Stewart, R. C. (1988). P-wave seismograms from underground explosions at the Shagan River Test Site recorded at four arrays, *AWE Report O-4/88*, HMSO, London, UK.
- Stimpson, I. G. (1988). Source parameters of explosions in granite at the French Test Site in Algeria, *AWE Report O-11/88*, HMSO, London, UK.
- Sykes, L. R. and G. Ekstrom (1989). Comparison of seismic and hydrodynamic yield determinations for the Soviet joint verification experiment of 1988, *Proc. Natl. Acad. Sci. USA*, **86**, 3456-3460.
- Sykes, L. R. and S. Ruggi (1989). Soviet nuclear testing, in *Nuclear Weapon Databook (Volume IV, Chapter 10)*, Natural Resources Defense Council, Washington D. C.
- U.S. Congress/Office of Technology Assessment (1988). Seismic verification of nuclear testing treaties, *OTA-ISC-361*, U.S. Government Printing Office, Washington, D.C.
- Vergino, E. S. (1989). Soviet test yields, *EOS, Trans. A.G.U.*, Nov 28, 1989.

m_b -Yield Calibration Curves

(THIS PAGE INTENTIONALLY LEFT BLANK)

APPENDIX

GEOTECH'S MAXIMUM-LIKELIHOOD NETWORK m_b : GLM90A

Short-period WWSSN vertical recordings (SPZ) of body waves from 96 nuclear explosions detonated at the Semipalatinsk Test Site, Eastern Kazakhstan, USSR, are being measured and added to our database to determine the optimal network magnitudes using the maximum-likelihood estimator (MLE), which accounts for the effects of data censoring due to clipping and to noise.^{1,2} As of now, our WWSSN database has been expanded to 124 events (totaling 366 usable "a", "b", and "max" event phases) from a variety of test sites. Only the stations at teleseismic distance (20 to 95 degrees) were used in the network m_b determination. (Therefore, some of the m_b values might be slightly different from those in an earlier report TGAL-87-05.) The 8501 good signals, 5699 noise measurements, and 1088 clipped recordings yield a δ_{MLE} 0.320.

The 124 events in Table A1 are grouped by test sites. The three numbers under the column "# of signals" represent the number of signals, noise, and clips associated with the P_{max} phase of each event. Except for the U.S. and French Sahara explosions which have specific code names, all the remaining events are identified with the dates and abbreviated test site codes shown below:

azg	Azgir, U.S.S.R.
pne	"PNE", Urals, U.S.S.R.
mek	Murzhik (Konystan), E. Kazakh, U.S.S.R.
dek	Degelen Mountain, E. Kazakh, U.S.S.R.
sek	Shagan River (Balapan), E. Kazakh, U.S.S.R.
nnz	Northern Novaya Zemlya, U.S.S.R.
snz	Southern Novaya Zemlya, U.S.S.R.
tu	Tuamotu Islands, France
raj	Rajasthan, India
ch	Lop Nor, Sinkiang, China

Table A2 lists the station correction terms determined jointly along with the network m_b values.

¹ Blandford, R. R., and R. H. Shumway (1982). Magnitude yield for nuclear explosions in granite at the Nevada Test Site and Algeria: joint determination with station effects and with data containing clipped and low-amplitude signals, *Technical Report VSC-TR-82-12*, Teledyne Geotech, Alexandria, Virginia.

² Jih, R.-S., and R. H. Shumway (1989). Iterative network magnitude estimation and uncertainty assessment with noisy and clipped data, *Bull. Seismo. Soc. Am.*, 79, 1122-1141.

Geotech Network m_b

Table A1. Geotech's Maximum-Likelihood Network m_b					
Event	# of Signals	$m_b(P_a)$	$m_b(P_b)$	$m_b(P_{\max})$	σ
ALMENDRO	26,0,2	5.730	6.026	6.233	0.060
BENHAM	42,1,7	5.772	6.103	6.359	0.045
BILBY	36,3,0	5.148	5.404	5.658	0.051
BOURBON	18,31,0	4.587	4.720	4.904	0.046
BOXCAR	32,0,4	5.849	6.189	6.412	0.053
CAMBRIC	12,34,0	4.091	4.340	4.551	0.047
CHANCELLOR	16,12,1	4.887	5.183	5.338	0.059
CHARTREUSE	31,16,1	4.884	5.010	5.249	0.046
CHATEAUGAY	17,28,2	4.478	4.884	5.066	0.047
CORDUROY	18,14,0	4.971	5.092	5.287	0.057
HANDCAR	16,33,0	4.308	4.495	4.629	0.046
HANDLEY	41,1,1	6.062	6.307	6.480	0.049
HARZER	31,5,1	5.011	5.312	5.536	0.053
KANKAKEE	24,27,0	4.347	4.597	4.847	0.045
MAST	29,1,0	5.403	5.739	5.981	0.058
NASH	31,21,0	4.758	4.918	5.149	0.044
PILEDRIIVER	38,12,1	4.925	5.194	5.435	0.045
REX	16,35,1	3.875	4.376	4.720	0.044
SCOTCH	38,8,1	5.079	5.344	5.600	0.047
CANNIKIN	49,0,20	6.408	6.663	6.911	0.039
MILROW	52,0,4	5.945	6.195	6.494	0.043
LONGSHOT	67,4,3	5.056	5.428	5.818	0.037
FAULTLESS	47,1,3	5.829	6.157	6.460	0.045
GASBUGGY	11,37,0	4.153	4.412	4.661	0.046
RIO BLANCO	15,20,0	4.068	4.545	4.810	0.054
RULISON	9,37,0	4.108	4.240	4.554	0.047
SHOAL	13,27,0	4.321	4.455	4.738	0.051
SALMON	6,33,0	3.439	3.974	4.180	0.051

Geotech Network m_b

Table A1. Geotech's Maximum-Likelihood Network m_b (Continued)					
Event	# of Signals	$m_b(P_a)$	$m_b(P_b)$	$m_b(P_{\max})$	σ
azg22apr66	3,10,0	3.867	4.101	4.183	0.089
azg22dec71	12,0,2	5.473	5.826	6.164	0.086
azg25apr75	1,16,0	—	3.904	3.944	0.078
azg29jul76	41,5,7	5.105	5.579	5.864	0.044
azg30sep77	21,30,1	4.049	4.588	4.828	0.044
azg17oct78	7,0,5	5.271	5.724	6.097	0.092
azg18dec78	9,0,3	5.374	5.748	6.119	0.092
azg17jan79	10,0,4	5.515	5.869	6.153	0.086
azg14jul79	10,0,1	4.831	5.371	5.699	0.097
azg24oct79	3,0,6	4.848	5.681	5.960	0.107
pne29aug74	27,18,0	3.994	4.397	4.722	0.048
mek18dec66	55,9,1	5.261	5.493	5.709	0.040
dek21nov65	48,15,1	4.875	5.152	5.362	0.040
dek13feb66	51,4,10	5.640	5.890	6.082	0.040
dek20mar66	50,9,8	5.335	5.624	5.850	0.039
dek07may66	9,26,1	3.992	4.233	4.486	0.053
dek26feb67	48,9,6	5.353	5.597	5.821	0.040
dek29sep68	50,8,6	5.125	5.432	5.627	0.040
dek23jul69	38,21,1	4.594	4.920	5.167	0.041
dek11sep69	19,39,0	3.975	4.234	4.576	0.042
dek25apr71	37,5,0	5.299	5.566	5.756	0.049
dek30dec71	16,3,0	4.982	5.347	5.524	0.073
dek28mar72	28,17,0	4.351	4.726	4.959	0.048
dek16aug72	24,23,1	4.337	4.620	4.885	0.046
dek10dec72	30,7,5	4.975	5.333	5.532	0.049
dek29mar77	25,14,0	4.304	4.700	4.981	0.051
dek30jul77	21,16,0	4.200	4.604	4.857	0.053
dek26mar78	25,6,0	4.948	5.272	5.497	0.057
dek22apr78	21,9,0	4.466	4.765	5.014	0.058

Geotech Network m_b

Table A1. Geotech's Maximum-Likelihood Network m_b (Continued)					
Event	# of Signals	$m_b(P_a)$	$m_b(P_b)$	$m_b(P_{\max})$	σ
sek15jan65	46,1,2	5.493	5.732	5.880	0.046
sek19jun68	28,3,2	4.618	5.000	5.261	0.056
sek30nov69	32,0,0	5.378	5.767	5.975	0.057
sek30juh71	31,19,1	4.470	4.766	5.038	0.045
sek10feb72	34,8,2	4.803	5.071	5.304	0.048
sek02nov72	29,1,15	5.590	5.938	6.187	0.048
sek10dec72	29,2,11	—	5.784	6.013	0.049
sek23jul73	38,1,1	5.753	5.996	6.181	0.051
sek14dec73	45,8,6	5.245	5.545	5.770	0.042
sek27apr75	18,1,1	4.904	5.242	5.491	0.072
sek04jul76	14,0,5	5.229	5.598	5.927	0.073
sek07dec76	17,2,1	4.961	5.416	5.606	0.072
sek11jun78	17,0,1	5.296	5.580	5.889	0.075
sek15sep78	30,1,5	5.431	5.691	5.884	0.053
sek23jun79	38,3,3	5.615	5.846	6.049	0.048
sek14sep80	29,5,6	5.439	5.752	5.987	0.051
nnz27oct66	56,0,14	6.063	6.295	6.436	0.038
nnz21oct67	53,5,3	5.400	5.590	5.765	0.041
nnz07nov68	59,1,5	5.580	5.831	6.025	0.040
nnz14oct69	59,2,7	5.760	5.957	6.129	0.039
nnz14oct70	35,0,22	6.424	6.633	6.813	0.042
nnz27sep71	23,0,21	6.259	6.475	6.619	0.048
nnz28aug72	32,0,11	5.989	6.247	6.371	0.049
nnz12sep73	23,0,21	6.347	6.672	6.763	0.048
nnz29aug74	25,0,18	6.126	6.394	6.578	0.049
nnz21oct75	23,0,17	6.095	6.333	6.541	0.051
nnz23aug75	28,0,12	6.112	6.367	6.488	0.051
nnz20oct76	25,34,1	4.031	4.350	4.659	0.041
nnz01sep77	26,2,2	5.099	5.415	5.561	0.058
nnz10aug78	39,3,18	5.392	5.625	5.856	0.041

Geotech Network m_b

Table A1. Geotech's Maximum-Likelihood Network m_b (Continued)					
Event	# of Signals	$m_b(P_a)$	$m_b(P_b)$	$m_b(P_{\max})$	σ
nnz11oct80	42,4,6	5.181	5.442	5.658	0.044
nnz01oct81	43,4,5	5.226	5.489	5.649	0.044
nnz18aug83	30,5,5	5.321	5.526	5.703	0.051
nnz25oct84	22,3,4	5.154	5.427	5.599	0.059
snz27sep73	32,3,1	5.196	5.490	5.729	0.053
snz27oc73a	14,0,24	6.647	6.873	7.092	0.052
snz27oc73b	9,28,0	—	3.999	4.150	0.053
snz27oc73c	4,34,0	3.544	3.886	3.908	0.052
snz02nov74	12,0,29	6.497	6.790	7.012	0.050
snz18oct75	21,0,21	6.227	6.518	6.834	0.049
BERYL	11,6,0	4.412	4.778	4.985	0.078
CORUNDON	11,42,0	3.797	3.899	4.212	0.044
EMERAUDE	14,25,0	—	4.261	4.566	0.051
GRENAT	32,32,1	4.292	4.494	4.763	0.040
OPALE	3,51,0	3.770	3.855	3.896	0.044
RUBIS	42,5,0	4.826	5.167	5.429	0.047
SAPHIR	52,5,5	5.182	5.464	5.716	0.041
TOURMALINE	27,39,0	4.106	4.427	4.644	0.039
TURQOISE	11,55,0	—	3.941	4.221	0.039
tu19feb77	16,28,0	—	4.370	4.622	0.048
tu19mar77	20,6,1	5.141	5.438	5.639	0.062
tu24nov77	33,0,0	5.051	5.369	5.662	0.056
tu25jul79	18,0,0	5.090	5.570	5.864	0.075
tu23mar80	27,14,3	4.677	5.105	5.358	0.048
tu19jul80	38,2,2	4.891	5.158	5.513	0.049
tu03dec80	32,11,0	4.689	4.981	5.331	0.049
tu25jul82	22,13,0	4.675	5.034	5.210	0.054
tu19apr83	22,1,0	4.993	5.199	5.495	0.067

Geotech Network m_b

Table A1. Geotech's Maximum-Likelihood Network m_b (Continued)					
Event	# of Signals	$m_b(P_a)$	$m_b(P_b)$	$m_b(P_{\max})$	σ
tu25may83	18,0,0	5.150	5.455	5.785	0.075
tu30nov78	40,7,2	4.820	5.234	5.611	0.046
raj18may74	7,23,0	4.022	4.303	4.563	0.058
ch22sep69	30,12,0	4.325	4.742	5.133	0.049
ch27oct75	12,24,0	4.131	4.396	4.585	0.053
ch17oct76	13,33,0	3.884	4.146	4.532	0.047
ch06oct83	17,13,1	4.769	5.029	5.243	0.057
ch03oct84	10,12,0	4.453	4.747	4.999	0.068
ch19dec84	3,10,0	4.017	3.999	4.381	0.089

Geotech Network m_b

Table A2. WWSSN Station Corrections					
Code	# of Signals	Site Term	Longitude	Latitude	Description
AAE	78,93,17	-0.243±0.023	38.765556	9.029166	Addis Ababa, Ethiopia
AAM	134,64,6	0.254±0.022	-83.656113	42.299721	Ann Arbor, Michigan
ADE	16,25,0	0.001±0.050	138.708893	-34.966946	Adelaide, Australia
AFI	27,65,0	-0.143±0.033	-171.777252	-13.909333	Afiamalu, Samoa Islands
AKU	71,69,0	-0.093±0.027	-18.106667	65.686668	Akureyri, Iceland
ALQ	99,15,19	0.039±0.028	-106.457497	34.942501	Albuquerque, New Mexico
ANP	20,67,0	-0.327±0.034	121.516670	25.183332	Anpu, Formosa
ANT	41,49,2	0.056±0.033	-70.415276	-23.705000	Antofagasta, Chile
AQU	66,44,13	-0.054±0.029	13.403055	42.353889	Aquila, Italy
ARE	83,40,0	0.101±0.029	-71.491280	-16.462084	Arequipa, Peru
ASP	1,2,0	-0.581±0.185	133.896667	-23.683332	Alice Springs, Australia
ATL	79,19,2	0.164±0.032	-84.337502	33.433334	Atlanta, Georgia
ATU	112,78,16	0.146±0.022	23.716667	37.972221	Athens Univ., Greece
BAG	132,68,8	-0.028±0.022	120.579720	16.410833	Baguio City, Philippine Islands
BDF	10,2,0	-0.009±0.092	-47.903332	-15.663834	Brasilia array, Brazil
BEC	45,102,3	-0.131±0.026	-64.681114	32.379444	Bermuda-Columbia, Atlantic Ocean
BHP	30,75,0	-0.176±0.031	-79.558052	8.960834	Balboa Heights, Panama
BKS	141,65,1	0.087±0.022	-122.235001	37.876667	Byerly, California
BLA	152,53,12	0.122±0.022	-80.420998	37.211304	Blacksburg, West Virginia
BOG	41,76,0	0.057±0.030	-74.065002	4.623055	Bogota, Colombia
BOZ	44,4,5	0.238±0.044	-111.633331	45.599998	Bozeman, Montana
BUL	149,34,9	0.049±0.023	28.613333	-20.143333	Bulawayo, Rhodesia
CAR	92,59,7	0.154±0.025	-66.927635	10.506667	Caracas, Venezuela
CCG	1,0,0	-0.186±0.320	-61.133335	77.166664	Camp Century, Greenland
CHG	97,16,36	-0.127±0.026	98.976944	18.790001	Chiangmai, Asia
CMC	50,27,0	-0.140±0.036	-115.083336	67.833336	Copper Mine, Canada
COL	259,47,28	0.087±0.018	-147.793335	64.900002	College Outpost, Alaska
COP	74,101,14	0.166±0.023	12.433333	55.683334	Copenhagen, Denmark
COR	77,59,3	0.111±0.027	-123.303192	44.585724	Corvallis, Oregon
CTA	57,16,4	0.214±0.036	146.254440	-20.088333	Charters Towers, Australia

Geotech Network m_b

Table A2. WWSSN Station Corrections (Continued)					
Code	# of Signals	Site Term	Longitude	Latitude	Description
DAG	21,13,5	0.001±0.051	-18.770000	76.769997	Danmarkshavn, Greenland
DAL	17,24,4	0.191±0.048	-96.783890	32.846111	Dallas, Texas
DAV	24,81,0	-0.276±0.031	125.574722	7.087778	Davao, Philippine Islands
DUG	170,17,29	0.075±0.022	-112.813332	40.195000	Dugway, Utah
EIL	25,3,43	0.075±0.038	34.950001	29.549999	Eilat, United Arab Republic
EPT	29,2,2	0.005±0.056	-106.505836	31.771667	El Paso, Texas-Mexico border
ESK	88,80,2	0.117±0.025	-3.205000	55.316666	Eskdalemuir, United Kingdom
FLO	80,20,9	0.064±0.031	-90.370003	38.801666	Florissant, Missouri
FVM	44,8,0	-0.008±0.044	-90.426003	37.984001	French Village, Missouri
GDH	154,126,1	-0.159±0.019	-53.533333	69.250000	Godhavn, Greenland
GEO	88,69,2	0.021±0.025	-77.066666	38.900002	Georgetown, Virginia
GIE	9,38,0	-0.188±0.047	-90.300003	-0.733333	Galapagos Islands
GOL	157,24,11	-0.216±0.023	-105.371109	39.700279	Golden, Colorado
GRM	1,20,0	-0.093±0.070	26.573334	-33.313332	Grahamstown, South Africa
GSC	89,22,16	0.089±0.028	-116.804611	35.301666	Goldstone, California
GUA	78,175,0	-0.250±0.020	144.911667	13.538333	Guam, Mariana Islands
HKC	85,84,0	-0.131±0.025	114.171890	22.303556	Hong Kong
HLW	47,36,32	-0.047±0.030	31.341667	29.858334	Helwan, United Arab Republic
HNR	30,92,0	0.188±0.029	159.947113	-9.432195	Honiara, Solomon Islands
HON	6,9,0	0.051±0.083	-158.008331	21.321667	Honolulu, Hawaii
HOW	1,10,0	0.258±0.097	88.309166	22.416666	Howrah, India-Bangladesh border
IST	102,79,25	0.186±0.022	28.995832	41.045555	Istanbul, Turkey
JCT	59,4,24	0.159±0.034	-99.802223	30.479445	Junction City, Texas
JER	89,45,25	0.039±0.025	35.197224	31.771944	Jerusalem, Dead Sea
KBL	14,0,46	0.142±0.041	69.043167	34.540833	Kabul, Afghanistan
KBS	55,40,0	-0.181±0.033	11.923889	78.917503	Kingsbay, Svalbard
KEV	121,102,4	-0.123±0.021	27.006666	69.755280	Kevo, Finland
KIP	84,153,0	0.107±0.021	-158.014999	21.423334	Kipapa, Hawaii
KOD	107,33,30	0.100±0.025	77.466667	10.233334	Kodaikanal, India
KON	129,65,70	0.102±0.020	9.598222	59.649082	Kongsberg, Norway

Geotech Network m_b

Table A2. WWSSN Station Corrections (Continued)

Code	# of Signals	Site Term	Longitude	Latitude	Description
KRK	8,7,0	-0.171±0.083	30.062500	69.724167	Kirkenes, Norway-USSR border
KTG	72,75,1	-0.247±0.026	-21.983334	70.416664	Kap Tobin, Greenland
LAH	5,17,3	0.428±0.064	74.333336	31.549999	Lahore, India-Pakistan border
LEM	54,82,0	-0.531±0.027	107.616669	-6.833333	Lembang, Java
LON	162,44,21	-0.034±0.021	-121.809998	46.750000	Longmire, Washington
LOR	74,8,16	0.154±0.032	3.851389	47.266666	Lormes, France
LPA	8,91,0	0.426±0.032	-57.931946	-34.908890	La Plata, Uruguay
LPB	58,39,3	-0.043±0.032	-68.098358	-16.532667	La Paz, Peru-Bolivia border
LPS	50,27,3	-0.071±0.036	-89.161942	14.292222	La Palma, Guatemala
LUB	40,30,3	0.214±0.037	-101.866669	33.583332	Lubbock, Texas
MAL	87,41,10	0.055±0.027	-4.411111	36.727501	Malaga, straits of Gibraltar
MAN	30,14,1	0.316±0.048	121.076859	14.662000	Manila, Philippine Islands
MAT	145,53,25	-0.112±0.021	138.206665	36.541668	Matsushiro, Japan
MDS	39,19,0	-0.032±0.042	-89.760002	43.372223	Madison, Wisconsin
MHI	5,2,2	0.358±0.107	59.494499	36.299999	Meshed, Iran-USSR border
MNN	8,6,2	0.179±0.080	-93.190002	44.914444	Minneapolis, Minnesota
MSH	31,19,9	0.226±0.042	59.587776	36.311111	Meshed, Iran-USSR border
MSO	46,7,2	0.061±0.043	-113.940552	46.829166	Missoula, Montana
MUN	39,41,0	0.015±0.036	116.208336	-31.978333	Mundaring, Australia
NAI	115,46,9	-0.089±0.025	36.803665	-1.273944	Nairobi, Kenya
NAT	27,27,0	0.070±0.044	-35.033333	-5.116667	Natal, Brazil
NDI	129,24,25	0.124±0.024	77.216667	28.683332	New Delhi, India
NHA	12,3,0	-0.127±0.083	109.211670	12.210000	Nhatranga, Asia
NIL	14,6,18	-0.008±0.052	73.251663	33.650002	Nilore, Pakistan
NNA	47,57,0	-0.162±0.031	-76.842140	-11.987556	Nana, Peru
NOR	78,50,3	-0.260±0.028	-16.683332	81.599998	Nord, Greenland
NUR	103,82,7	0.051±0.023	24.651417	60.508999	Nurmijarvi, Finland
OGD	135,63,6	-0.119±0.022	-74.595833	41.087502	Ogdensburg, New York
OXF	79,10,17	0.347±0.031	-89.409164	34.511806	Oxford, Mississippi
PDA	31,103,3	0.050±0.027	-25.663334	37.746666	Ponta Delgada, Azores Islands

Geotech Network m_b

Table A2. WWSSN Station Corrections (Continued)					
Code	# of Signals	Site Term	Longitude	Latitude	Description
PEL	29,39,3	0.052±0.038	-70.685280	-33.143612	Peldehue, Chile-Argentina
PMG	82,58,2	-0.005±0.027	147.153885	-9.409166	Port Moresby, New Guinea
POO	133,40,28	0.037±0.023	73.849998	18.533333	Pcona, India
PRE	65,42,0	-0.074±0.031	28.190001	-25.753334	Pretoria, South Africa
PTO	84,52,5	-0.140±0.027	-8.602222	41.138611	Porto Serro Do, Portugal
QUE	82,23,41	-0.412±0.026	66.949997	30.188334	Quetta, Pakistan
QUI	9,67,0	0.007±0.037	-78.500504	-0.200139	Quito, Ecuador
RAB	45,135,0	-0.177±0.024	152.169830	-4.191278	Rabaul, New Britain
RAR	12,30,0	-0.070±0.049	-159.773331	-21.212500	Rarotonga, Cook Islands
RCD	28,22,3	0.439±0.044	-103.208336	44.075001	Rapid City, South Dakota
RIV	9,22,0	0.355±0.057	151.158340	-33.829361	Riverview, Australia
SBA	2,12,0	-0.619±0.086	166.756104	-77.850281	Scott Base, Antarctica
SCP	167,68,21	0.055±0.020	-77.864998	40.794998	State College, Pennsylvania
SDB	75,17,9	0.083±0.032	13.571944	-14.925834	Sa Da Bandeira, Angola
SEO	97,76,12	-0.076±0.024	126.966667	37.566666	Seoul Keizyo, South Korea
SHA	76,65,0	0.346±0.027	-88.142807	30.694361	Spring Hill, Mississippi
SHI	77,14,30	0.298±0.029	52.519943	29.638306	Shiraz, Iran
SHK	41,76,0	-0.324±0.030	132.677505	34.532223	Shiraki, Honshu, Japan
SHL	83,15,41	0.033±0.027	91.883331	25.566668	Shillong, India-Bangladesh border
SJG	129,57,0	-0.248±0.023	-66.150002	18.111666	San Juan, Puerto Rico
SNA	6,11,0	0.108±0.078	-2.325000	-70.315002	Sanae, Antarctica
SNG	44,31,3	-0.072±0.036	100.620003	7.173333	Songkhla, Malay Peninsula
SPA	13,7,0	-0.756±0.072	0.000000	-90.000000	South Pole, Antarctica
STU	172,94,20	0.094±0.019	9.195000	48.771946	Stuttgart, Germany
TAB	76,53,5	0.216±0.028	46.326668	38.067501	Tabriz, Iran-USSR border
TAU	12,14,0	-0.115±0.063	147.320419	-42.909916	Tasmania Univ., Tasmania
TOL	112,52,23	0.211±0.023	-4.048611	39.881390	Toledo, Spain
TRI	128,85,25	-0.105±0.021	13.764167	45.708889	Trieste, Italy
TRN	112,70,1	0.101±0.024	-61.402779	10.648916	Trinidad, Trinidad
TUC	57,3,21	0.077±0.036	-110.782219	32.309723	Tucson, Arizona

Geotech Network m_b

Table A2. WWSSN Station Corrections (Continued)

Code	# of Signals	Site Term	Longitude	Latitude	Description
UME	123,53,2	0.170±0.024	20.236666	63.814999	Umea, Sweden
UNM	10,13,1	-0.236±0.065	-99.178085	19.329000	Nat. University of Central Mexico
UPA	2,1,0	-0.261±0.185	-79.533997	8.981500	Univ. de Panama, Panama
VAL	122,122,12	0.015±0.020	-10.244166	51.939445	Valentia Eire
WEL	8,12,0	0.139±0.072	174.768326	-41.286110	Wellington, New Zealand
WES	135,118,6	-0.139±0.020	-71.322083	42.384693	Weston, New England
WIN	32,29,0	-0.186±0.041	17.100000	-22.566668	Windhoek, South-West Africa

Geotech Network m_b

(THIS PAGE INTENTIONALLY LEFT BLANK)

Prof. Thomas Ahrens
Seismological Lab, 252-21
Division of Geological & Planetary Sciences
California Institute of Technology
Pasadena, CA 91125

Prof. Charles B. Archambeau
CIRES
University of Colorado
Boulder, CO 80309

Prof. Muawia Barazangi
Institute for the Study of the Continent
Cornell University
Ithaca, NY 14853

Dr. Douglas R. Baumgardt
ENSCO, Inc
5400 Port Royal Road
Springfield, VA 22151-2388

Prof. Jonathan Berger
IGPP, A-025
Scripps Institution of Oceanography
University of California, San Diego
La Jolla, CA 92093

Dr. Lawrence J. Burdick
Woodward-Clyde Consultants
566 El Dorado Street
Pasadena, CA 91109-3245

Dr. Karl Coyner
New England Research, Inc.
76 Olcott Drive
White River Junction, VT 05001

Prof. Vernon F. Cormier
Department of Geology & Geophysics
U-15, Room 207
The University of Connecticut
Storrs, CT 06268

Professor Anton W. Dainty
Earth Resources Laboratory
Massachusetts Institute of Technology
42 Carleton Street
Cambridge, MA 02142

Prof. Steven Day
Department of Geological Sciences
San Diego State University
San Diego, CA 92182

Dr. Zoltan A. Der
ENSCO, Inc.
5400 Port Royal Road
Springfield, VA 22151-2388

Prof. John Ferguson
Center for Lithospheric Studies
The University of Texas at Dallas
P.O. Box 830688
Richardson, TX 75083-0688

Prof. Stanley Flatte
Applied Sciences Building
University of California
Santa Cruz, CA 95064

Dr. Alexander Florence
SRI International
333 Ravenswood Avenue
Menlo Park, CA 94025-3493

Prof. Henry L. Gray
Vice Provost and Dean
Department of Statistical Sciences
Southern Methodist University
Dallas, TX 75275

Dr. Indra Gupta
Teledyne Geotech
314 Montgomery Street
Alexandria, VA 22314

Prof. David G. Harkrider
Seismological Laboratory
Division of Geological & Planetary Sciences
California Institute of Technology
Pasadena, CA 91125

Prof. Donald V. Helmberger
Seismological Laboratory
Division of Geological & Planetary Sciences
California Institute of Technology
Pasadena, CA 91125

Prof. Eugene Herrin
Institute for the Study of Earth and Man
Geophysical Laboratory
Southern Methodist University
Dallas, TX 75275

Prof. Robert B. Herrmann
Department of Earth & Atmospheric Sciences
St. Louis University
St. Louis, MO 63156

Prof. Bryan Isacks
Cornell University
Department of Geological Sciences
SNEE Hall
Ithaca, NY 14850

Dr. Rong-Song Jih
Teledyne Geotech
314 Montgomery Street
Alexandria, VA 22314

Prof. Lane R. Johnson
Seismographic Station
University of California
Berkeley, CA 94720

Prof. Alan Kafka
Department of Geology & Geophysics
Boston College
Chestnut Hill, MA 02167

Dr. Richard LaCoss
MIT-Lincoln Laboratory
M-200B
P. O. Box 73
Lexington, MA 02173-0073 (3 copies)

Prof Fred K. Lamb
University of Illinois at Urbana-Champaign
Department of Physics
1110 West Green Street
Urbana, IL 61801

Prof. Charles A. Langston
Geosciences Department
403 Deike Building
The Pennsylvania State University
University Park, PA 16802

Prof. Thorne Lay
Institute of Tectonics
Earth Science Board
University of California, Santa Cruz
Santa Cruz, CA 95064

Prof. Arthur Lerner-Lam
Lamont-Doherty Geological Observatory
of Columbia University
Palisades, NY 10964

Dr. Christopher Lynnes
Teledyne Geotech
314 Montgomery Street
Alexandria, VA 22314

Prof. Peter Malin
University of California at Santa Barbara
Institute for Crustal Studies
Santa Barbara, CA 93106

Dr. Randolph Martin, III
New England Research, Inc.
76 Olcott Drive
White River Junction, VT 05001

Dr. Gary McCartor
Mission Research Corporation
735 State Street
P.O. Drawer 719
Santa Barbara, CA 93102 (2 copies)

Prof. Thomas V. McEvilly
Seismographic Station
University of California
Berkeley, CA 94720

Dr. Keith L. McLaughlin
S-CUBED
A Division of Maxwell Laboratory
P.O. Box 1620
La Jolla, CA 92038-1620

Prof. William Menke
Lamont-Doherty Geological Observatory
of Columbia University
Palisades, NY 10964

Stephen Miller
SRI International
333 Ravenswood Avenue
Box AF 116
Menlo Park, CA 94025-3493

Prof. Bernard Minster
IGPP, A-025
Scripps Institute of Oceanography
University of California, San Diego
La Jolla, CA 92093

Prof. Brian J. Mitchell
Department of Earth & Atmospheric Sciences
St. Louis University
St. Louis, MO 63156

Mr. Jack Murphy
S-CUBED, A Division of Maxwell Laboratory
11800 Sunrise Valley Drive
Suite 1212
Reston, VA 22091 (2 copies)

Dr. Bao Nguyen
GL/LWH
Hanscom AFB, MA 01731-5000

Prof. John A. Orcutt
IGPP, A-025
Scripps Institute of Oceanography
University of California, San Diego
La Jolla, CA 92093

Prof. Keith Priestley
University of Cambridge
Bullard Labs, Dept. of Earth Sciences
Madingley Rise, Madingley Rd.
Cambridge CB3 0EZ, ENGLAND

Prof. Paul G. Richards
L-210
Lawrence Livermore National Laboratory
Livermore, CA 94550

Dr. Wilmer Rivers
Teledyne Geotech
314 Montgomery Street
Alexandria, VA 22314

Prof. Charles G. Sammis
Center for Earth Sciences
University of Southern California
University Park
Los Angeles, CA 90089-0741

Prof. Christopher H. Scholz
Lamont-Doherty Geological Observatory
of Columbia University
Palisades, NY 10964

Prof. David G. Simpson
Lamont-Doherty Geological Observatory
of Columbia University
Palisades, NY 10964

Dr. Jeffrey Stevens
S-CUBED
A Division of Maxwell Laboratory
P.O. Box 1620
La Jolla, CA 92038-1620

Prof. Brian Stump
Institute for the Study of Earth & Man
Geophysical Laboratory
Southern Methodist University
Dallas, TX 75275

Prof. Jeremiah Sullivan
University of Illinois at Urbana-Champaign
Department of Physics
1110 West Green Street
Urbana, IL 61801

Prof. Clifford Thurber
University of Wisconsin-Madison
Department of Geology & Geophysics
1215 West Dayton Street
Madison, WI 53706

Prof. M. Nafi Toksoz
Earth Resources Lab
Massachusetts Institute of Technology
42 Carleton Street
Cambridge, MA 02142

Prof. John E. Vidale
University of California at Santa Cruz
Seismological Laboratory
Santa Cruz, CA 95064

Prof. Terry C. Wallace
Department of Geosciences
Building #77
University of Arizona
Tucson, AZ 85721

Dr. Raymond Willeman
GL/LWH
Hanscom AFB, MA 01731-5000

Dr. Lorraine Wolf
GL/LWH
Hanscom AFB, MA 01731-5000

Prof. Francis T. Wu
Department of Geological Sciences
State University of New York
at Binghamton
Vestal, NY 13901

OTHERS (United States)

Dr. Monem Abdel-Gawad
Rockwell International Science Center
1049 Camino Dos Rios
Thousand Oaks, CA 91360

Prof. Keiiti Aki
Center for Earth Sciences
University of Southern California
University Park
Los Angeles, CA 90089-0741

Prof. Shelton S. Alexander
Geosciences Department
403 Deike Building
The Pennsylvania State University
University Park, PA 16802

Dr. Kenneth Anderson
BBNSTC
Mail Stop 14/1B
Cambridge, MA 02238

Dr. Ralph Archuleta
Department of Geological Sciences
University of California at Santa Barbara
Santa Barbara, CA 93102

Dr. Thomas C. Bache, Jr.
Science Applications Int'l Corp.
10210 Campus Point Drive
San Diego, CA 92121 (2 copies)

J. Barker
Department of Geological Sciences
State University of New York
at Binghamton
Vestal, NY 13901

Dr. T.J. Bennett
S-CUBED
A Division of Maxwell Laboratory
11800 Sunrise Valley Drive, Suite 1212
Reston, VA 22091

Mr. William J. Best
907 Westwood Drive
Vienna, VA 22180

Dr. N. Biswas
Geophysical Institute
University of Alaska
Fairbanks, AK 99701

Dr. G.A. Bollinger
Department of Geological Sciences
Virginia Polytechnical Institute
21044 Derring Hall
Blacksburg, VA 24061

Dr. Steven R. Bratt
Center for Seismic Studies
1300 North 17th St., Suite 1450
Arlington, VA 22209

Michael Browne
Teledyne Geotech
3401 Shiloh Road
Garland, TX 75041

Mr. Roy Burger
1221 Serry Road
Schenectady, NY 12309

Dr. Robert Burrige
Schlumberger-Doll Research Center
Old Quarry Road
Ridgefield, CT 06877

Dr. Jerry Carter
Rondout Associates
P.O. Box 224
Stone Ridge, NY 12484

Dr. W. Winston Chan
Teledyne Geotech
314 Montgomery Street
Alexandria, VA 22314-1581

Dr. Theodore Cherry
Science Horizons, Inc.
710 Encinitas Blvd., Suite 200
Encinitas, CA 92024 (2 copies)

Prof. Jon F. Claerbout
Department of Geophysics
Stanford University
Stanford, CA 94305

Prof. Robert W. Clayton
Seismological Laboratory
Division of Geological & Planetary Sciences
California Institute of Technology
Pasadena, CA 91125

Prof. F. A. Dahlen
Geological and Geophysical Sciences
Princeton University
Princeton, NJ 08544-0636

Prof. Adam Dziewonski
Hoffman Laboratory
Harvard University
20 Oxford St
Cambridge, MA 02138

Prof. John Ebel
Department of Geology & Geophysics
Boston College
Chestnut Hill, MA 02167

Eric Fielding
SNEE Hall
INSTOC
Cornell University
Ithaca, NY 14853

Prof. Donald Forsyth
Department of Geological Sciences
Brown University
Providence, RI 02912

Dr. Cliff Frolich
Institute of Geophysics
8701 North Mopac
Austin, TX 78759

Prof. Art Frankel
Mail Stop 922
Geological Survey
790 National Center
Reston, VA 22092

Dr. Anthony Gangi
Texas A&M University
Department of Geophysics
College Station, TX 77843

Dr. Freeman Gilbert
Inst. of Geophysics & Planetary Physics
University of California, San Diego
P.O. Box 109
La Jolla, CA 92037

Mr. Edward Giller
Pacific Sierra Research Corp.
1401 Wilson Boulevard
Arlington, VA 22209

Dr. Jeffrey W. Given
Sierra Geophysics
11255 Kirkland Way
Kirkland, WA 98033

Prof. Stephen Grand
University of Texas at Austin
Department of Geological Sciences
Austin, TX 78713-7909

Prof. Roy Greenfield
Geosciences Department
403 Deike Building
The Pennsylvania State University
University Park, PA 16802

Dan N. Hagedorn
Battelle
Pacific Northwest Laboratories
Battelle Boulevard
Richland, WA 99352

Kevin Hutchenson
Department of Earth Sciences
St. Louis University
3507 Laclede
St. Louis, MO 63103

Prof. Thomas H. Jordan
Department of Earth, Atmospheric
and Planetary Sciences
Massachusetts Institute of Technology
Cambridge, MA 02139

Robert C. Kemerait
ENSCO, Inc.
445 Pineda Court
Melbourne, FL 32940

William Kikendall
Teledyne Geotech
3401 Shiloh Road
Garland, TX 75041

Prof. Leon Knopoff
University of California
Institute of Geophysics & Planetary Physics
Los Angeles, CA 90024

Prof. L. Timothy Long
School of Geophysical Sciences
Georgia Institute of Technology
Atlanta, GA 30332

Prof. Art McGarr
Mail Stop 977
Geological Survey
345 Middlefield Rd.
Menlo Park, CA 94025

Dr. George Mellman
Sierra Geophysics
11255 Kirkland Way
Kirkland, WA 98033

Prof. John Nabelek
College of Oceanography
Oregon State University
Corvallis, OR 97331

Prof. Geza Nagy
University of California, San Diego
Department of Ames, M.S. B-010
La Jolla, CA 92093

Prof. Amos Nur
Department of Geophysics
Stanford University
Stanford, CA 94305

Prof. Jack Oliver
Department of Geology
Cornell University
Ithaca, NY 14850

Prof. Robert Phinney
Geological & Geophysical Sciences
Princeton University
Princeton, NJ 08544-0636

Dr. Paul Pomeroy
Rondout Associates
P.O. Box 224
Stone Ridge, NY 12484

Dr. Jay Pulli
RADIX System, Inc.
2 Taft Court, Suite 203
Rockville, MD 20850

Dr. Norton Rimer
S-CUBED
A Division of Maxwell Laboratory
P.O. Box 1620
La Jolla, CA 92038-1620

Prof. Larry J. Ruff
Department of Geological Sciences
1006 C.C. Little Building
University of Michigan
Ann Arbor, MI 48109-1063

Dr. Richard Sailor
TASC Inc.
55 Walkers Brook Drive
Reading, MA 01867

Thomas J. Sereno, Jr.
Science Application Int'l Corp.
10210 Campus Point Drive
San Diego, CA 92121

John Sherwin
Teledyne Geotech
3401 Shiloh Road
Garland, TX 75041

Prof. Robert Smith
Department of Geophysics
University of Utah
1400 East 2nd South
Salt Lake City, UT 84112

Prof. S. W. Smith
Geophysics Program
University of Washington
Seattle, WA 98195

Dr. Stewart Smith
IRIS Inc.
1616 North Fort Myer Drive
Suite 1440
Arlington, VA 22209

Dr. George Sutton
Rondout Associates
P.O. Box 224
Stone Ridge, NY 12484

Prof. L. Sykes
Lamont-Doherty Geological Observatory
of Columbia University
Palisades, NY 10964

Prof. Pradeep Talwani
Department of Geological Sciences
University of South Carolina
Columbia, SC 29208

Prof. Ta-liang Teng
Center for Earth Sciences
University of Southern California
University Park
Los Angeles, CA 90089-0741

Dr. R.B. Tittmann
Rockwell International Science Center
1049 Camino Dos Rios
P.O. Box 1085
Thousand Oaks, CA 91360

Dr. Gregory van der Vink
IRIS, Inc.
1616 North Fort Myer Drive
Suite 1440
Arlington, VA 22209

Professor Daniel Walker
University of Hawaii
Institute of Geophysics
Honolulu, HI 96822

William R. Walter
Seismological Laboratory
University of Nevada
Reno, NV 89557

Dr. Gregory Wojcik
Weidlinger Associates
4410 El Camino Real
Suite 110
Los Altos, CA 94022

Prof. John H. Woodhouse
Hoffman Laboratory
Harvard University
20 Oxford St.
Cambridge, MA 02138

Dr. Gregory B. Young
ENSCO, Inc.
5400 Port Royal Road
Springfield, VA 22151-2388

GOVERNMENT

Dr. Ralph Alewine III
DARPA/NMRO
1400 Wilson Boulevard
Arlington, VA 22209-2308

Mr. James C. Battis
GL/LWH
Hanscom AFB, MA 01731-5000

Dr. Robert Blandford
DARPA/NMRO
1400 Wilson Boulevard
Arlington, VA 22209-2308

Eric Chael
Division 9241
Sandia Laboratory
Albuquerque, NM 87185

Dr. John J. Cipar
GL/LWH
Hanscom AFB, MA 01731-5000

Mr. Jeff Duncan
Office of Congressman Markey
2133 Rayburn House Bldg.
Washington, DC 20515

Dr. Jack Evernden
USGS - Earthquake Studies
345 Middlefield Road
Menlo Park, CA 94025

Art Frankel
USGS
922 National Center
Reston, VA 22092

Dr. T. Hanks
USGS
Nat'l Earthquake Research Center
345 Middlefield Road
Menlo Park, CA 94025

Dr. James Hannon
Lawrence Livermore Nat'l Laboratory
P.O. Box 808
Livermore, CA 94550

Paul Johnson
ESS-4, Mail Stop J979
Los Alamos National Laboratory
Los Alamos, NM 87545

Janet Johnston
GL/LWH
Hanscom AFB, MA 01731-5000

Dr. Katharine Kadinsky-Cade
GL/LWH
Hanscom AFB, MA 01731-5000

Ms. Ann Kerr
IGPP, A-025
Scripps Institute of Oceanography
University of California, San Diego
La Jolla, CA 92093

Dr. Max Koontz
US Dept of Energy/DP 5
Forrestal Building
1000 Independence Avenue
Washington, DC 20585

Dr. W.H.K. Lee
Office of Earthquakes, Volcanoes,
& Engineering
345 Middlefield Road
Menlo Park, CA 94025

Dr. William Leith
U.S. Geological Survey
Mail Stop 928
Reston, VA 22092

Dr. Richard Lewis
Director, Earthquake Engineering & Geophysics
U.S. Army Corps of Engineers
Box 631
Vicksburg, MS 39180

James F. Lewkowicz
GL/LWH
Hanscom AFB, MA 01731-5000

Mr. Alfred Lieberman
ACDA/VI-OA State Department Bldg
Room 5726
320 - 21st Street, NW
Washington, DC 20451

Stephen Mangino
GL/LWH
Hanscom AFB, MA 01731-5000

Dr. Frank F. Pilotte
HQ AFTAC/TT
Patrick AFB, FL 32925-6001

Dr. Robert Masse
Box 25046, Mail Stop 967
Denver Federal Center
Denver, CO 80225

Katie Poley
CIA-OSWR/NED
Washington, DC 20505

Art McGarr
U.S. Geological Survey, MS-977
345 Middlefield Road
Menlo Park, CA 94025

Mr. Jack Rachlin
U.S. Geological Survey
Geology, Rm 3 C136
Mail Stop 928 National Center
Reston, VA 22092

Richard Morrow
ACDA/VI, Room 5741
320 21st Street N.W
Washington, DC 20451

Dr. Robert Reinke
WL/NTESG
Kirtland AFB, NM 87117-6008

Dr. Keith K. Nakanishi
Lawrence Livermore National Laboratory
P.O. Box 808, L-205
Livermore, CA 94550

Dr. Byron Ristvet
HQ DNA, Nevada Operations Office
Attn: NVCG
P.O. Box 98539
Las Vegas, NV 89193

Dr. Carl Newton
Los Alamos National Laboratory
P.O. Box 1663
Mail Stop C335, Group ESS-3
Los Alamos, NM 87545

Dr. George Rothe
HQ AFTAC/TGR
Patrick AFB, FL 32925-6001

Dr. Kenneth H. Olsen
Los Alamos Scientific Laboratory
P.O. Box 1663
Mail Stop C335, Group ESS-3
Los Alamos, NM 87545

Dr. Alan S. Ryall, Jr.
DARPA/NMRO
1400 Wilson Boulevard
Arlington, VA 22209-2308

Howard J. Patton
Lawrence Livermore National Laboratory
P.O. Box 808, L-205
Livermore, CA 94550

Dr. Michael Shore
Defense Nuclear Agency/SPSS
6801 Telegraph Road
Alexandria, VA 22310

Mr. Chris Paine
Office of Senator Kennedy
SR 315
United States Senate
Washington, DC 20510

Donald L. Springer
Lawrence Livermore National Laboratory
P.O. Box 808, L-205
Livermore, CA 94550

Colonel Jerry J. Perrizo
AFOSR/NP, Building 410
Bolling AFB
Washington, DC 20332-6448

Mr. Charles L. Taylor
GL/LWG
Hanscom AFB, MA 01731-5000

Dr. Thomas Weaver
Los Alamos National Laboratory
P.O. Box 1663, Mail Stop C335
Los Alamos, NM 87545

DARPA/PM
1400 Wilson Boulevard
Arlington, VA 22209

J.J. Zucca
Lawrence Livermore National Laboratory
Box 808
Livermore, CA 94550

Defense Technical Information Center
Cameron Station
Alexandria, VA 22314 (5 copies)

GL/SULL
Research Library
Hanscom AFB, MA 01731-5000 (2 copies)

Defense Intelligence Agency
Directorate for Scientific &
Technical Intelligence/DTIB
Washington, DC 20340-6158

Secretary of the Air Force
(SAFRD)

Washington, DC 20330

AFTAC/CA
(STINFO)
Patrick AFB, FL 32925-6001

Office of the Secretary Defense
DDR & E
Washington, DC 20330

TACTEC
Battelle Memorial Institute
505 King Avenue
Columbus, OH 43201 (Final Report Only)

HQ DNA
Attn: Technical Library
Washington, DC 20305

DARPA/RMO/RETRIEVAL
1400 Wilson Boulevard
Arlington, VA 22209

DARPA/RMO/Security Office
1400 Wilson Boulevard
Arlington, VA 22209

Geophysics Laboratory
Attn: XO
Hanscom AFB, MA 01731-5000

Geophysics Laboratory
Attn: LW
Hanscom AFB, MA 01731-5000

CONTRACTORS (Foreign)

Dr. Ramon Cabre, S.J.
Observatorio San Calixto
Casilla 5939
La Paz, Bolivia

- Prof. Hans-Peter Harjes
Institute for Geophysik
Ruhr University/Bochum
- P.O. Box 102148
4630 Bochum 1, FRG

Prof. Eystein Husebye
NTNF/NORSAR
P.O. Box 51
N-2007 Kjeller, NORWAY

Prof. Brian L.N. Kennett
Research School of Earth Sciences
Institute of Advanced Studies
G.P.O. Box 4
Canberra 2601, AUSTRALIA

Dr. Bernard Massinon
Societe Radiomana
27 rue Claude Bernard
75005 Paris, FRANCE (2 Copies)

Dr. Pierre Mecheler
Societe Radiomana
27 rue Claude Bernard
75005 Paris, FRANCE

Dr. Svein Mykkeltveit
NTNF/NORSAR
P.O. Box 51
N-2007 Kjeller, NORWAY

FOREIGN (Others)

Dr. Peter Basham
Earth Physics Branch
Geological Survey of Canada
1 Observatory Crescent
Ottawa, Ontario, CANADA K1A 0Y3

Dr. Eduard Berg
Institute of Geophysics
University of Hawaii
Honolulu, HI 96822

Dr. Michel Bouchon
I.R.I.G.M.-B.P. 68
38402 St. Martin D'Herès
Cedex, FRANCE

Dr. Hilmar Bungum
NTNF/NORSAR
P.O. Box 51
N-2007 Kjeller, NORWAY

Dr. Michel Campillo
Observatoire de Grenoble
I.R.I.G.M.-B.P. 53
38041 Grenoble, FRANCE

Dr. Kin Yip Chun
Geophysics Division
Physics Department
University of Toronto
Ontario, CANADA M5S 1A7

Dr. Alan Douglas
Ministry of Defense
Blacknest, Brimpton
Reading RG7-4RS, UNITED KINGDOM

Dr. Roger Hansen
NTNF/NORSAR
P.O. Box 51
N-2007 Kjeller, NORWAY

Dr. Manfred Henger
Federal Institute for Geosciences & Nat'l Res.
Postfach 510153
D-3000 Hanover 51, FRG

Ms. Eva Johannisson
Senior Research Officer
National Defense Research Inst.
P.O. Box 27322
S-102 54 Stockholm, SWEDEN

Dr. Fekadu Kebede
Seismological Section
Box 12019
S-750 Uppsala, SWEDEN

Dr. Tormod Kvaerna
NTNF/NORSAR
P.O. Box 51
N-2007 Kjeller, NORWAY

Dr. Peter Marshal
Procurement Executive
Ministry of Defense
Blacknest, Brimpton
Reading RG7-4RS, UNITED KINGDOM

Prof. Ari Ben-Menahem
Department of Applied Mathematics
Weizman Institute of Science
Rehovot, ISRAEL 951729

Dr. Robert North
Geophysics Division
Geological Survey of Canada
1 Observatory Crescent
Ottawa, Ontario, CANADA K1A 0Y3

Dr. Frode Ringdal
NTNF/NORSAR
P.O. Box 51
N-2007 Kjeller, NORWAY

Dr. Jorg Schlittenhardt
Federal Institute for Geosciences & Nat'l Res.
Postfach 510153
D-3000 Hannover 51, FEDERAL REPUBLIC OF
GERMANY